A STUDY OF THE HYDROLYSIS REACTIONS OF $PhSiCl_3$
AND Me_2SiCl_2 IN A LAMINAR FLOW TUBULAR REACTOR

Dissertation for the Degree of Ph. D.
MICHIGAN STATE UNIVERSITY
JOHN HOWARD CAMERON
1975

This is to certify that the

thesis entitled

A STUDY OF THE HYDROLYSIS REACTIONS OF

PhSiCl$_3$ AND Me$_2$SiCl$_2$ IN A LAMINAR

FLOW TUBULAR REACTOR

presented by

John Howard Cameron

has been accepted towards fulfillment
of the requirements for

Ph.D.   degree in Chemical Engineering

Major professor

Date July 11, 1975

O-7639

ABSTRACT

A STUDY OF THE HYDROLYSIS REACTIONS OF PhSiCl$_3$ AND Me$_2$SiCl$_2$ IN A LAMINAR FLOW TUBULAR REACTOR

By

John Howard Cameron

This work contains a study of the hydrolysis reactions of PhSiCl$_3$ and Me$_2$SiCl$_2$ in a laminar flow tubular reactor. The aims of this work were to model these reactions, investigate the mechanisms involved, determine the effect of HCl on these reactions, and estimate the effects of the plug flow and isothermal assumptions for the reactor.

The hydrolysis reactions of chlorosilanes consist of the replacement of the chlorines by hydroxyl groups. Little work has been done on these reactions due to their fast rate and complexity. There are three reasons for the fast rate of these reactions relative to similar carbon reactions. These are the ionic nature of the silicon-halogen bond, the larger diameter of silicon compared to carbon, and silicon's unfilled 3-d orbitals. The complexity of these reactions is due to the effect of HCl on the system and a competing condensation reaction. HCl has the ability to either catalyze or suppress the hydrolysis reactions of chlorosilanes and is also known to catalyze the condensation reaction.

In this study, the individual hydrolysis reactions of the chlorosilanes were followed using an infrared spectrophotometer. The absorption spectrum of the chlorosilanes and their hydrolysis products were obtained. Using these spectra, infrared band assignments were made for the reactants, unstable intermediates and products.

A variable length reactor surrounded by a heat exchanger and coupled with an infrared spectrophotometer was used to monitor the reactions. The silane solvent mixture entered the reactor through a long needle, similar to a hypodermic needle. By varying the position of this needle in the reactor, the length of the reaction zone was varied. Using this technique, data on concentrations versus residence time was obtained.

The hydrolysis reactions of $PhSiCl_3$ can be written as a series of three irreversible reactions.

$$PhSiCl_3 + H_2O \xrightarrow{K_1} PhSiCl_2(OH) + HCl$$

$$PhSiCl_2(OH) + H_2O \xrightarrow{K_2} PhSiCl(OH)_2 + HCl$$

$$PhSiCl(OH)_2 + H_2O \xrightarrow{K_3} PhSi(OH)_3 + HCl$$
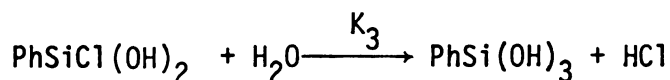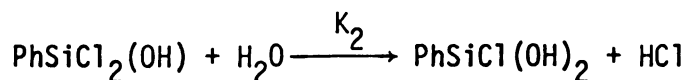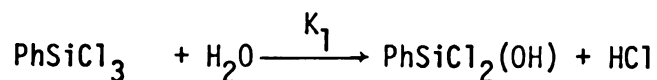
To determine the effect of HCl on the reactions, the initial concentration of HCl in the system was varied. The mechanism of this effect is complex, with the reaction being catalyzed through the stabilization of the transition state intermediate by

the chloride ion and being suppressed by the reaction of water with the proton to form the hydronium ion. However, the principal effect of HCl was to suppress the rate of these hydrolysis reactions. The effect of HCl was incorporated into the set of differential equations describing the reactions by using the term $[HCl]^n$. The rate constants and n were found to have the following values at 0°C: K_1 = 220, K_2 = 16.5, K_3 = 40.6 $(liters/mole)^{1+n}/seconds$ and n = -0.612.

The second system studied was the hydrolysis reactions of Me_2SiCl_2. The following series of reactions were found to describe these hydrolysis reactions.

$$Me_2SiCl_2 \quad + \quad H_2O \xrightarrow{\quad K_1 \quad} Me_2SiCl(OH) + HCl$$

$$Me_2SiCl(OH) + H_2O \underset{K_2'}{\overset{K_2}{\rightleftharpoons}} Me_2Si(OH)_2 + HCl$$
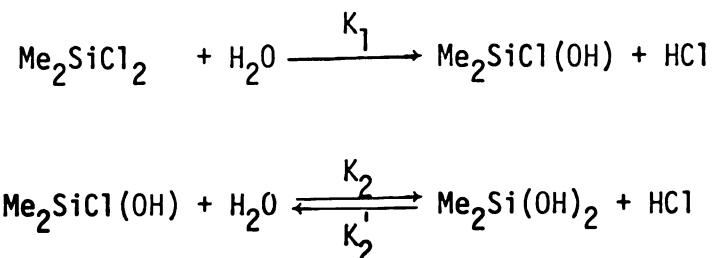
The rate constants found to describe these reactions at 0°C are K_1 = 38.3, K_2 = 11.1, K_2' = 20.2 (mole/liter-second). By studying these reactions at different temperatures, the activation energies were determined: ΔE_1 = 3.6 kcal/mole, ΔE_2 = 10.5 kcal/mole, $\Delta E_2'$ = 14.0 kcal/mole.

These reactions were modeled assuming that plug flow existed and that the system was isothermal. A principal aspect of this study was to determine the magnitude of the error introduced by these assumptions. The study of these assumptions begins with

John Howard Cameron

a material and energy balance on a laminar flow tubular reactor. The model is based on a ring-shaped element in the reactor with conduction and convection of energy in the axial direction and conduction in the radial direction. Partial differential equations describing the temperature and concentration profiles in the reactor are developed. Using a finite difference technique and physical constants similar to those found in the hydrolysis reactions of Me_2SiCl_2, a computer program is employed to integrate these equations. Second order rate constants needed to give the same conversion in a laminar flow reactor with heat transfer are compared to those in an isothermal plug flow reactor. It was determined that the rate constants determined assuming isothermal plug flow are approximately 10 percent lower than those determined assuming laminar flow with heat transfer. This produces a bound of 10 percent between these two models.

A STUDY OF THE HYDROLYSIS REACTIONS OF

$PhSiCl_3$ AND Me_2SiCl_2 IN A LAMINAR

FLOW TUBULAR REACTOR

By

John Howard Cameron

A DISSERTATION

Submitted to
Michigan State University
in partial fulfillment of the requirements
for the degree of

DOCTOR OF PHILOSOPHY

Department of Chemical Engineering

1975

ACKNOWLEDGMENTS

The author wishes to express his sincere appreciation to Dr. Martin C. Hawley for his guidance and advice throughout the course of this work. Appreciation is also extended to the members of my Thesis Guidance Committee for their advice and suggestions.

The author is indebted to the Division of Engineering Research for their support of this project and to the Dow Corning Corporation for furnishing the necessary reagents. The advice and effort of Don Childs in the fabrication of the experimental apparatus is appreciated.

Special thanks is given to my wife, Pam, for her understanding and encouragement.

TABLE OF CONTENTS

LIST OF TABLES

LIST OF FIGURES

CHAPTER I

INTRODUCTION

A. General Chemistry of Silicon

The hydrolysis reactions of halosilanes are faster than those of similar carbon compounds. Frequently, these reactions are too fast to be studied by conventional techniques and techniques designed for fast reactions must be employed to study them. Their complexity and fast rate are the primary reasons for the lack of study on the hydrolysis reactions of halosilanes.

Silicon compounds are generally tetravalent. From the study of these compounds and orbital energy considerations, it is concluded that silicon like carbon makes use of sp^3-σ bonding (1: p. 3). However, due to the unfilled 3-d orbitals, silicon has the ability to expand its valence shell to include pentacovalent and hexacovalent silicon. Unlike carbon, the double oxygen bond in silicon is unstable (2: p. 1). Instead, silicon forms single bonds with oxygen and silicon-oxygen chains known as polyorgano-siloxanes. The silicon in polyorganosiloxanes may have one, two or three organic groups attached to it. The possible forms of this silicon unit in the polyorganosiloxanes are:

```
       O                O                R                R
       |                |                |                |
O - Si - O       O - Si - R       O - Si - O       O - Si - R
       |                |                |                |
       O                O                R                R
```

1
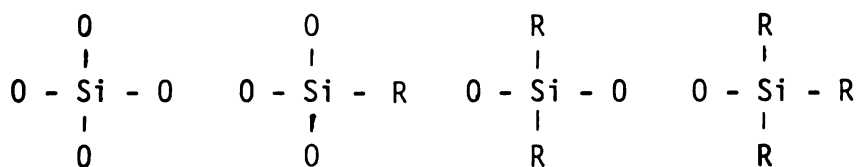
Polyorganosiloxanes are normally produced from monomeric organosilicon compounds containing both organic and silicon functional groups. These silicon functional groups are hydrolyzable groups attached to the silicon atom. Polyorganosiloxanes are formed by the reaction of these monomeric organosilicon compounds with water. During this hydrolysis reaction, the functional groups are replaced by hydroxyl groups. These silanols further react by condensation accompanied by loss of water to form polyorganosiloxanes. The hydrolysis and condensation reactions of monomeric organosilicon compounds containing 1, 2, 3, or 4 functional groups are:

Silane	Unstable Intermediate	Siloxane Unit
R_3SiX	$\rightarrow R_3Si(OH)$	$\rightarrow R_3SiO_{1/2}$
R_2SiX_2	$\rightarrow R_2Si(OH)_2$	$\rightarrow R_2SiO$
$RSiX_3$	$\rightarrow RSi(OH)_3$	$\rightarrow RSiO_{3/2}$
SiX_4	$\rightarrow Si(OH)_4$	$\rightarrow SiO_2$
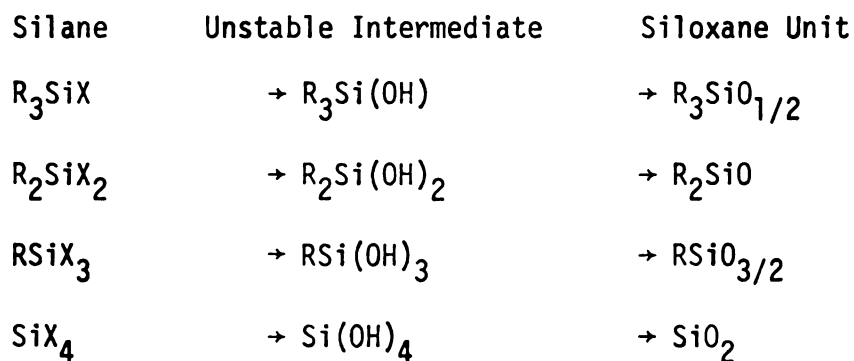
The silicon-halogen bond is extremely reactive and reactions involving this bond are generally fast. There are three principal reasons for the reactivity of the silicon-halogen bond. First, the silicon-halogen bond is strongly polar. Second, the radius of a silicon atom is 1.17 Å compared to 0.77 Å for a carbon atom. Therefore, an attacking nucleophile would have easier access to the silicon atom in a silicon compound than to a carbon atom in a similar carbon compound. Third, since the 3-d orbitals

of the silicon atom are unfilled, these orbitals may take part in the transition intermediate. In cases where a lower energy state for the intermediate occurs due to the incorporation of the 3-d orbitals, the silicon species would be more reactive.

Industrially, the most important monomeric organosilicon compounds are those containing chlorine atoms as the functional groups. Through a variety of methods and conditions, these organochlorosilanes are hydrolyzed with water to form organosilanols which condense to form the various polyorganosiloxanes.

Sommer (1: p. 78) studied the hydrolysis reactions of optically active compounds R_3Si^*Cl.

$$(+) \ R_3Si^*Cl + H_2O \xrightarrow{\text{ether}} (+) \ R_3Si^*OH + HCl$$

$$+ 6.4° \qquad\qquad\qquad + 20.5°$$
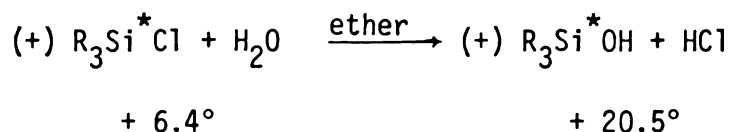
Such reactions were found to be 90 percent sterospecific and to proceed with inversion of configuration; for example, cis-chlorosilane gives a trans-silanol. From such reactions, it has been proposed that the hydrolysis reactions involving organo-chlorosilanes take place through backside attack by the water molecule. The transition intermediate for such reactions would involve a separation of charges. A typical intermediate for these reactions is:

$$S[^{\delta+} H_2O \cdots \overset{\textstyle|}{\underset{\textstyle/\ \backslash}{Si}} \cdots Cl^{\delta-}] S$$
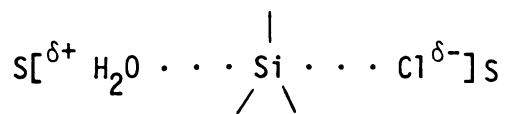
This intermediate would be stabilized by solvent molecules (S). Since such intermediates contain a separation of charges, the more polar the solvent molecules, the greater their ability to stabilize the intermediates.

B. Scope of Past Work

The hydrolysis reactions of the halosilanes that have been studied are principally those of the monohalosilanes. These reactions are generally slower and less complex than those of the di- or trihalosilanes. Recent studies of those reactions include those of Milishkevick et al. 1971 (3), Allen and Modena 1957 (4), and Chipperfield and Prince 1963 (5). Shaffer and Flanigen 1957 (6) investigated the combined hydrolysis-condensation reactions of alkyl and aryl chlorosilanes in batch experiments.

The studies of Shaffer and Flanigen (6) and Chipperfield and Prince (5) both used electrolytic conductance to follow the hydrolysis of the chlorosilanes. Shaffer and Flanigen (6) slowed the reactions by saturating the solution with HCl and cooling the reactants. This allowed the reactions to be followed by conductometric titration. Chipperfield and Prince (5) designed a flow reactor and monitored the electrolytic conductivity as a function of reactor length. Both of these techniques follow the HCl concentration, which allows observation of only the rate limiting hydrolysis or condensation step.

Shaffer and Flanigen (6) expressed the rate of reaction with respect to the change in water concentration as:

$$- \frac{d(H_2O)}{dt} = k \ (H_2O)^m \ (\equiv SiCl)^n \ (HCl)^p \qquad (2.1)$$

The hydrolysis reactions were found to be first order with respect to water. Hence, the value of m in equation (2.1) is 1. The value of n for the reactions of $PhSiCl_3$ was found to be 1.9. However, for the reactions of $(CH_3)_2SiCl_2$, n was found to be -1/3. This decrease in initial rate of reaction with an increase in dimethyldichlorosilane was not understood. No corrections were made for any equilibriums in the system. This was mentioned as a possible source of error in the work of Shaffer and Flanigen.

No value of p was given in the paper. However, it was observed that an increase in HCl concentration decreased the rate of the hydrolysis reactions. For the hydrolysis of $PhSiCl_3$, a 10 percent increase in HCl concentration can double the half-time of the reaction.

1,2-dimethoxyethane saturated with HCl was used as the solvent for the majority of the hydrolysis experiments. However, the hydrolysis reactions of CH_3SiCl_3, $C_6H_5SiCl_3$, and $(CH_3)_2SiCl_2$ were also measured in a dioxane-HCl solution. The rates of reaction of CH_3SiCl_3 and $(CH_3)_2SiCl_2$ were found to be three times as fast in dioxane-HCl than in 1,2-dimethoxyethane HCl. However, the hydrolysis of $C_6H_5SiCl_3$ was observed to be slower in dioxane-HCl.

When titrating $PhSiCl_3$ in an initially neutral solution at 0°C, Shaffer and Flanigen determined that only completely condensed polysiloxanes $(RSiO_{3/2})_x$ were formed. While at -78°C, $(RSiCl_2)O$ was found to be an intermediate product. Only in the case of

$(C_6H_5)_2SiCl_2$ were indications of stable groups such as $\underset{\overset{|}{Cl}}{=Si-OH}$
found.

From their research, Shaffer and Flanigen reached the following generalizations. First, the rate of hydrolysis reactions of a series of silanes $SiCl_4$ - R_3SiCl are related in the following manner.

$$SiCl_4 > RSiCl_3 > R_2SiCl_2 > R_3SiCl$$
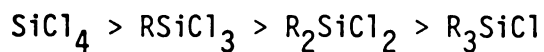
Second, for a silane containing more than one chlorine, the rate of hydrolysis of the first chlorine atom is much faster than that of the remaining chlorines.

Kleinhenz and Hawley 1970 (7) studied the hydrolysis reactions of $PhSiCl_3$ at 0°C in an experimental flow system similar to the one used in this study. The reactions were followed using an infrared spectrophotometer.

The hydrolysis reactions of $PhSiCl_3$ were modeled as three irreversible reactions in series, first order with respect to water and silane, and second order overall. The rate equations used to describe these reactions are:

$$\frac{d[PhSiCl_3]}{dt} = -k_1 \ [PhSiCl_3] \ [H_2O] \qquad (2.2)$$

$$\frac{d[PhSiCl_2(OH)]}{dt} = k_1 \ [PhSiCl_3] \ [H_2O] - k_2$$

$$[PhSiCl_2(OH)] \ [H_2O] \qquad (2.3)$$

$$\frac{d[PhSiCl(OH)_2]}{dt} = k_2 \quad [PhSiCl_2(OH)] \quad [H_2O] - k_3$$

$$[PhSiCl(OH)_2] \quad [H_2O] \qquad\qquad (2.4)$$

$$[PhSi(OH)_3] = [PhSiCl_3]_0 + [PhSiCl_2(OH)]_0 + [PhSiCl(OH)_2]_0$$

$$+ [PhSi(OH)_3]_0 - [PhSiCl_3] - [PhSiCl_2(OH)]$$

$$- [PhSiCl(OH)_2] \qquad\qquad (2.5)$$

Equation (2.5) is a material balance on the system with $[PhSiCl_3]_0$, $[PhSiCl_2(OH)]_0$, and $[PhSiCl(OH)_2]_0$ representing the initial concentrations of $PhSiCl_3$, $PhSiCl_2(OH)$, and $PhSiCl(OH)_2$, respectively.

To fit the rate constants, the reactions were modeled for both plug and laminar flow. In laminar flow the velocity distribution is:

$$U = 2 \quad Ub \quad (1 - (r/R)^2) \qquad\qquad (2.6)$$

The residence time for each element in the cylindrical cross section is:

$$t = L/U \qquad\qquad (2.7)$$

The velocity distribution was used as a weighing factor to obtain the bulk concentrations by integrating the point concentrations over the reactor cross section.

$$C_b = \frac{2\pi \int_0^R C(L,r/R,U_b) \; U(r/R,U_b)r \; dr}{\pi \, U_b \, R^2} \qquad (2.8)$$

Using this analysis, rate constants, which give the same conversions for either plug or laminar flow, were determined for different order reactions. For second order irreversible reactions, the average ratio of the rate constant determined assuming laminar flow to that determined assuming plug flow is 1.176. The rate constants for equations (2.2) through (2.4) were determined by bracketing the data points between a model for laminar flow and a model for plug flow. Using this method, the rate constants were determined to be $k_1 = 1500.0$, $k_2 = 77.5$, $k_3 = 1000.0$ liters/mole-seconds. All hydrolysis experiments were run with no initial HCl concentration and no attempt was made to determine the effect of HCl on the system.

C. Scope of This Work

The literature available on the hydrolysis reactions of halosilanes deals almost exclusively with the monohalosilanes. Though the reactions of the monohalosilanes are of little industrial importance, they have been studied to a considerably greater extent than those of the di- or trihalosilanes. This occurred since monohalosilanes reactions tend to be slower and less complex than those of the di- or trihalosilanes. Their hydrolysis reactions can be followed through either an increase in the HCl concentration or a decrease in water concentration.

In order to adequately determine the kinetics of such reactions, it is necessary to determine the individual reactants and product concentrations during the reactions. A technique has been developed in this research which allows the determination of the concentrations of the initial chlorosilanes, unstable intermediates, and products of the hydrolysis reactions to be followed during these reactions.

When Kleinhenz and Hawley (7) studied the hydrolysis reactions of $PhSiCl_3$, no effort was made to determine the effect of HCl on these reactions. Shaffer and Flanigen (6) observed a marked decrease in the rate of reaction with an increase in the HCl concentration. They gave the decrease of the rate of the combined hydrolysis and condensation reactions of $PhSiCl_3$ as an example of this effect. Here, a definite decrease in the rate of reaction was observed with an increase in the HCl concentration. To minimize this effect, Shaffer and Flanigen studied the reactions in a saturated solution of HCl. One of the objects of this present study was to determine the effect of HCl on the hydrolysis reactions.

The hydrolysis reactions of $PhSiCl_3$ and Me_2SiCl_2 were studied during this research. These compounds and their hydrolysis reactions are industrially important in the manufacture of polyorganosiloxanes. A laminar flow tubular reactor coupled with an infrared spectrophotometer was utilized to follow the hydrolysis reactions. Infrared spectra of the reactants, unstable intermediates, and products were obtained during the experiments. Peak assignments were made for the various compounds which are

present during the reactions and extinction coefficients determined for these compounds. Using these spectra, concentration data versus time in the reactor were obtained.

The experimental apparatus was modified to handle corrosive solutions of HCl. This enabled the initial concentration of HCl to be varied and the effect of HCl on the hydrolysis reactions to be determined.

In this study models for the hydrolysis reactions of $PhSiCl_3$ and Me_2SiCl_2 are presented. These models are based on an S_n2-Si type reaction and describe the individual hydrolysis reactions. S_n2-Si reactions are nucleophilic substitution reactions of silicon having a transition state intermediate containing a separation of charges. Rate constants are determined from experimental data for the individual hydrolysis reactions. With the exception of the work of Kleinhenz and Hawley (7), previous work on these reactions has only described the rates of the combined hydrolysis-condensation reactions.

The temperature effect on the hydrolysis reactions of Me_2SiCl_2 is described. The effect of HCl on the hydrolysis reactions is clarified by describing the conditions under which HCl catalyzes or suppresses the hydrolysis reactions of the chlorosilanes. By describing the individual rates of the hydrolysis reactions, the temperature effect, and the effect of HCl, the knowledge of these hydrolysis reactions is significantly increased. Finally, a model of a laminar flow reactor is presented. This model may be used to determine under what conditions the plug flow and isothermal assumptions are justified when investigating reaction rates in a flow reactor.

D. Organization of This Work

The body of this work is contained in five chapters.
Chapter II describes the experimental apparatus and techniques
employed to study the hydrolysis reactions.

Chapter III describes the hydrolysis reactions of $PhSiCl_3$.
This chapter begins with the interpretation of the infrared spec-
tra obtained during the hydrolysis experiments. The competing
condensation reaction is then described. The conditions for the
hydrolysis reactions of $PhSiCl_3$ are discussed and a model for
these reactions presented. The solvent effects are then investi-
gated. The chapter ends with some concluding remarks on these
hydrolysis reactions.

Chapter IV describes the hydrolysis reactions of Me_2SiCl_2.
This chapter begins with an interpretation of the infrared spectra
obtained during the hydrolysis reactions of Me_2SiCl_2. The com-
peting condensation reactions for this system are then discussed
along with any possible effect of the condensation reactions on
this study of the hydrolysis reactions. The experimental condi-
tions for these hydrolysis reactions are described and a model
developed. The temperature effect on these reactions is then dis-
cussed. This chapter ends with concluding remarks on the hydrolysis
reactions of Me_2SiCl_2.

Chapter V contains a development of a laminar flow reactor
model with heat transfer. This chapter begins with a discussion
of past work that has been done on this type of model. The basis

for the model is introduced and the model developed. The chapter ends with a discussion of conclusions reached through this analysis.

Chapter VI contains a general discussion of conclusions reached during this study. Appendix A contains the data from the laminar flow reactor used to model the reactions. Appendix B contains the development of the computer program used to solve the partial differential equations describing the temperature and concentration profiles in the reactor.

CHAPTER II

EXPERIMENTAL

A. Apparatus

Figure 1 illustrates the apparatus used for the hydrolysis experiments. The reactants-solvent mixtures were contained in two polyethylene tanks. The driving force for the system was a tank of dry nitrogen. The line pressure from the nitrogen tank was maintained at approximately 10 p.s.i.g. during the runs. This pressure forced the solutions from the tanks through the rotameters. The rotameters were calibrated and these calibrations checked after each run. After the reactants-solvent mixtures left the rotameters, they flowed through the temperature bath and then into the reactor. Polyethylene tubing (1/4 inch O.D.) was used for the flow lines to the rotameters, from the rotameters to the constant temperature bath, and from the constant temperature bath to the reactor. The polyethylene tanks and tubing, being resistive to the corrosive nature of chlorosilanes and hydrogen chloride, were found to be ideal for handling solutions of these reagents. The heat exchanger consisted of a series of coiled stainless steel tubing, which insured good heat transfer. Since the contact time between the reactants and stainless steel was very short, only a minimum of corrosive reaction occurred here.

13
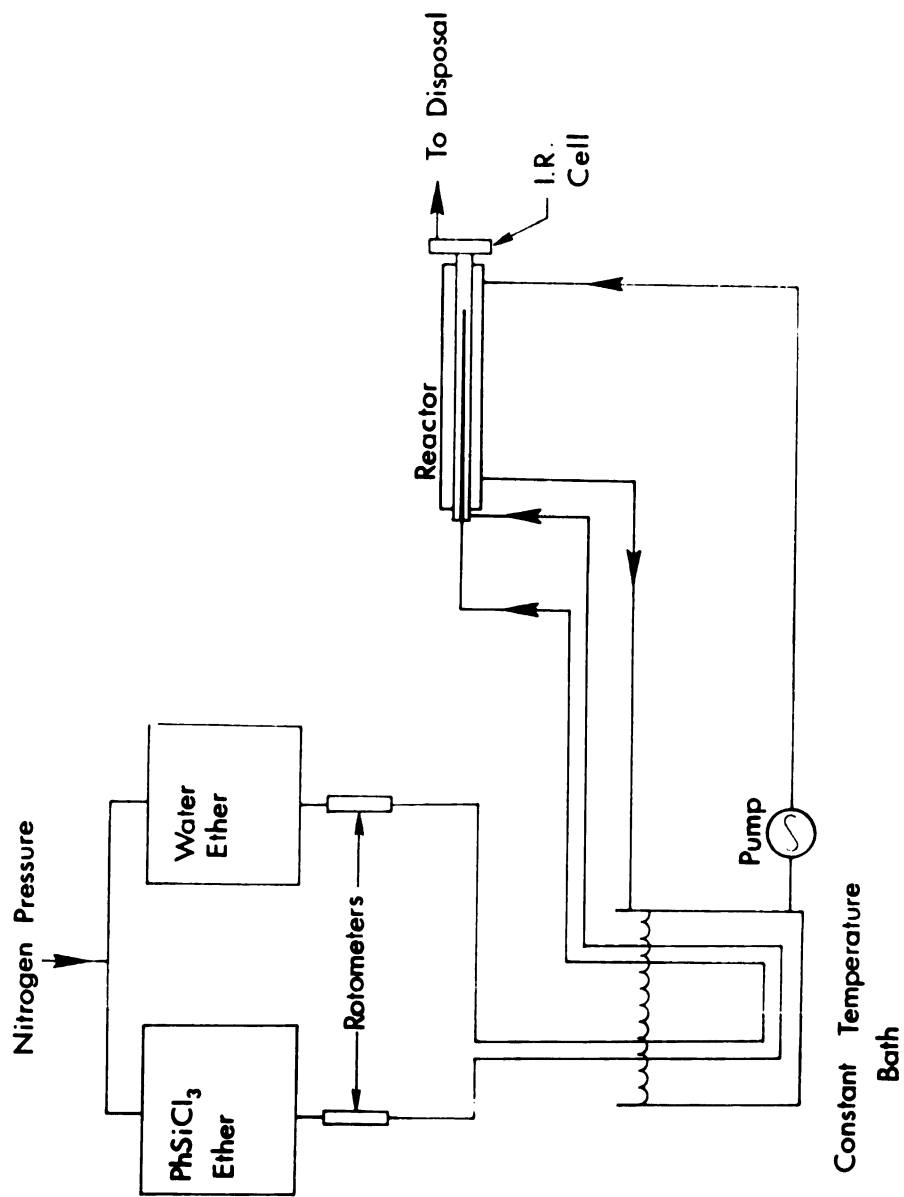
Figure 1.--Reactor Apparatus.

The polyethylene tubing proved a good insulating material. Besides being constructed from polyethylene, the tubes from the heat exchanger to the reactor were wrapped in 1/2 inch of insulation, which kept the temperature rise during this portion of the reactants' journey to a minimum.

The reactor is shown in Figure 2. It consisted of a stainless steel tube, 0.216 cm in diameter, surrounded by a heat exchanger. Water was pumped from the constant temperature bath through the heat exchanger. This aided in maintaining a constant temperature during the reaction.

The silane-solvent mixture entered the reactor at a side port near its base, and the water-solvent mixture entered the reactor through a needle. This needle is similar to a hypodermic needle and has three small holes at 120° from each other at its end. As the water-solvent mixture was forced through these holes, it mixed with silane-solvent mixture. This point is defined as the beginning of the reaction zone. Based on the stability of the infrared spectra, it was found that the holes in the hypodermic needle are small enough to insure good mixing in the reactor and prevent the development of streamline regions of high concentration, which flow through the reactor without mixing.

From the reactor, the reactants flowed into the infrared cell, Figure 3. Considerable turbulence occurred where the reactor makes a 60° turn when entering the infrared cell and again at a 90° turn where the reactants flowed up between the salt plates. It was necessary to place a gasket between the reactor and salt plates
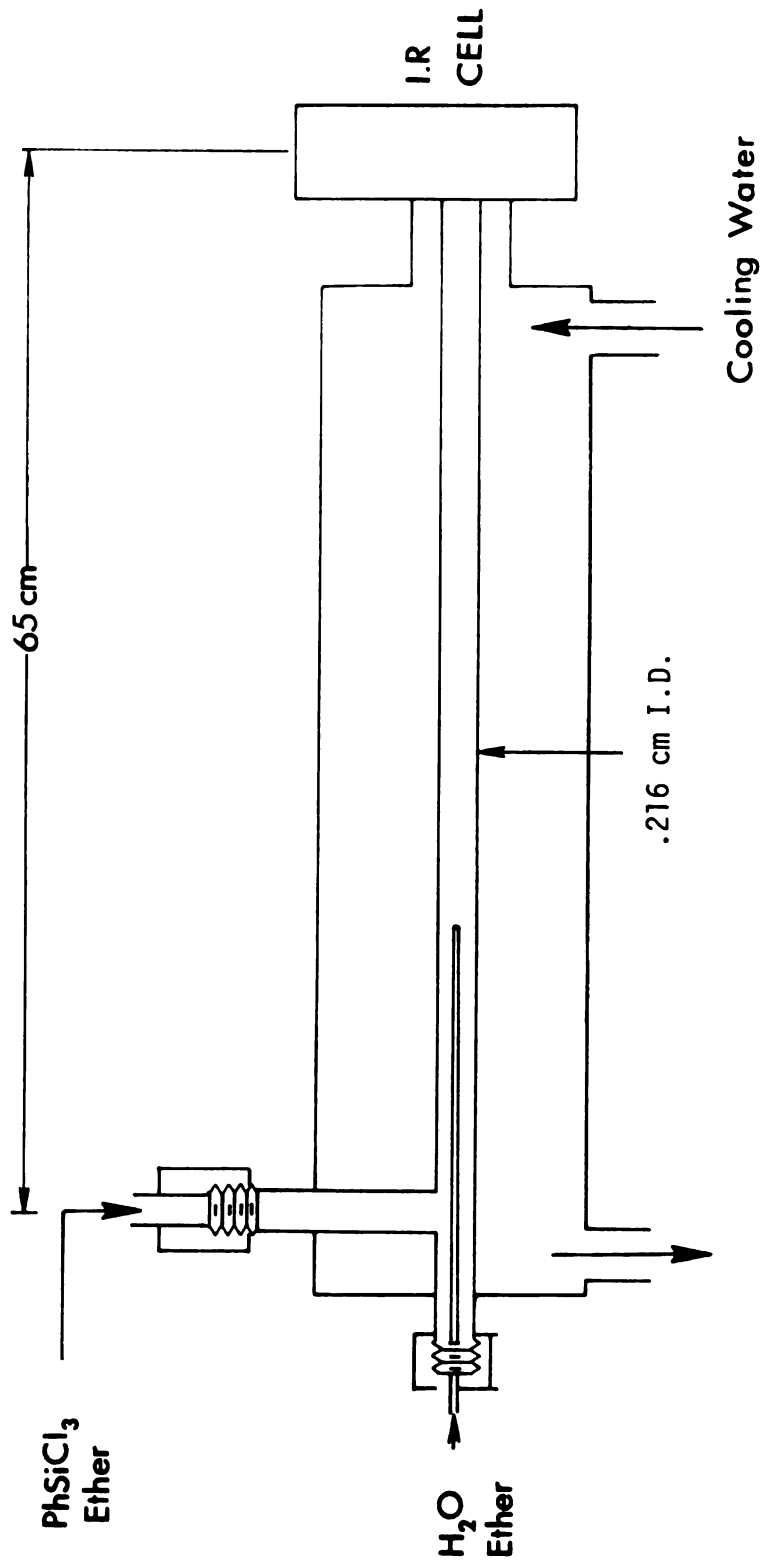
Figure 2.--Reactor and Surrounding Heat Exchanger.
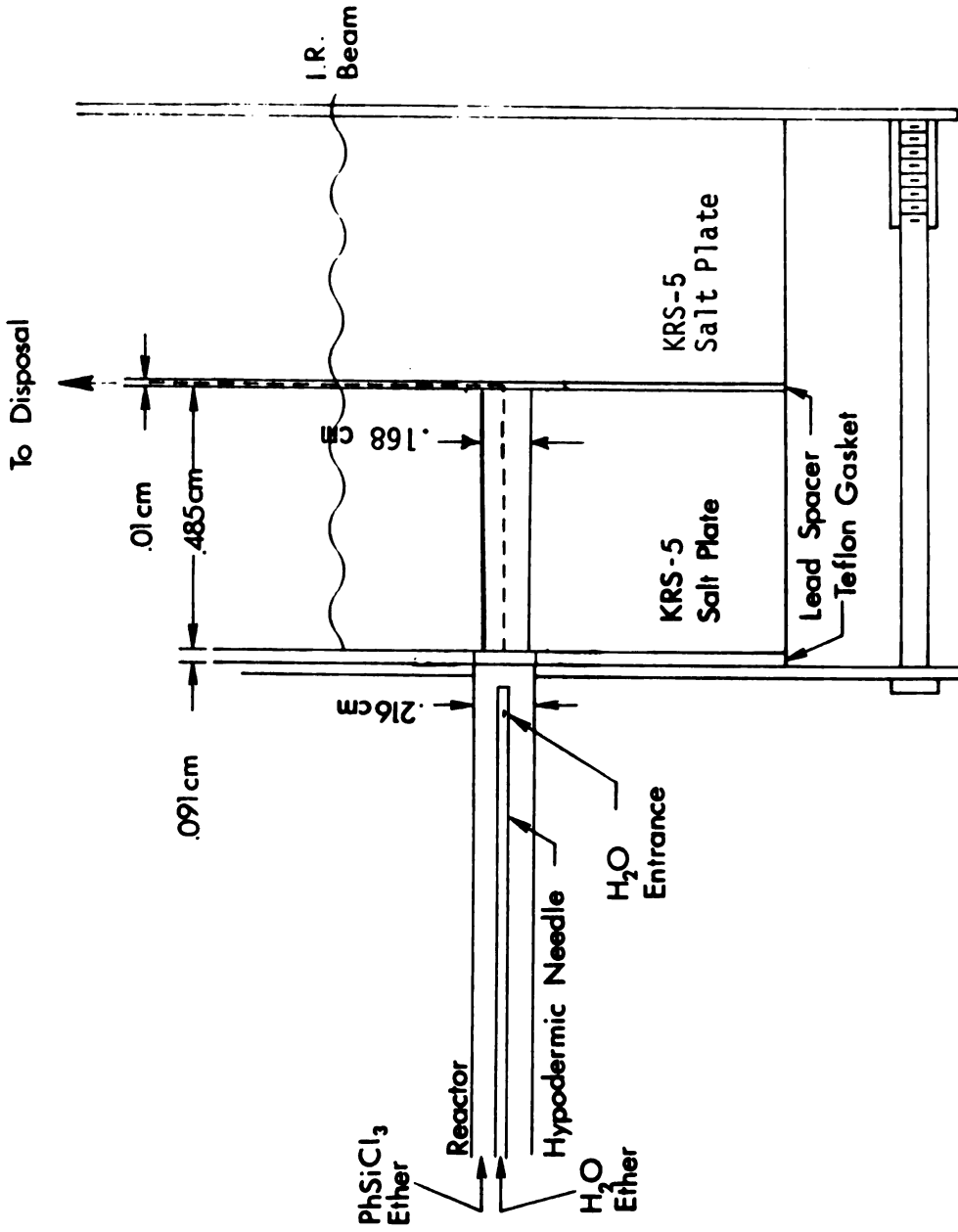
Figure 3.--Constant Flow Infrared Cell and Cell Holder.

to prevent any reactants from leaking at this junction. The salt plates were made of thallium bromide-iodine (KRS-5). These plates allowed observation of the low infrared region characteristic of the silane-chlorine vibrations (650 cm^{-1} to 400 cm^{-1}). The reactants entered the infrared cell at its base and left at the top. From here, they flowed into a container for disposal.

The spectrophotometer employed for this study was a dual beam, Perkin-Elmer 337 model. The dual beam arrangement compensated for the solvent absorption.

B. Temperature Control

The reactants were cooled to 0°C using a constant temperature bath containing distilled water and ice. To maintain temperatures above 0°C, an on-off type heater and cooling coil were employed. Tap water at approximately 16°C was constantly circulated through the coil. A centrifugal pump was employed to maintain constant circulation of water in the bath.

To maintain temperatures below 0°C, a methanol-water bath was employed. Here, methanol was added to the water to lower the freezing point to the desired temperature. Dry ice was then added to the mixture until a liquid-solid equilibrium occurred. Using this method it was possible to maintain the temperature to within 0.5°C of the desired temperature during each experiment.

C. Reagents

The solvent used in the majority of the experiments was 1,2-dimethoxyethane (Ansul Ether 121*). This solvent has the necessary characteristics of being a solvent for water, halosilanes, and silanols, and of not absorbing strongly in the lower infrared region. The ether was dried over $CaSO_4$ and distilled from KOH in a nitrogen atmosphere. Only the middle fraction of the distillate, that of a constant boiling point, was used. The distillation process removed inhibitors found in the ether.

A procedure was developed to recycle the ether after it had been used. The used ether was first titrated with aniline to remove the hydrogen chloride. It was then filtered to remove the aniline hydrochloride. Next it was distilled from KOH and then stored with $CaSO_4$, to further dry the ether. The ether was distilled a second time before use. An infrared spectrum of the ether showed that no silanes remained in the recycled ether.

Matheson gaseous HCl was used to prepare the HCl ether solutions for the runs requiring initial concentrations of HCl. The solutions were prepared by passing the gaseous HCl through the ether. The concentration of HCl was then determined by electrolytically titrating the HCl ether solutions with a standard solution of NaOH.

To prepare the silane solutions, the silane was distilled in a nitrogen atmosphere directly into the ether. This procedure avoided any reaction between the silane and atmospheric moisture.

---

*Ansul Company, Marinette, Wisconsin.

The silane solvent mixture was then weighed to calculate the concentration of silane.

D. Experimental Technique

Before each experiment, the experimental apparatus was flushed with acetone and then dried with nitrogen. By first evacuating the tank and then drawing the reagents in under this vacuum, it was possible to avoid any contact with atmospheric moisture.

At the beginning of each run, an initial spectrum of the silane was obtained before any water had been added to the system. This spectrum allowed the initial concentrations of the reactants to be calculated. During the runs, the flow rates of both the water-solvent and silane-solvent mixtures were monitored using rotameters. The initial concentrations of the reactants were corrected for the dilution due to the mixing of the streams.

To obtain concentration data versus residence time in the reactor, the hypodermic needle was pushed the maximum distance into the reactor and the spectrum (650 cm^{-1} to 400 cm^{-1}) scanned. The hypodermic needle was calibrated, by centimeters, such that its distance in the reactor could be read at the needle input to the reactor. Using the flow rates from the rotameters, the reactor area, and reaction zone, the residence time could be calculated. The needle was then moved out to a desired distance increasing the residence time and again the spectrum was recorded. Using this technique, a series of concentrations versus residence times was obtained.

CHAPTER III

THE HYDROLYSIS REACTIONS OF PHENYLTRICHLOROSILANE

The experimental techniques described in Chapter II were
used to study the hydrolysis reactions of phenyltrichlorosilane.
The object of this study was to obtain experimental data on the
hydrolysis reactions, model the reactions at 0°C, determine the
rate constants for this model, and determine the effects of hydro-
gen chloride on these reactions.

To obtain experimental data on these reactions, the posi-
tion of the hypodermic needle through which the water-solvent
mixture entered the reactor was varied. A steady state of con-
centration of reactants occurred along the length of the reactor.
Therefore, by varying the length of the reaction zone, the resi-
dence of the reaction was also varied.

The hydrolysis reactions of phenyltrichlorosilane were
studied in three parts. First, these reactions were studied at
0°C with varying concentrations of HCl. Here, the initial con-
centration of HCl was varied from 0.330 to 1.46 moles/liter.
The concentration of silanes present was varied for 0.073 to
0.095 moles/liter with enough water initially present (0.215 to
0.291 moles/liter) to ensure complete reaction. Next the hydroly-
sis reactions were studied with no HCl initially present at 0°C.

The amount of water initially present varied from 0.259 to 0.0807 moles/liter. At an initial water concentration of 0.259 moles/ liter, the chlorosilanes were completely converted to silanols. However, with an initial water concentration of 0.0807 moles/ liter, the reaction stopped with mainly unstable intermediates present. This allowed the reaction to be studied when complete hydrolysis did not occur. A total of five runs with approximately nine data points per run at times from 0.066 to 2.0 seconds were used to model the hydrolysis reactions of phenyltrichlorosilane in 1,2-dimethoxyethane.

To determine the effect of solvent on the rate of the hydrolysis reactions, two hydrolysis runs were made using acetonitrile as the solvent. Approximately 0.07 moles/liter of silane and an excess of water were used for these runs. Approximately 18 data points were obtained, which allowed the rate of these reactions in acetonitrile to be compared with the rate in 1,2-dimethoxyethane.

The data collected during the experiments consisted of the infrared absorption of several peaks versus residence time in the reactor. In order to utilize this data, it was necessary to assign these peaks to the various reactants, unstable intermediates and products of the hydrolysis reactions.

A. Interpretation of the Infrared Spectra
Obtained During the Hydrolysis Reactions
of Phenyltrichlorosilane

The assignments which were made for the absorption peaks

of $PhSiCl_3$ and its hydrolysis products are listed in Table 1.

TABLE 1.--Infrared Assignments for $PhSiCl_3$ and Its Hydrolysis
Products.

$PhSiCl_3$	590 cm^{-1} and 518 cm^{-1}
$PhSiCl_2(OH)$	572 cm^{-1} and 527 cm^{-1}
$PhSiCl(OH)_2$	542 cm^{-1}
$PhSi(OH)_3$	485 cm^{-1} and 465 cm^{-1}

The infrared spectra characteristics of $PhSiCl_3$, the hydroly-
sis reaction products of $PhSiCl_3$ and $(PhSiCl_2)_2O$ are shown in Figure
4. These spectra along with spectra of the hydrolysis experiments
were used to deduce the species present during the hydrolysis
experiments. Figure 5 shows the infrared spectrum of $PhSiCl_3$
obtained during the hydrolysis experiments. H. Kriegsmann and
K. H. Schowlka (8) conducted an extensive study of the various si-
lanes and assigned the 590 cm^{-1} peak of the $PhSiCl_3$ spectrum to the
asymmetric vibration of $SiCl_3$ and the 518 cm^{-1} peak to its symmet-
ric vibration. The 620 cm^{-1} peak was assigned to the Ph-Si vibra-
tion. Smith (9) also made these assignments for $PSiCl_3$ and noted
that the 590 cm^{-1} peak has a shoulder at approximately 583 cm^{-1}.

Preliminary hydrolysis experiments with no initial HCl

present and with excess water produced spectra similar to that of
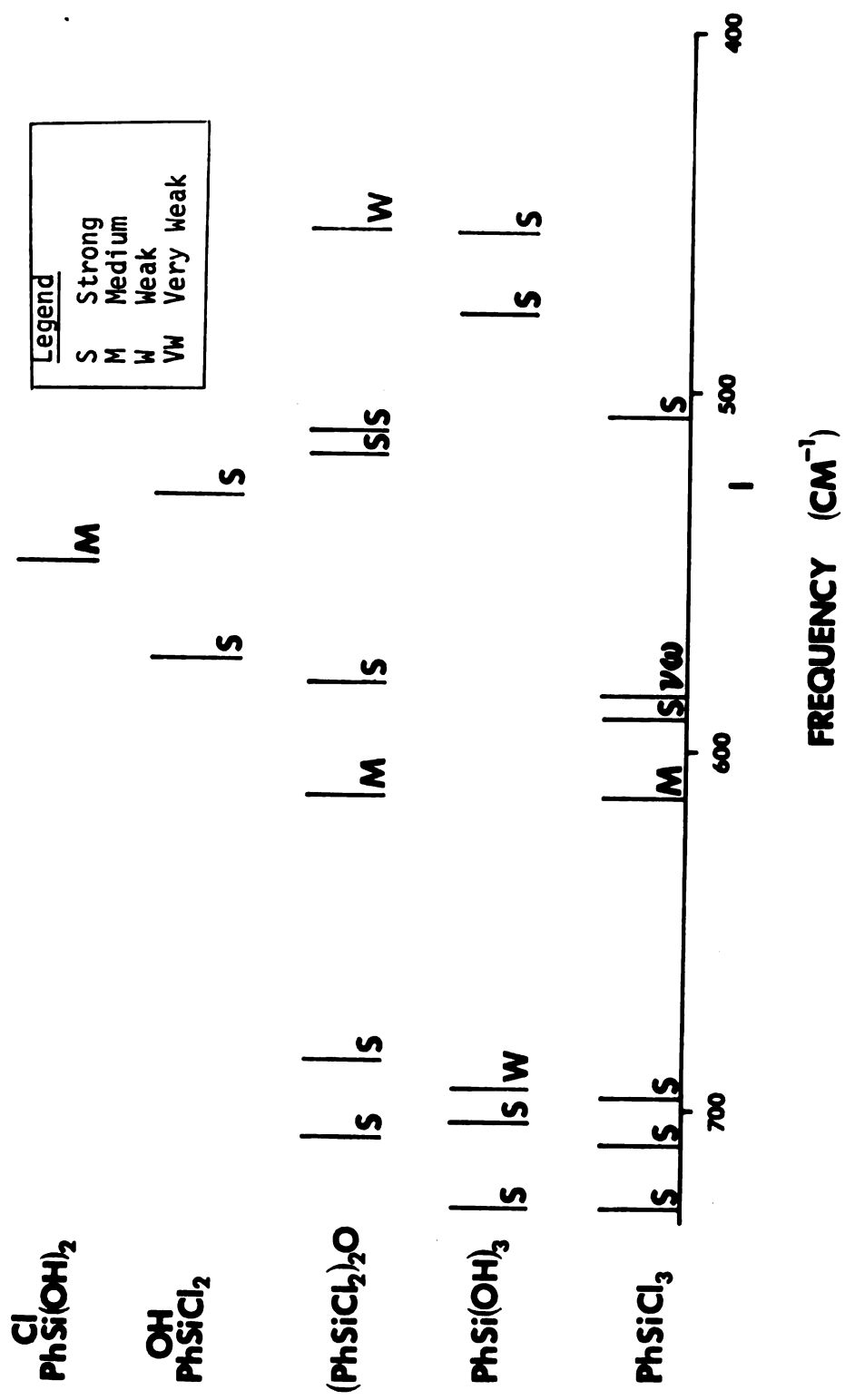
Figure 4.--Infrared Spectrum of PhSiCl$_3$, Hydrolysis Reaction Products and (PhSiCl$_2$)O.
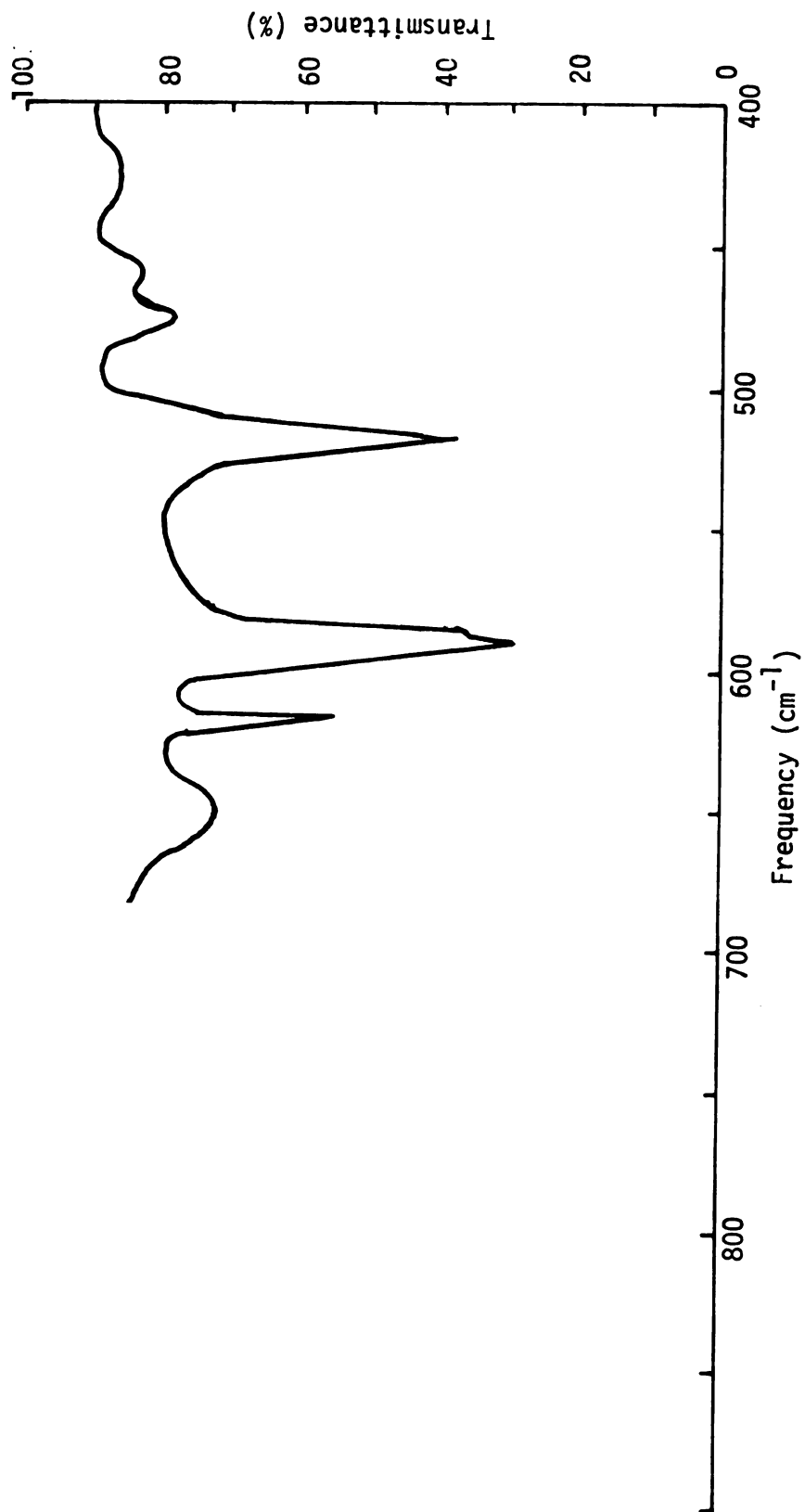
Figure 5.--Infrared Spectrum of PhSiCl$_3$.

PhSi(OH)$_3$ over the range of from 400 cm^{-1} to 740 cm^{-1} at long

reactor lengths. At shorter reactor lengths, intermediate bands

appeared at 572 cm^{-1}, 542 cm^{-1}, and 527 cm^{-1}. The 572 cm^{-1} and

527 cm^{-1} peaks appeared immediately after the water was added to

the system, were well correlated, and decreased as the reactor

length was increased. The 572 cm^{-1} and 527 cm^{-1} peaks were

present and similar in appearance during all runs. For Ph$_2$SiCl$_2$,

the symmetric and asymmetric peaks of =SiCl$_2$ occur at 540 cm^{-1} and

572 cm^{-1}, respectively. Therefore, the 572 cm^{-1} peak was assigned

to the asymmetric vibration of SiCl$_2$ in PhSiCl$_2$(OH) and the 527

cm^{-1} peak was assigned to the symmetric vibration. At all times

the 542 cm^{-1} peak was quite small and somewhat obscure due to the

absorption of a solvent peak at 547 cm^{-1}. Therefore, the quanti-

tative interpretation of the peak was difficult.

$$\begin{array}{ccc} Cl & & Cl \\ | & & | \\ Ph-Si-O-Si-Ph \\ | & & | \\ Cl & & Cl \end{array}$$

The absorption spectra characteristic of Ph-Si-O-Si-Ph
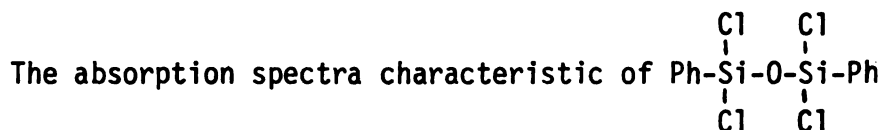
was not seen during the experiment. Also, a separate experiment

showed that the condensation reaction was considerably slower than

the hydrolysis reaction at low concentrations of HCl.

B. Preparation of PhSi(OH)$_3$

The infrared spectrum of phenylsilanetriol from 4000 cm^{-1}

to 650 cm^{-1} has been published (10). However, the spectrum

between 650 cm^{-1} and 400 cm^{-1} was not available in the literature.

Therefore, to confirm that phenylsilanetriol was the final product

from the hydrolysis reaction of phenyltrichlorosilane and to study

its condensation reaction, it was necessary to prepare phenyl-
silanetriol and obtain its spectrum.

Phenylsilanetriol has been prepared by several authors.
Takiguchi (11) prepared phenylsilanetriol by direct hydrolysis of
phenyltrichlorosilane using aniline as an hydrogen chloride
accepter. This procedure was somewhat complex and involved the
evaporation of a considerable amount of solvent.

Tyler (12) prepared phenylsilanetriol through the hydroly-
sis of phenyltrimethmoxysilane at 10°C using acetic acid as a
catalyst. On standing, condensation gradually occurred in some
of Tyler's samples, while others were kept for one year with no
signs of decomposition.

Phenylsilanetriol was prepared using a method similar to
that of Tyler's. In a three-neck, one-liter flask, 198 g (1.0
mole) of phenyltrimethmoxysilane were added to 108 g (6.0 moles)
of water. No acetic acid was added in order to minimize the amount
of condensation occurring. After constant agitation at 16°C for
four hours, shiny, white, flat crystals precipitated. After six
hours of constant agitation, the crystals were filtered and dried
overnight. The product weighed 75 g (0.49 moles), which gives
approximately a 50 percent yield. Figure 6 shows the spectrum
of phenylsilanetriol from 800 cm^{-1} to 400 cm^{-1}. The phenyl-
silanetriol spectrum has two peaks at 745 cm^{-1} and 705 cm^{-1} which
compare with those of the published spectrum plus peaks at 485
cm^{-1} and 465 cm^{-1}.
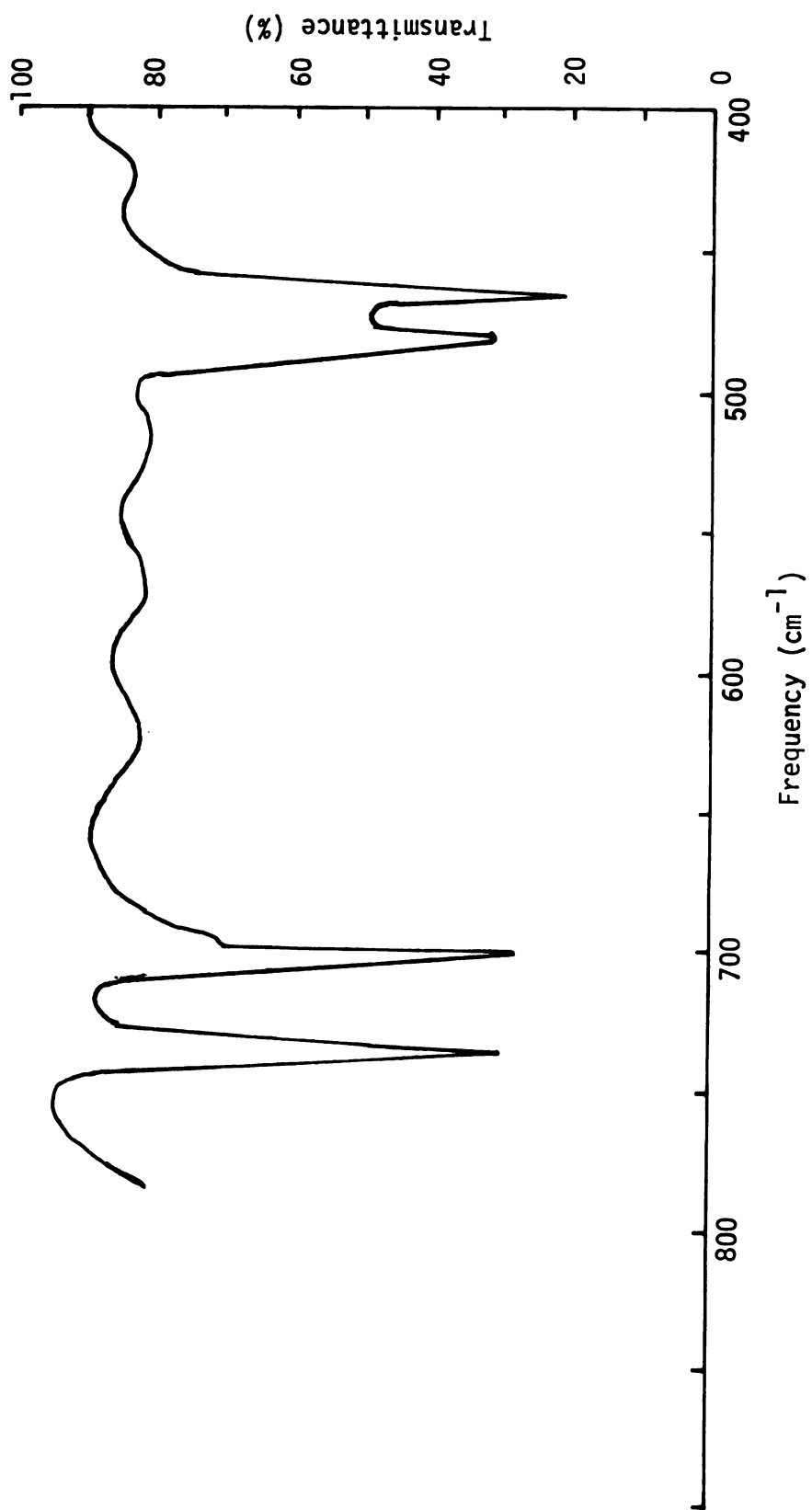
Figure 6.--Infrared Spectrum of $PhSi(OH)_3$.

C. Condensation Reactions

To determine the effect of the condensation reaction, the reaction between $PhSiCl_3$ and $PhSi(OH)_3$ was studied. Kleinhenz and Hawley (7) reported that no reaction occurred when $PhSiCl_3$ and $PhSi(OH)_3$ were mixed in the reactor at 0°C. Here a 14 weight percent mixture of $PhSi(OH)_3$ in ether and a 4.95 weight percent mixture of $PhSiCl_3$ in ether were mixed in the reactor. No significant changes in infrared absorption of either $PhSi(OH)_3$ or $PhSiCl_3$ were observed with changes in the reaction zone. This indicated that with no hydrogen chloride present the condensation reaction is very slow.

During the hydrolysis reaction, HCl is produced. It has also been observed that HCl catalyzes the hydrolysis reaction through the following mechanism (13):

First, the hydrogen ion joins the silanol oxygen.

$$(1) \quad H^+ + Si\text{-}OH \rightleftharpoons Si\text{-}OH_2^+$$
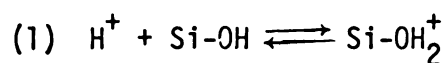
The second reaction consists of a nucleophilic attack by the oxygen on one silanol on the silicon of the silanol molecule in the oxonium form.

$$(2) \quad SiOH + Si\text{-}OH_2^+ \longrightarrow Si\text{-}O\text{-}Si + H^+ + H_2O$$
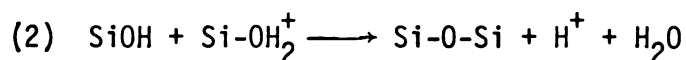
The first reaction is quite rapid, while the second occurs more slowly and is the rate controlling step.

To determine the effect of HCl on the condensation reaction, $PhSiCl_3$ and $PhSi(OH)_3$ were mixed in the reactor with an

initial HCl concentration of 0.390 moles/liter. The conditions
for this reaction are given in Table 2.

TABLE 2.--Conditions for Condensation Reaction of PhSi(OH)$_3$.

Temperature	0°C
Flow Rates	33.9 ml/min
Initial Concentrations	Moles/Liter
PhSi(OH)$_3$	0.073
PhSiCl$_3$	0.114
PhSiCl$_2$(OH)	0.056
PhSiCl(OH)$_2$	0.0
Total Silanes	0.243
HCl	0.390

In the hydrolysis reactions with no initial concentration
of HCl, the concentration of HCl reaches approximately 0.3 moles/
liter at the end of the reaction. At this time, the trichlorosilane
and dichlorosilane have reacted leaving principally phenylsilane-
triol, approximately 0.1 moles/liter. Hence, the conditions of
the condensation reaction study with HCl initially present were
considerably harsher than those encountered during the hydrolysis
experiments with no initial concentration of HCl.

A reaction was detected during this condensation study by
a decrease in the PhSiCl$_3$ and PhSi(OH)$_3$ and an increase in the
PhSiCl$_2$(OH) peak. Some of the possible reactions occurring here are:

31

(1)   Ph-Si-OH + Ph-Si-OH ⟶ Ph-Si-O-Si-Ph + H_2O

(2)   Ph-Si-OH + Ph-Si-Cl ⟶ Ph-Si-O-Si-Ph + HCl

(3) $PHSiCl_3$ + H_2O ⟶ $PhSiCl_2(OH)$ + HCl
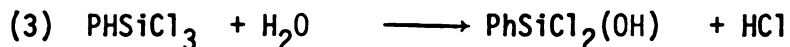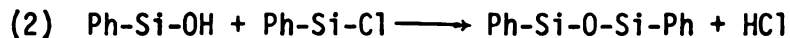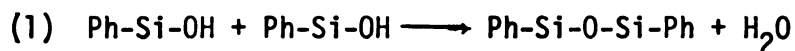
The decrease in the $PhSiCl_3$ concentration and increase in $PhSiCl_2(OH)$ may be explained by [1] reaction (1) followed by reactions (2) and (3), or [2] an unknown amount of H_2O in the $PhSi(OH)_3$ stream. The decrease in the $PhSi(OH)_3$ peaks can only be explained through a condensation reaction. Either reactions (1) or (2) are occurring, or both reactions are occurring simultaneously. Hence, the rate of the condensation reaction may best be determined through the decrease in $PhSi(OH)_3$. The concentrations of the various silanes versus residence times are given in Appendix A-7. Figure 7 is a plot of absorption of $PhSi(OH)_3$ versus time during the condensation reaction. The mean time on the figures refers to the residence time in the reactor. The half life, the time required for one-half of the initial concentration to react, of $PhSi(OH)_3$ is approximately 0.5 sec. In run 24 the half life of $PhSiCl_3$ is approximately 0.0015 sec. and that of $PhSiCl_2(OH)$ is 0.1 sec. Therefore, for the hydrolysis reactions with an initial HCl concentration greater than 1.0 moles/liter, the condensation effect can be seen at long reaction times where the amount of $PhSi(OH)_3$ present falls below that predicted by the model.
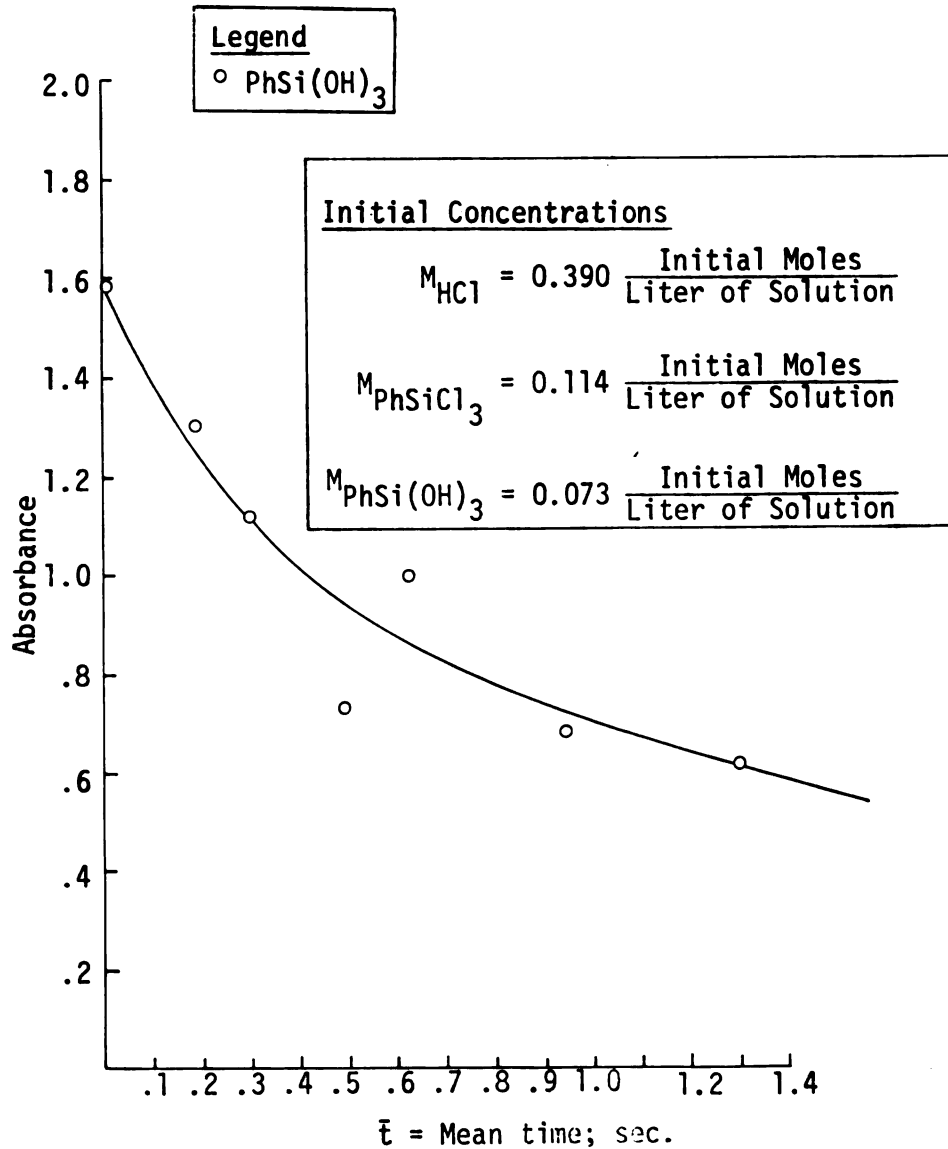
Figure 7.--Absorbance of PhSi(OH)$_3$ Versus Residence Time.

D. Calculation of Concentrations

Kleinhenz and Hawley (7) experimentally determined, using infrared spectrophotometry, that the difference of the absorption of $PhSiCl_3$, A, and the corresponding base-line absorption, A_0, was proportional to the product of the concentration, C, of $PhSiCl_3$ in the ether solution and the infrared cell path length, d (i.e., the Beer's law relationship is applicable). Figure 8 illustrates Beer's Law application to the 620 cm^{-1} and 517 cm^{-1} peaks of $PhSiCl_3$ for concentrations of $PhSiCl_3$ below 0.1 moles/liter.

$$A_0 - A = \varepsilon dC \qquad (3.1)$$

It was assumed that the same relations were valid for each reaction species being monitored. Here, ε is the extinction coefficient or proportionality constant.

The base-line technique was used to measure the absorption of each peak. The extinction coefficient, ε, for the 465 cm^{-1} peak of $PhSi(OH)_3$ was found by reacting $PhSiCl_3$ with an excess of water at long reaction times. The 518 cm^{-1} peak was used to determine the concentration of $PhSiCl_3$ and the 527 cm^{-1} peak was used for $PhSiCl_2(OH)$. The extinction coefficients for these peaks were determined using a least squares fit for absorption data obtained at different reaction times when reacting 1 mole of $PhSiCl_3$ with 1/2 mole of water. The extinction coefficients obtained are:

TABLE 3.--Extinction Coefficients for $PhSiCl_3$ and Its Hydrolysis Products.

ε_{517}	= 446	$(Mxcm)^{-1}$
ε_{527}	= 390	$(Mxcm)^{-1}$
ε_{465}	= 237	$(Mxcm)^{-1}$
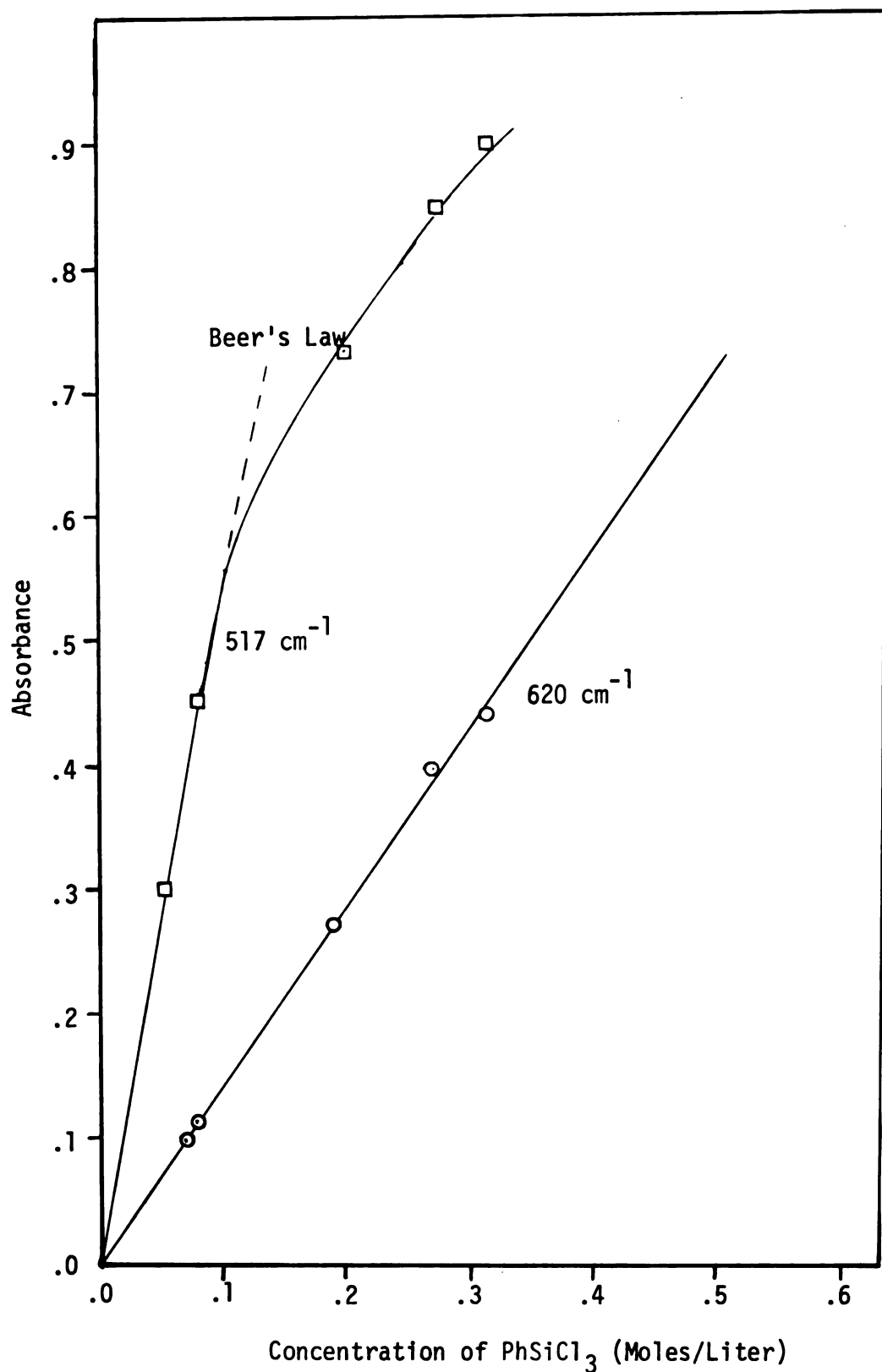
Figure 8.--Beer's Law Application: the 620 cm^{-1} and 517 cm^{-1} Bands of PhSiCl$_3$.

E. Conditions for the Hydrolysis
Reactions of PhSiCl$_3$

The reagents were prepared and drawn into the holding tanks as described earlier in Chapter II. The initial concentrations of the silanes were determined from the reference spectrum and are shown in Table A-1 along with the initial water and hydrogen chloride concentrations. Since a major object of this investigation was to study the HCl effect, the initial HCl concentration was varied from 0.0 to 1.46 moles per liter for different runs. During each run approximately 0.3 moles per liter of HCl were produced. The total silane present was varied from 0.072 to 0.095 moles per liter and the initial H$_2$O concentration from 0.0807 to 0.291 moles per liter for the various runs. At the higher water concentrations, complete hydrolysis of PhSiCl$_3$ occurred. This allowed the final hydrolysis products of PhSiCl$_3$ to be studied. At lower water concentrations, unstable intermediate products occurred and reached a steady state. This allowed the assignments for these products to be made.

Some of the spectra obtained during two different hydrolysis experiments, runs 21 and 24, are shown in Figures 9 and 10. These two experiments illustrate the hydrolysis reactions in media where no HCl is initially present and where a high concentration of HCl is initially present. Run 24 contained no initial concentration of HCl, while run 21 contained 1.46 moles per liter of HCl initially. At the end of run 24, the spectrum closely approximates that obtained for PhSi(OH)$_3$.

36
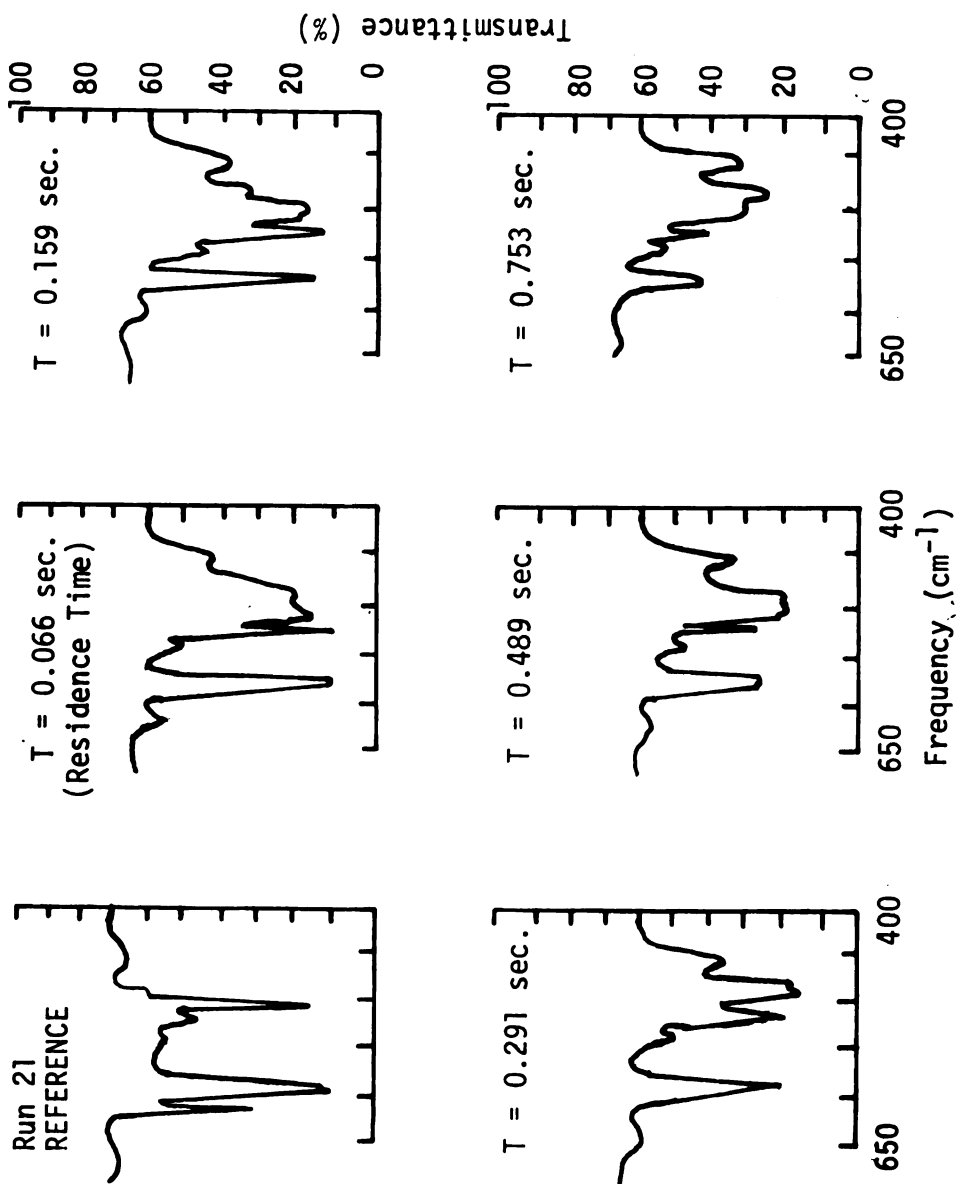
Figure 9.--Spectra Obtained During the Hydrolysis Reactions of PhSiCl$_3$, Run 21. [HCl]$_o$ = 1.46 Moles/Liter.
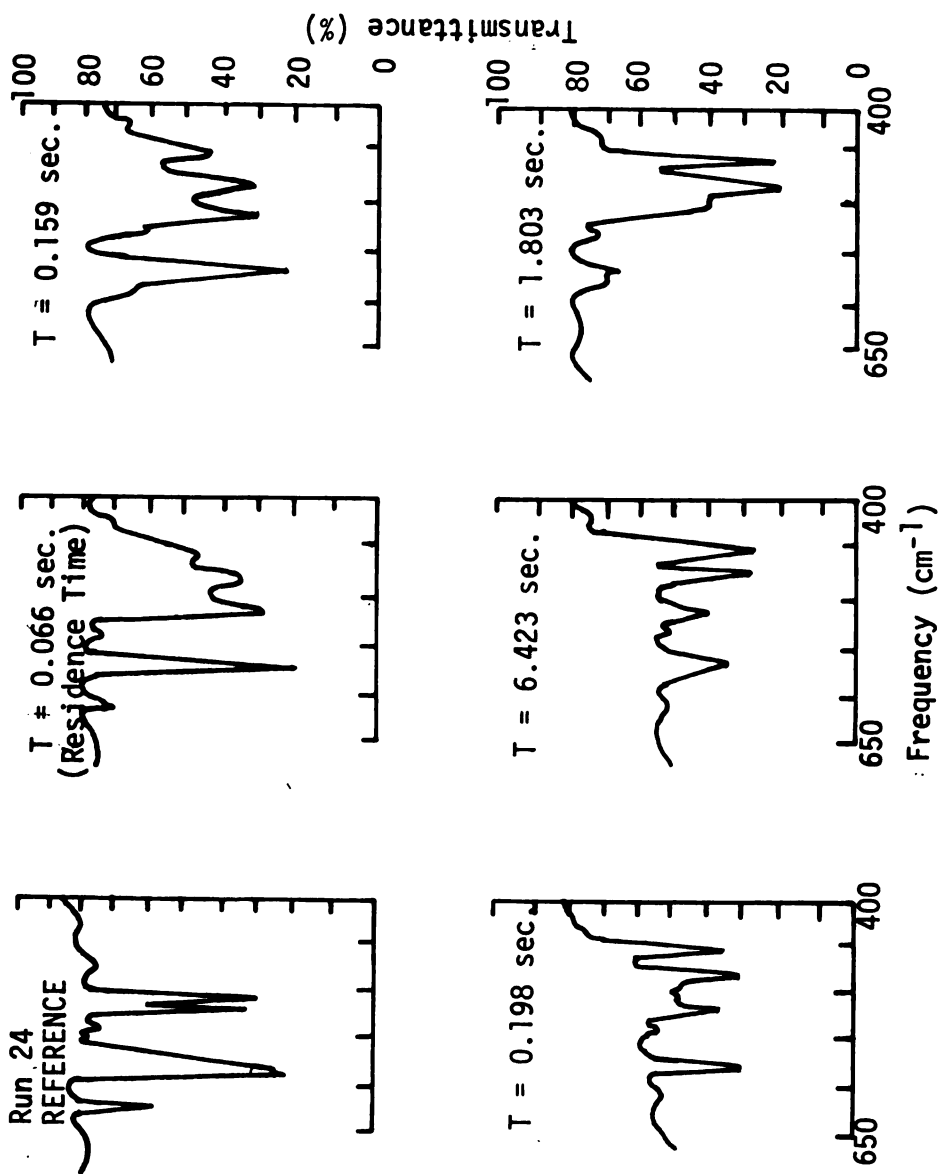
Figure 10.--Spectra Obtained During the Hydrolysis Reactions of PhSiCl$_3$, Run 24. [HCl]$_o$ = 0.0 Moles/Liter.

To determine the cell length, d, the empty sample cell transmittance was measured and a number of interference bands obtained. Smith (14) reported that the cell length, d, is related to these bands by:

$$d = n/\left(2(\mu_1 - \mu_2)\right) \qquad (3.2)$$

Here n is the number of maxima between the wave numbers μ_1 and μ_2.

Due to the high concentration of HCl, the rate of the hydrolysis reaction in run 21 is considerably slower than that of run 24. Also, the peaks at 485 cm^{-1} and 465 cm^{-1} are smaller and less distinct than those in run 24. Some condensation does take place in run 21 and this effect can be seen in Figure 12 (on page 42), where the amount of silanes present (points) falls below that predicted by the model (solid lines).

F. Results and Discussions

The following reaction steps were used to model the hydrolysis of $PhSiCl_3$.

(1) $PhSiCl_3$ + H_2O $\xrightarrow{K_1}$ $PhSiCl_2(OH)$ + HCl

(2) $PhSiCl_2(OH)$ + H_2O $\xrightarrow{K_2}$ $PhSiCl(OH)_2$ + HCl

(3) $PhSiCl(OH)_2$ + H_2O $\xrightarrow{K_3}$ $PhSi(OH)_3$ + HCl
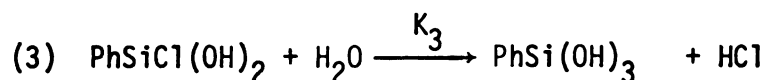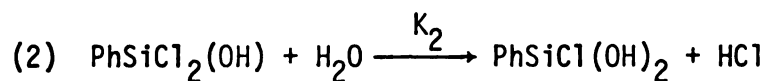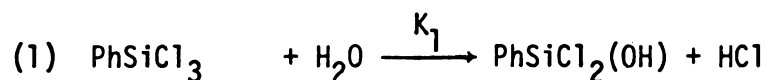
Under the conditions used in this study, these reactions were found to be essentially irreversible. It was assumed that the reactions were first order with respect to H_2O and the silanes. The effect of HCl was incorporated into the rate expressions using the term $[HCl]^n$. The rate expressions used to describe these reactions are:

$$\frac{d\ [PhSiCl_3]}{dt} = -K_1\ [PhSiCl_3]\ [H_2O]\ [HCl]^n \qquad (3.3)$$

$$\frac{d\ [PhSiCl_2(OH)]}{dt} = K_1\ [PhSiCl_3]\ [H_2O]\ [HCl]^n$$

$$- K_2\ [PhSiCl_2(OH)]\ [H_2O]\ [HCl]^n \qquad (3.4)$$

$$\frac{d\ [PhSiCl(OH)_2]}{dt} = K_2\ [PhSiCl_2(OH)]\ [H_2O]\ [HCl]^n$$

$$- K_3\ [PhSiCl(OH)]\ [H_2O]\ [HCl]^n \qquad (3.5)$$

$$\frac{d\ [PhSi(OH)_3]}{dt} = K_3\ [PhSiCl(OH)_2]\ [H_2O]\ [HCl]^n \qquad (3.6)$$

$$[H_2O] = [H_2O]_0 - [PhSiCl_2(OH)] - 2[PhSiCl(OH)_2]$$

$$- 3[PhSi(OH)_3] \qquad (3.7)$$

$$[HCl] = [HCl]_0 + [PhSiCl_2(OH)] + 2[PhSiCl(OH)_2]$$

$$+ 3\ [PhSi(OH)_3] \qquad (3.8)$$

Here, $[HCl]_0$ and $[H_2O]_0$ are the initial concentrations of HCl and H_2O, respectively.

Increasing the initial HCl concentration had the effect of decreasing the rate of the hydrolysis reaction. Using an unweighted squares type curve fitting program (14), the constants listed in Table 4 were determined to fit the various data sets. Figures 11 through 15 are plots of the data points and model (solid lines) versus mean residence time for the various runs. The solid lines through the data points represent twice the estimated standard deviation of the data.

The kinetic parameters were determined assuming that the reactor was isothermal and that plug flow existed in the reactor. The effect of the plug flow assumption has been studied by Klein-henz and Hawley (7) for reaction orders between 0 and 3. Their analysis employed an integration of the concentration-velocity product for each reaction over the flow cross-sectional area. They concluded that for first and second order reactions, the rate

TABLE 4.--Parameters Used to Model the Hydrolysis Reactions of PhSiCl$_3$.

Parameter	Linear Estimate of Standard Deviation
$K_1 = 220.$ (liters/mole)$^{1+n}$/sec.	121.
$K_2 = 16.5$ (liters/mole)$^{1+n}$/sec.	1.05
$K_3 = 40.6$ (liters/mole)$^{1+n}$/sec.	4.90
$n = -0.612$	0.0809

Legend
- ○ PhSiCl₂(OH)
- □ PhSi(OH)₃

Initial Concentrations
Run 20
$M_{Si} = .073$ Moles of Total Silane / Liters of Solution
$M_{H_2O} = .215$ Moles H₂O Added / of S
$M_{HCl} = 1.21$ Moles HCl Added / of S
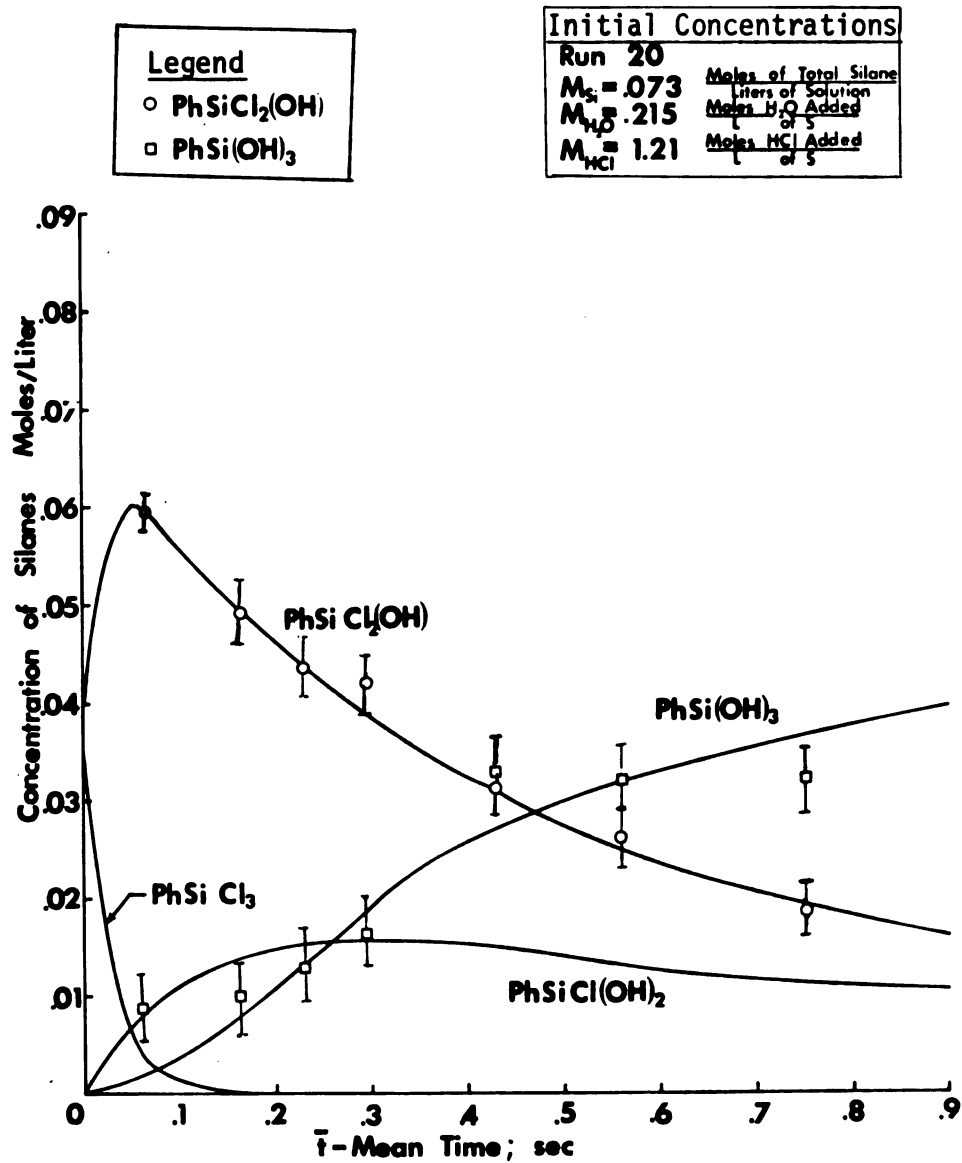
Figure 11.--Concentration of Silanes Versus Mean Reaction
Time for the Hydrolysis of PhSiCl₃, Run 20.
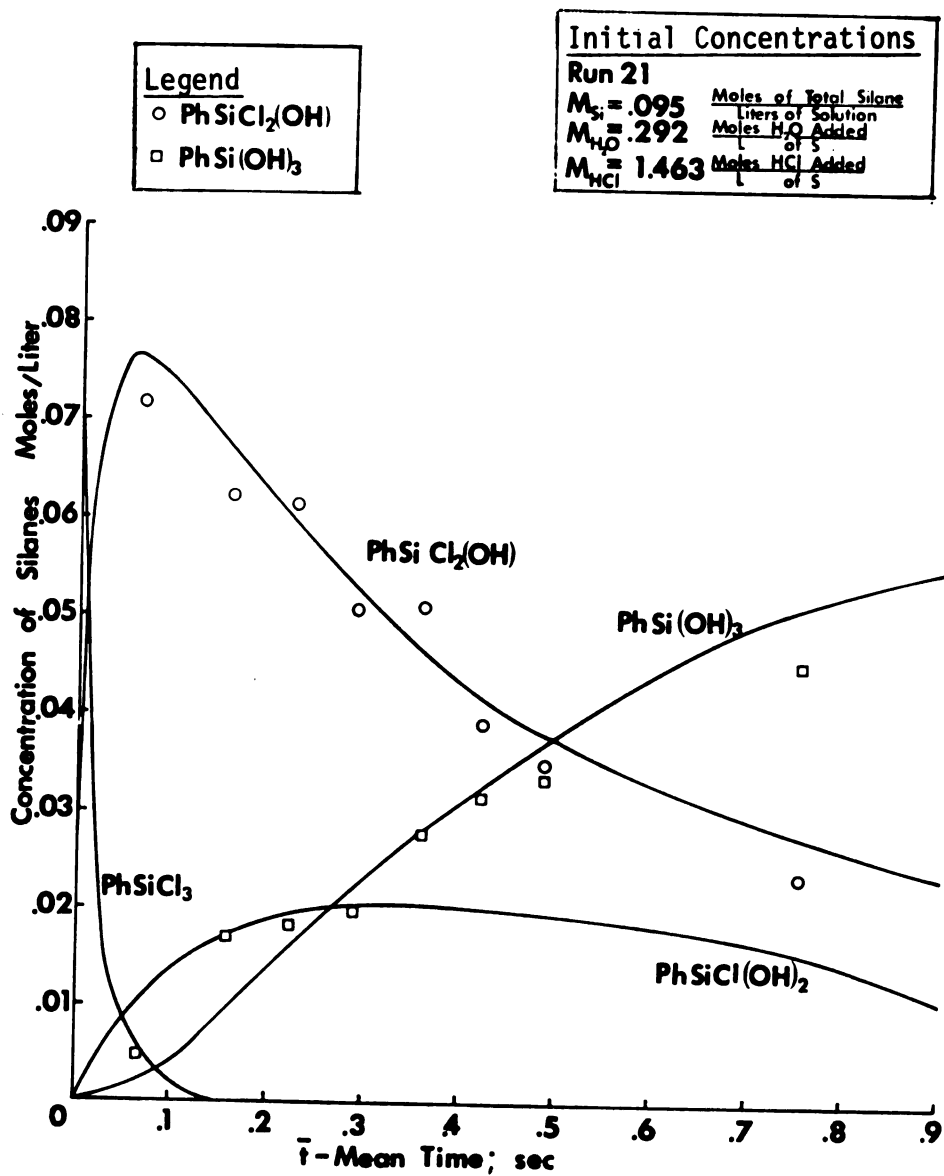
Figure 12.--Concentration of Silanes Versus Mean Reaction
Time for the Hydrolysis of PhSiCl$_3$, Run 21.

Legend

○ PhSiCl$_2$(OH)

□ PhSi(OH)$_3$

Initial Concentrations

Run 22

$M_{Si} = .0918$ Moles of Total Silane / Liters of Solution

$M_{H_2O} = .242$ Moles H$_2$O Added / of S

$M_{HCl} = .338$ Moles HCl Added / of S

Concentration of Silanes Moles/Liter

.09

.08

.07

.06 PhSiCl$_2$(OH)

.05

.04

PhSiCl$_3$

.03

.02 PhSi(OH)$_3$

.01 PhSiCl(OH)$_2$

0

0 .1 .2 .3 .4 .5 .6 .7 .8 .9

$\bar{t}$ – Mean Time; sec
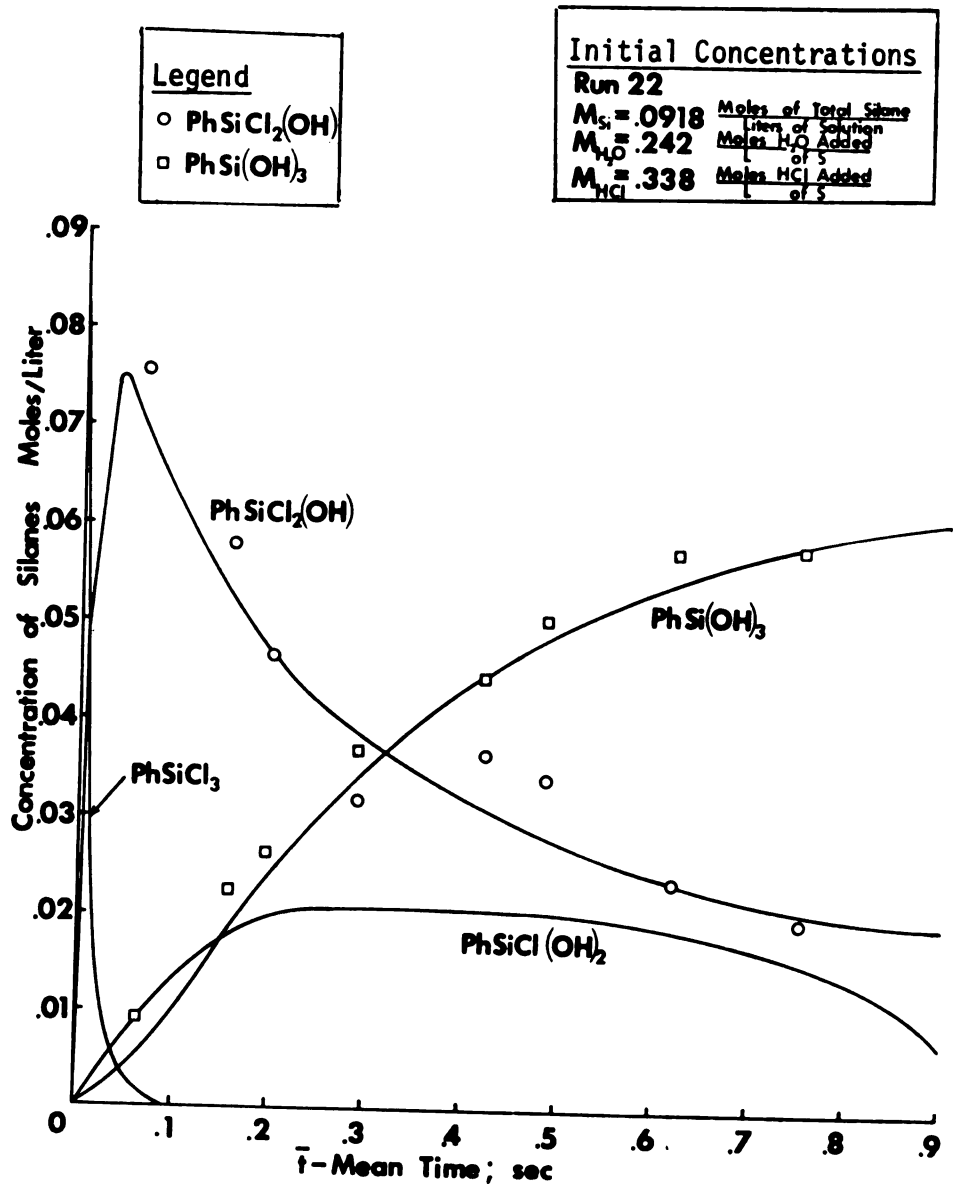
Figure 13.--Concentration of Silanes Versus Mean Reaction
Time for the Hydrolysis of PhSiCl$_3$, Run 22.

Legend
○ PhSiCl$_2$(OH)
□ PhSi(OH)$_3$

Initial Concentrations
Run 24
M_{Si} = .0776 $\frac{\text{Moles of Total Silane}}{\text{Liters of Solution}}$
M_{H_2O} = .313 $\frac{\text{Moles H}_2\text{O Added}}{\text{of S}}$
M_{HCl} = .000 $\frac{\text{Moles HCl Added}}{\text{of S}}$

Concentration of Silanes   Moles/Liter

PhSi(OH)$_3$

PhSiCl$_2$(OH)

PhSiCl(OH)$_2$
PhSiCl$_3$

$\bar{t}$-Mean Time; sec
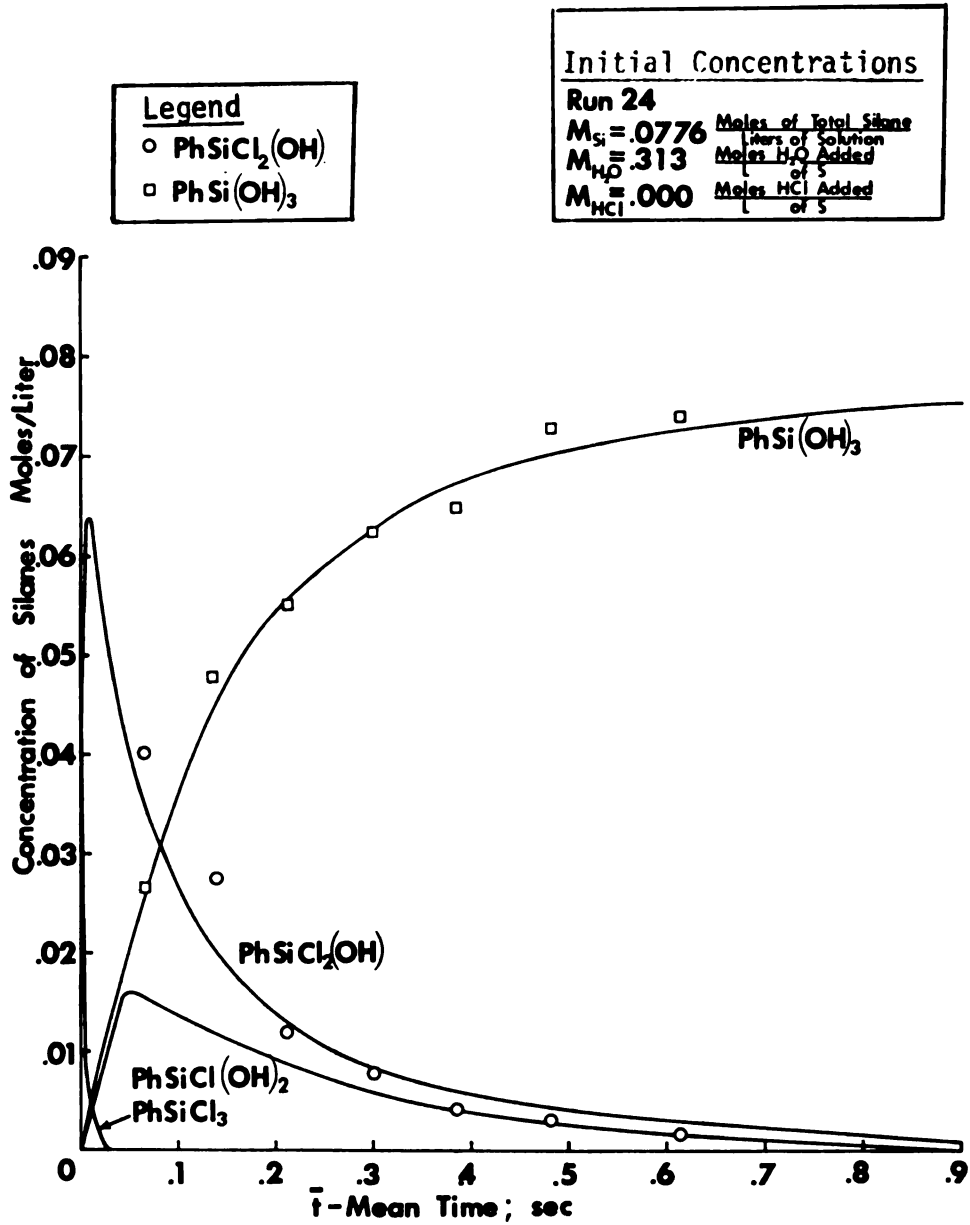
Figure 14.--Concentration of Silanes Versus Mean Reaction
Time for the Hydrolysis of PhSiCl$_3$, Run 24.
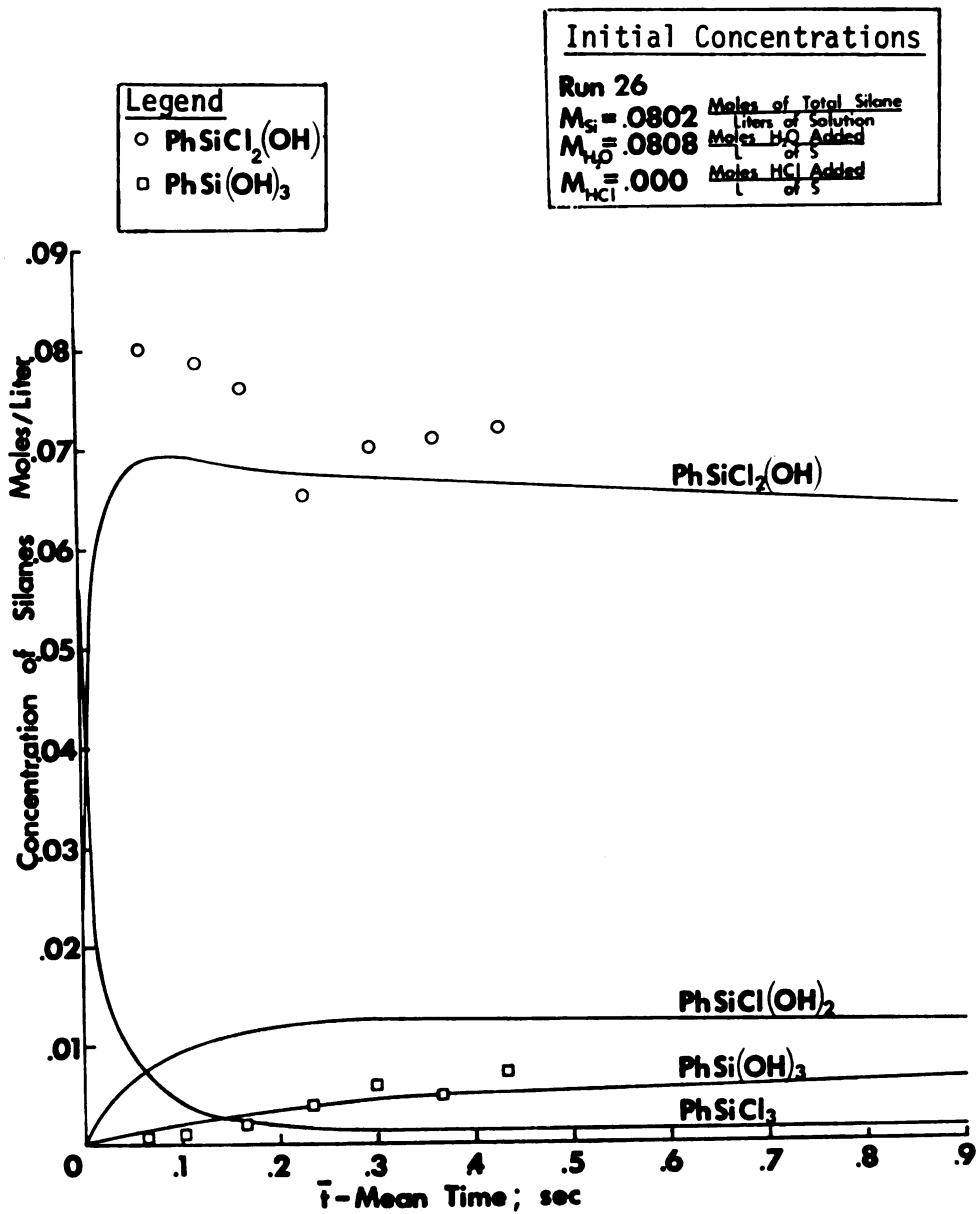
Figure 15.--Concentration of Silanes Versus Mean Reaction Time for the Hydrolysis of PhSiCl$_3$, Run 26.

constants determined assuming a plug flow reactor are approximately 16 percent lower than the actual rate constants in a laminar flow reactor. This produces a 16 percent bound between two extremes, that of laminar flow and that of plug flow.

Chapter V of this study analyzes both the plug flow and isothermal assumptions. These two assumptions tend to counteract each other. The plug flow assumption produces a lower rate constant, while the isothermal assumption produces a higher rate constant. For a second order reaction with thermodynamic and rate constants similar to those found in the hydrolysis reactions, the rate constants determined using both assumptions are approximately 10 percent lower than the rate constants in a laminar flow reactor with heat transfer.

In the actual system neither of the models completely describes the situation. Although the Reynold's number is well within the laminar flow region, there is considerable mixing in the reactor where the reactants are combined and again where the reactor effluent enters the infrared cell. Also, there is a certain amount of mixing in the system due to radial diffusion. Therefore, the kinetic parameters determined with the plug flow isothermal assumptions are within this 10 percent bound.

The rate of hydrolysis of the first chlorine atom in $PhSiCl_3$ is extremely fast and near the limit of the system to determine. Therefore, this first rate constant K_1 should only be considered an estimate of its actual value. The parameters

K_2, K_3 and n are well defined based on the fit of the data and the linear estimates of the standard deviations.

G. Solvent Effect

To determine the solvent effect on the hydrolysis reactions of $PhSiCl_3$, the reactions were studied in acetonitrile. Acetonitrile has the necessary characteristics of not absorbing in the 600-400 cm^{-1} region and of being a solvent for both water and the silane.

The physical constants of acetonitrile and 1,2-dimethoxyethane are shown in Table 5. The dipole moment of acetonitrile is 37.5 Debyes, while that of 1,2-dimethoxyethane is 7.2. The higher the dipole moment the greater the ionization ability of the solvent. For an S_n2-Si reaction mechanism, the rate controlling transition intermediate would be of the form:

$$^{\delta+}H_2O - \overset{\displaystyle \diagdown \diagup}{\underset{|}{Si}} - Cl^{\delta-}$$
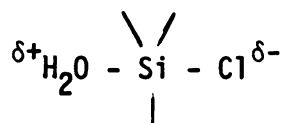
TABLE 5.--Physical Constants of Acetonitrile and 1,2-Dimethoxyethane.

	Acetonitrile	1,2-Dimethoxyethane
Molecular weight	41.053	90.123
Boiling point (°C)	81.6	93.0
Density at 20°C	0.78	0.8665
Refractive index	1.344	1.3796
Dipole moment (Debyes)	37.5 at 20°C	7.20 at 25°C

This transition state involves the separation of charges. Any solvent which stabilizes this intermediate would increase the reaction rate. Hence, if this mechanism is correct, the rate of reaction would be faster in acetonitrile than in 1,2-dimethoxy-ethane.

The infrared spectra of 1,2-dimethoxyethane and acetonitrile are shown in Figures 16 and 17, respectively. Acetonitrile has no absorption bands in the 400 to 600 cm^{-1} region. Some of the spectra obtained during run 17 are shown in Figure 18. The spectra are quite similar to those obtained using 1,2-dimethoxyethane as a solvent. The spectra obtained during the hydrolysis reaction at long reaction times are similar to those of $PhSi(OH)_3$.

Reagent grade acetonitrile was prepared by drying over calcium sulfate (Drierite) followed by distillation from phosphorous pentoxide. Only the middle fraction, approximately 80 percent, was used for the hydrolysis study. To prevent poly-merization of acetonitrile, the phosphorous pentoxide was limited from 5 to 10 grams per liter of solution. The amount of water remaining in the acetonitrile can be calculated from the initial spectrum of $PhSiCl_3$ by comparing the amount of $PhSiCl_3$ and $PhSiCl_2(OH)$ initially present. Using this method, the amount of water present was determined to be less than 0.5 moles per liter of solution.

Since the effect of hydrogen chloride was not studied in acetonitrile, the reactions were modeled as three irreversible S_n2-Si reactions in series.
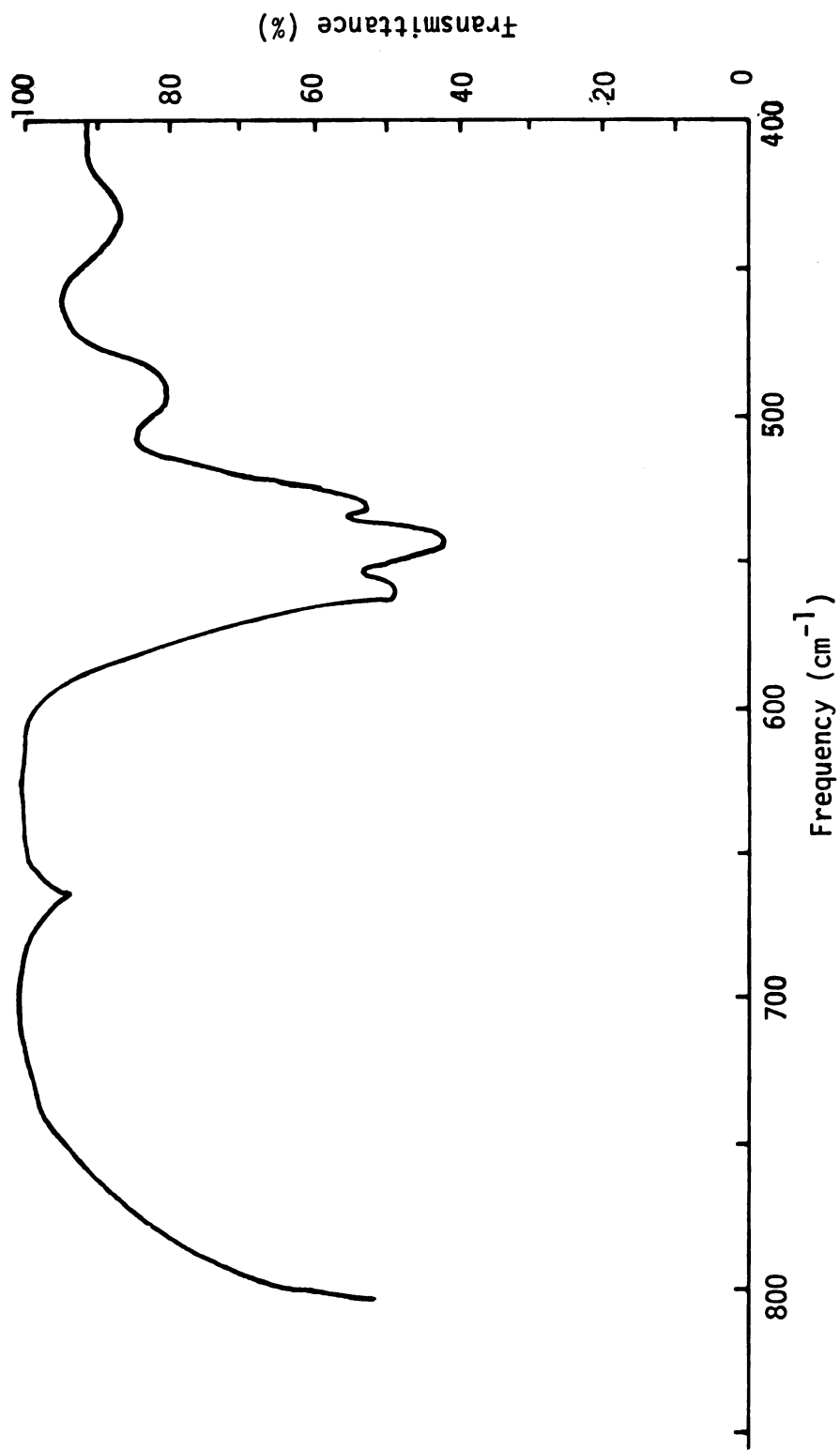
Figure 16.--Infrared Spectrum of 1,2-Dimethoxyethane.
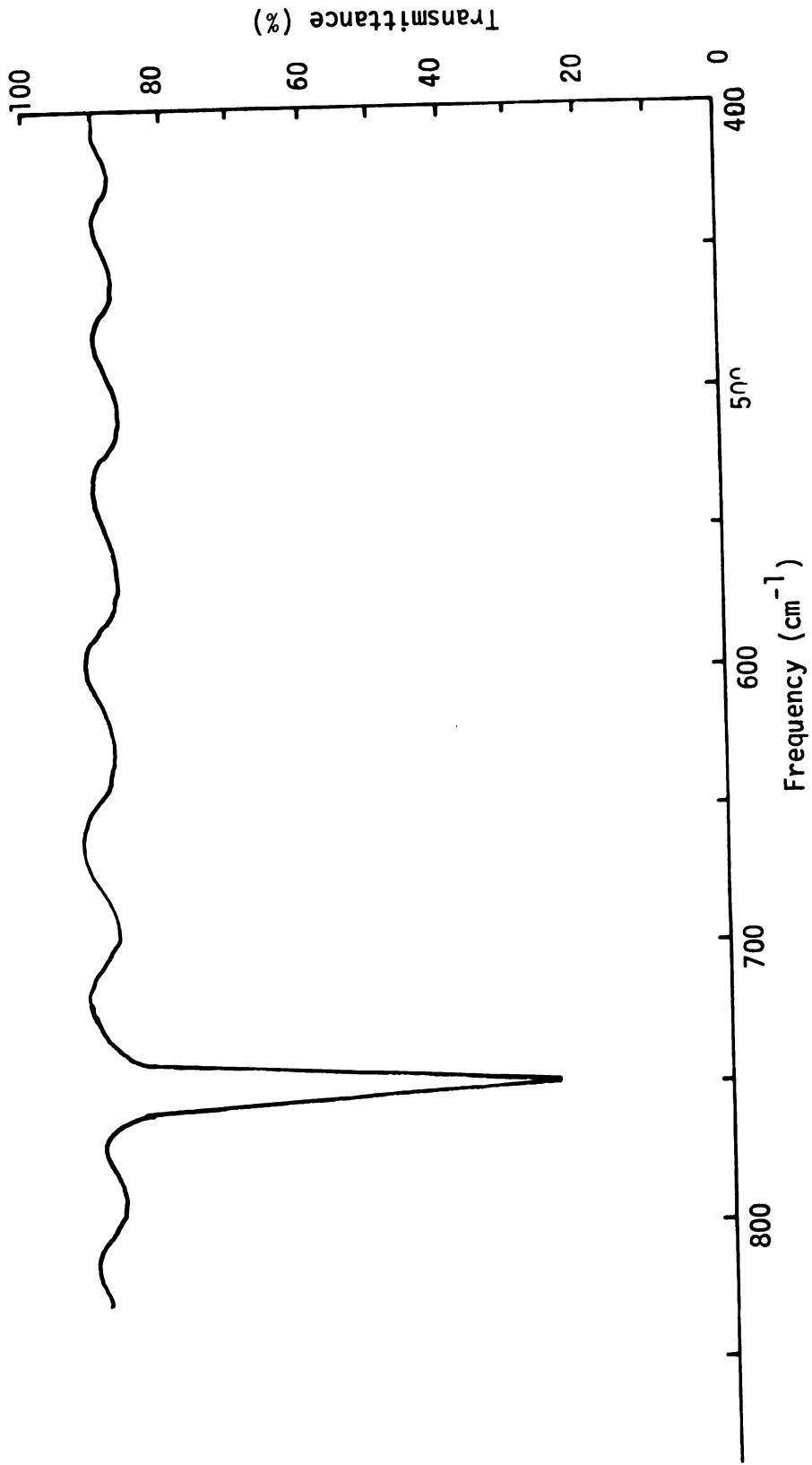
Figure 17.--Infrared Spectrum of Acetonitrile.
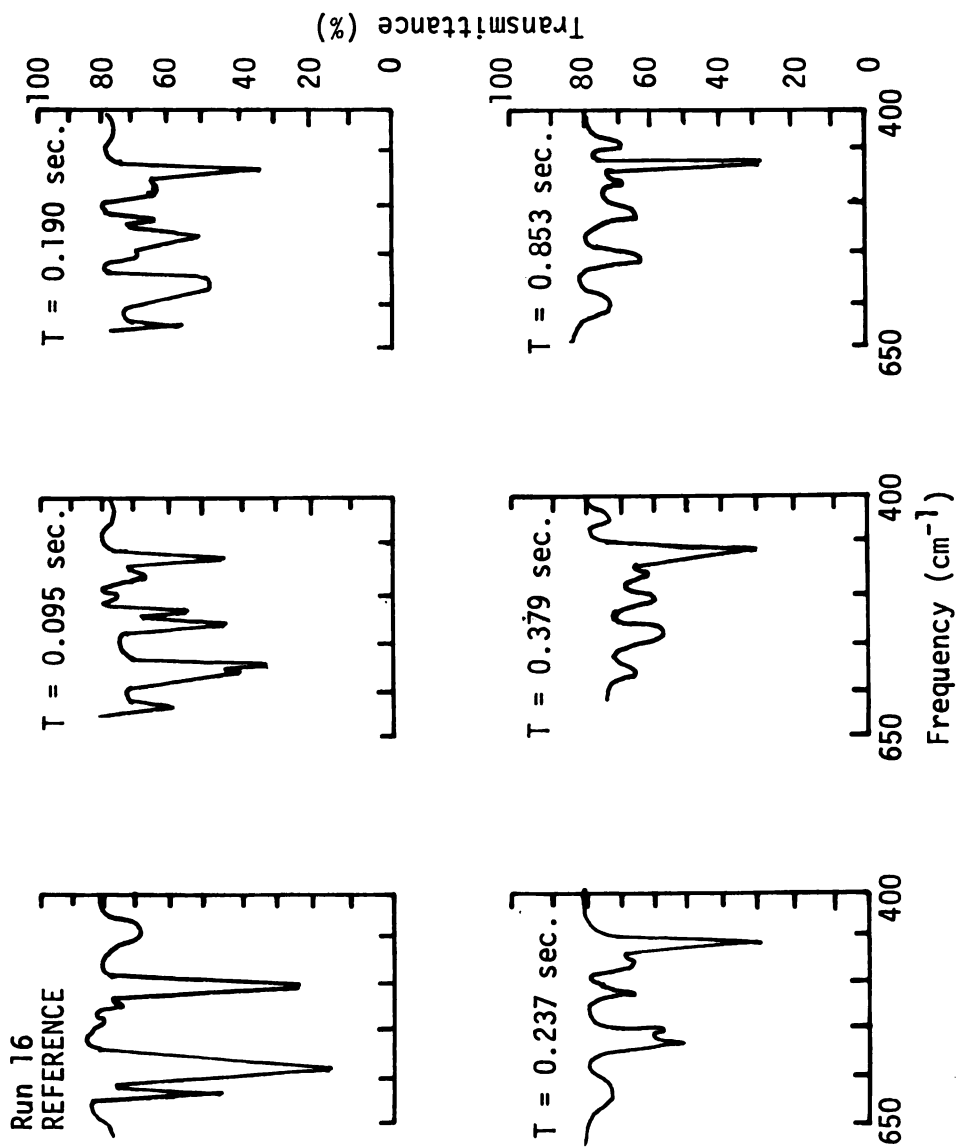
Figure 18.--Infrared Spectrum Obtained During the Hydrolysis of PhSiCl$_3$ in Acetonitrile.

(1) $PhSiCl_3$ + H_2O $\xrightarrow{K_1}$ $PhSiCl_2(OH)$ + HCl

(2) $PhSiCl_2(OH)$ + H_2O $\xrightarrow{K_2}$ $PhSiCl(OH)_2$ + HCl

(3) $PhSiCl(OH)_2$ + H_2O $\xrightarrow{K_3}$ $PhSi(OH)_3$ + HCl
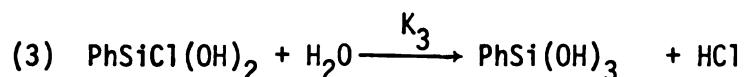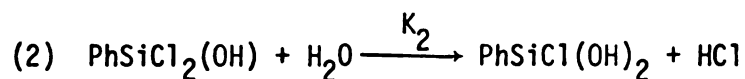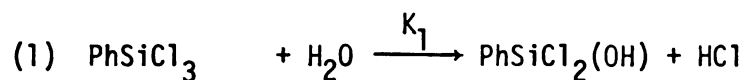
It was observed that the third reaction (3) was faster than the second and that a steady state approximation was applicable to $PhSiCl(OH)_2$. The rate expressions for these reactions may then be written as:

$$\frac{d\,[PhSiCl]_3}{dt} = -K_1\,[PhSiCl_3]\quad[H_2O] \qquad (3.9)$$

$$\frac{d\,[PhSiCl_2(OH)]}{dt} = K_1\,[PhSiCl_3]\quad[H_2O] -$$

$$-K_2[PhSiCl_2(OH)]\quad[H_2O] \qquad (3.10)$$

$$\frac{d\,[PhSiCl(OH)]_2}{dt} = K_2\,[PhSiCl_2(OH)]\quad[H_2O]$$

$$- K_3\,[PhSiCl(OH)_2]\quad[H_2O] \qquad (3.11)$$

$$\frac{d\,[PhSi(OH)_3]}{dt} = K_3\,[PhSiCl(OH)_2]\quad[H_2O] \qquad (3.12)$$

Assuming a steady state on $PhSiCl(OH)_2$.

$$K_2 \ [PhSiCl_2(OH)] \quad [H_2O] - K_3 \ [PhSiCl(OH)_2] \quad [H_2O] = 0 \qquad (3.13)$$

$$[PhSiCl(OH)_2] = \frac{K_2}{K_3} \ [PhSiCl_2(OH)]$$

Equation 3.12 may now be written as:

$$\frac{d \ [PhSi(OH)_3]}{dt} = K_2 \ [PhSiCl_2(OH)] \ [H_2O] \qquad (3.14)$$

Using this steady state approximation, the hydrolysis series reactions for $PhSiCl_3$ can be written with two rate constants K_1 and K_2.

The following reasoning was used to estimate the extinction coefficients of the reactants in acetonitrile. The intensity of an absorption band in solvents of refractive indexes n_1 and n_2 has been expressed by Brown (16) as:

$$\frac{A_2}{A_1} = \frac{n_1}{n_2} \left[\frac{1 + C - C/n_2^2}{1 + C - C/n_1^2} \right]^2 \qquad (3.15)$$

Here, A is the absorption in the two solvents, and C is a constant which depends on the geometry of the solute molecule. The refractive index of acetonitrile is 1.34 and that of 1,2-dimethoxyethane is 1.38. Since these refractive indexes are essentially the same, one would expect the same band intensity in both solvents. Not enough data was obtained in acetonitrile to calculate all band intensities used in the hydrolysis study of $PhSiCl_3$. However, the 465 cm^{-1} band for $PhSi(OH)_3$ was determined to be 255 liters/mole-centimeter. This compares with 237 for the same band in

1,2-dimethoxyethane. Therefore, the extinction for acetonitrile were assumed to be the same as those for 1,2-dimethyoxyethane.

To determine the rate constants K_1 and K_2, a least squares program was employed. The values and linear estimate of standard deviation are shown in Table 6. Due to the fast rate of reaction, the first rate constant K_1 is near the limit of the system to determine. This is evident from the large value of the linear estimate of standard deviation. Therefore, K_1 should only be considered an estimate of its actual value.

Figures 19 and 20 show the concentrations of the silanes versus the residence time for runs 17 and 18. The initial conditions for these experiments are given in Table A-3 in Appendix A.

The significance of this study of the reactions in acetonitrile is the marked increase in the rate of reaction rather than a model for the system in acetonitrile. This increase in rate is especially evident from the value of K_2. Kleinhenz and Hawley (7) determined a value of 77.5 liters/mole-second for this rate constant in 1,2-dimethoxyethane using a similar irreversible S_n2-Si mechanism. This compares with a value of 122 liters/

TABLE 6.--Parameters Used to Describe the Hydrolysis Reactions of $PhSiCl_3$ in Acetonitrile.

Rate Constant	Linear Estimate of Standard Deviation
K_1 = 180. liter/mole-sec.	147.
K_2 = 122. liter/mole-sec.	37.9
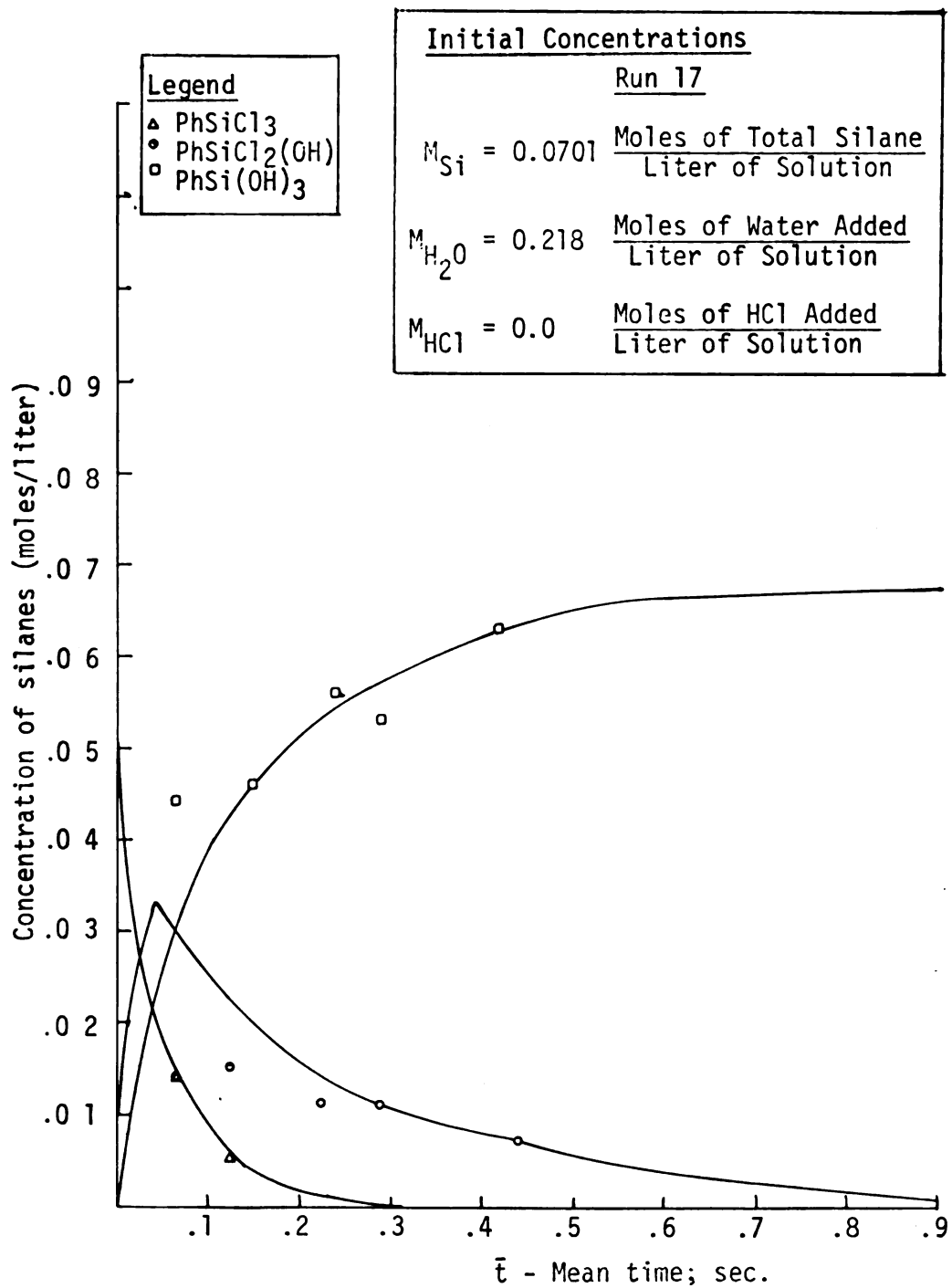
Figure 19.--Concentration of Silanes Versus Mean Reaction Time
for the Hydrolysis of $PhSiCl_3$, Run 17.
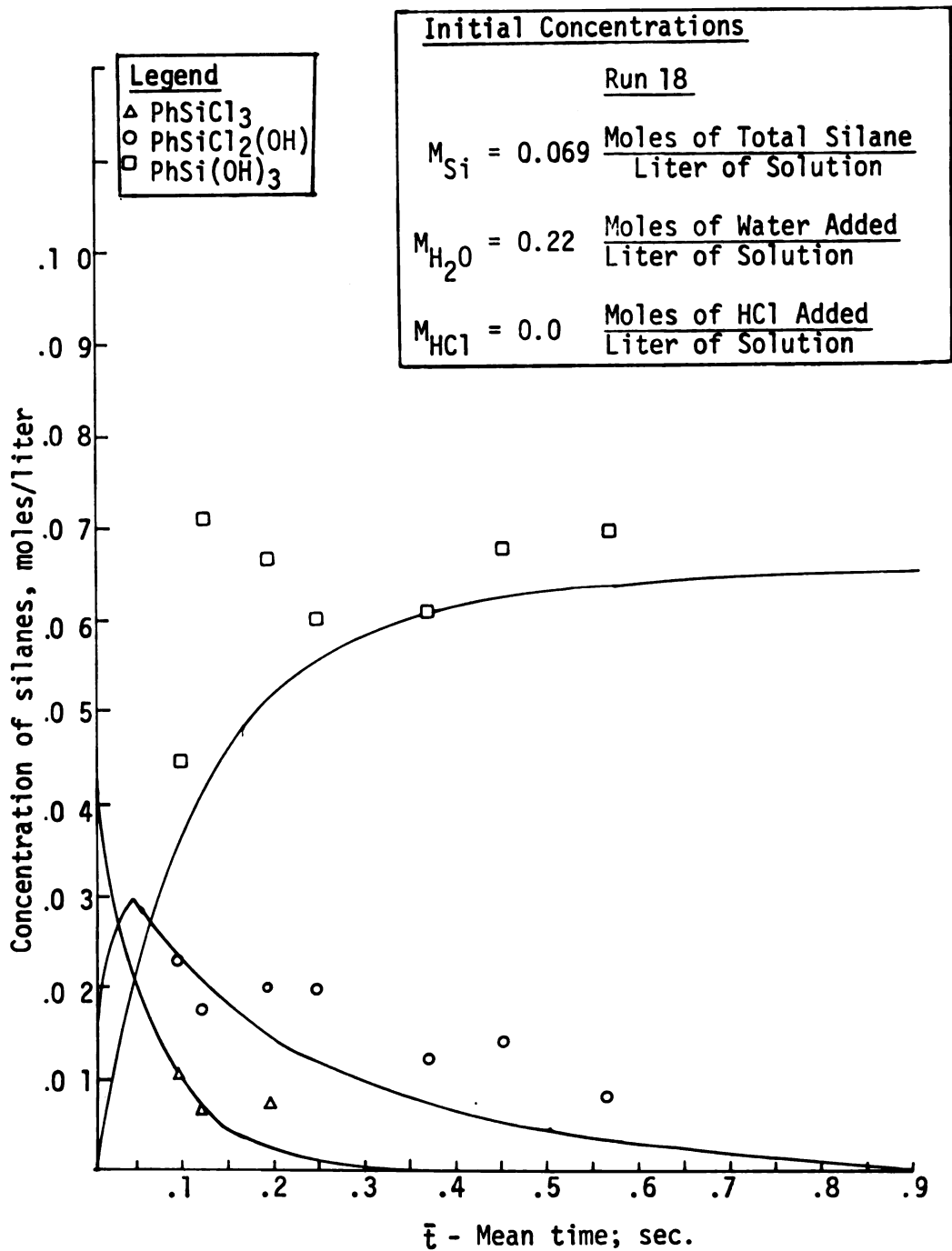
Figure 20.--Concentration of Silanes Versus Mean Reaction Time for the Hydrolysis of PhSiCl$_3$, Run 18.

mole-second for K_2 in acetonitrile. This increase in rate can be accounted for by the higher dipole moment of acetonitrile compared with 1,2-dimethoxyethane. This increase in dipole moment enables the solvent to better stabilize the transition state intermediate.

H. Concluding Remarks

It was found that the hydrolysis of the first chlorine atom of $PhSiCl_3$ is much faster than that of the remaining two. This is similar to the observation of Shaffer and Flanigen (6), that the first hydrolysis reaction in a series is faster than the following hydrolysis reactions. The second and third hydrolysis reactions were much closer in their rates. However, the hydrolysis of the third chlorine was slightly faster than that of the second. Hence, a small amount of $PhSiCl(OH)_2$ was present during the reaction.

A major observation was the effect of HCl, which decreased the rate of hydrolysis. This observation was supported by the study of Shaffer and Flanigen (6), who observed the decrease in the rate of hydrolysis of $PhSiCl_3$ by saturing 1,2-dimethoxyethane solution with HCl. The effect of HCl was incorporated into the kinetic equations in the form of $[HCl]^n$ and the value of n determined using a least squares fit.

The effect of HCl can be accounted for by considering the equilibrium of H^+, Cl^- in the solvent with water.

$$H^+ + Cl^- + H_2O \rightleftharpoons H_3O^+ + Cl^-$$
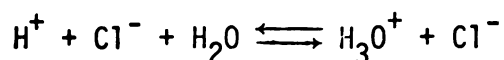
The hydronium ion H_3O^+ should be considerably less reactive than water. As the amount of HCl increases, more water becomes tied up as hydronium ion. Therefore, an increase in the HCl concentration would suppress the hydrolysis reaction.

However, the effect of HCl is complicated by changes in the medium with changes in the amount of HCl present. The chloride ion has the ability to stabilize the transition state intermediate and increase the rate of reaction. However, for the hydrolysis of $PhSiCl_3$ with a relatively small amount of water present, the prominent effect of HCl is to decrease the rate of reaction through formation of the hydronium ion.

HCl is also known to catalyze the condensation reaction. During the residence times used for these studies, no indication of condensation was observed in the experiments where there was no initial concentration of HCl. However, in the experiments with an initial HCl concentration the condensation effect can be seen at long residence times where the amount of silanes present falls below that predicted by the model. Therefore, the dual effect of HCl of suppressing hydrolysis and catalyzing condensation causes condensation to occur before hydrolysis is complete at high HCl concentrations. In a saturated solution, it might be reasonable

$$
\begin{array}{ccc}
& Cl & Cl \\
& | & | \\
\text{to expect such groups as } Ph-Si-O-Si-Ph, \text{ which were indicated by} \\
& | & | \\
& Cl & Cl
\end{array}
$$

Shaffer and Flanigan's (6) study, to exist. Hence HCl has a major role in determining the products obtained during the hydrolysis of halosilanes.

The hydrolysis reactions of $PhSiCl_3$ were modeled assuming that they were first order with respect to both water and silane. Such a model is consistent with the S_n2-Si mechanism that has been proposed to describe these reactions (1: p. 93). These studies were conducted in a polar solvent. In a nonpolar or slightly polar solvent, the rate of reaction with respect to water or silane should be greater than one. The addition of water or silane to a slightly polar solvent would increase the ability of the medium to stabilize the transition state intermediate. Hence, the rate of reaction with respect to water or silane would be greater than one.

CHAPTER IV

THE HYDROLYSIS REACTIONS OF DIMETHYLDICHLOROSILANE

The hydrolysis reactions of dimethyldichlorosilane were studied using the experimental techniques discussed in Chapter II. The objects of this study were to obtain experimental data on these reactions, model these reactions, determine the rate constants for this model, investigate the effects of hydrogen chloride on these reactions and determine the temperature effect. The data was collected by varying the length of the laminar flow reactor. Since a steady state occurred in the reactor, it was possible to study the concentrations at one residence time. By varying the length of the reactor, data on concentrations versus residence time were obtained.

The hydrolysis reactions of Me_2SiCl_2 were studied in three parts. First, these reactions were studied with initial concentrations of 0.57 and 0.48 moles/liter of HCl and silane concentrations of approximately 0.1 moles/liter at 0°C. Since at most 0.2 moles/liter of HCl are formed during these reactions, more HCl is initially present in these runs than is formed during the hydrolysis reactions. Approximately ten data points at times from 0.064 to 3.62 seconds were obtained during each of these runs.

Next, three runs at 0°C with no initial concentration of HCl were made. The concentration of silane varied from 0.10 to

0.12 moles/liter with excess water initially present. Again ten data points were obtained during each run at times ranging from 0.18 to 2.13 seconds.

To determine the effect of temperature on these reactions, the reactions were also studied at 267.5 and 252.0°K. Using the data from these runs, the runs at 273.0°K, and measurements on the equilibrium shift with temperature, the activation energies of the various reactions were determined.

The data obtained consisted of a series of absorption peaks versus residence time. In order to utilize this data, it was necessary to assign these peaks to the various reactants, unstable intermediates, and products of the hydrolysis reactions of Me_2SiCl_2.

A. Interpretation of Infrared Spectra Obtained During the Hydrolysis Reactions of Dimethyldichlorosilane

The following spectra assignments were made for the absorption bands of Me_2SiCl_2 and its hydrolysis products:

TABLE 7.--Infrared Assignments for Me_2SiCl_2 and Its Hydrolysis Products.

Me_2SiCl_2	532 cm^{-1} and 470 cm^{-1}
$Me_2SiCl(OH)$	572 cm^{-1} and 542 cm^{-1}
$Me_2Si(OH)_2$	510 cm^{-1}

The infrared spectrum of Me_2SiCl_2 is shown in Figure [21].
This spectrum was obtained using a 0.1 M solution of dimethyl-
dichlorosilane in 1,2-dimethoxyethane. The asymmetric and symmetric
vibrations of $SiCl_2$ occurred at 532 cm^{-1} and 470 cm^{-1}, respectively.
Smith [17] published an infrared spectrum of gaseous Me_2SiCl_2 with
the asymmetric and symmetric vibrations of $SiCl_2$ occurring at
553 cm^{-1} and 473 cm^{-1}, respectively. The shift in frequencies of
these vibrations may be accounted for by the difference between the
gaseous and liquid states (18: p. 41). Similar differences were
noted by Smith [17] for $SiCl_4$.

After water was added to the system, the bands at 532 cm^{-1}
and 470 cm^{-1} gradually decreased and new peaks appeared at 542 cm^{-1}
and 572 cm^{-1}. The 572 cm^{-1} peak was assigned to the Si-O vibration
and the 542 cm^{-1} peak to the Si-Cl vibration in $Me_2SiCl(OH)$. Since
$Me_2SiCl(OH)$ is an unstable hydrolysis intermediate, its infrared
spectrum has not been published. However, the 542 cm^{-1} assignment
for Si-Cl falls in the range (465 cm^{-1} to 560 cm^{-1}) given by Smith
[9] for the Si-Cl vibrations.

As the residence time was increased, the peaks at 572 cm^{-1}
and 542 cm^{-1} gradually decreased and a new peak appeared at 510
cm^{-1}. This peak was assigned to the Si-O vibration in $Si(OH)_2$.
No published infrared spectrum for $Me_2Si(OH)_2$ includes the infrared
region below 900 cm^{-1}. The reason for this lack of information on
the spectrum of $Me_2Si(OH)_2$ is the highly unstable nature of
$Me_2Si(OH)_2$. Since several authors have reported preparing $Me_2Si(OH)_2$
using a variety of techniques, $Me_2Si(OH)_2$ does not appear to be
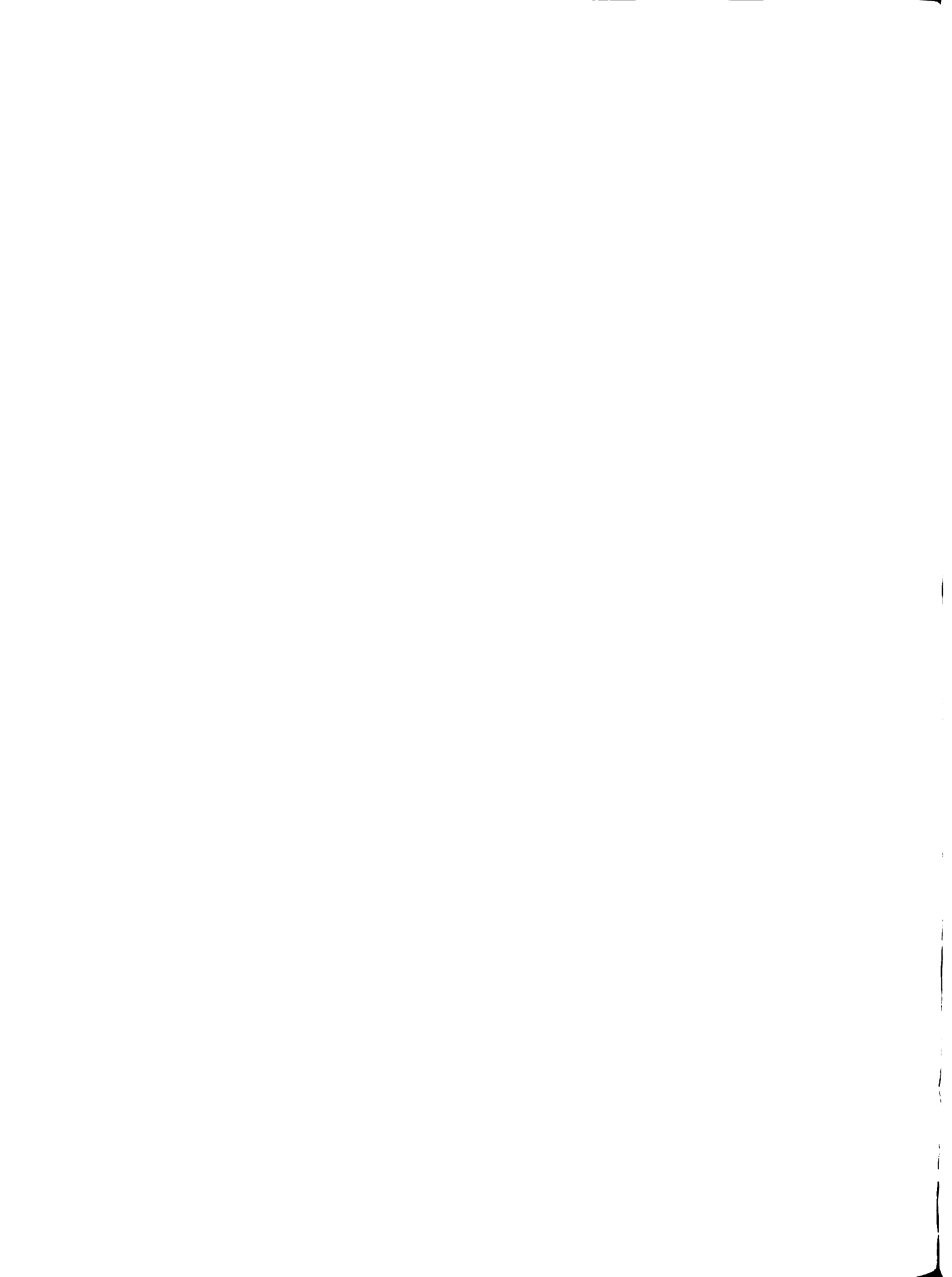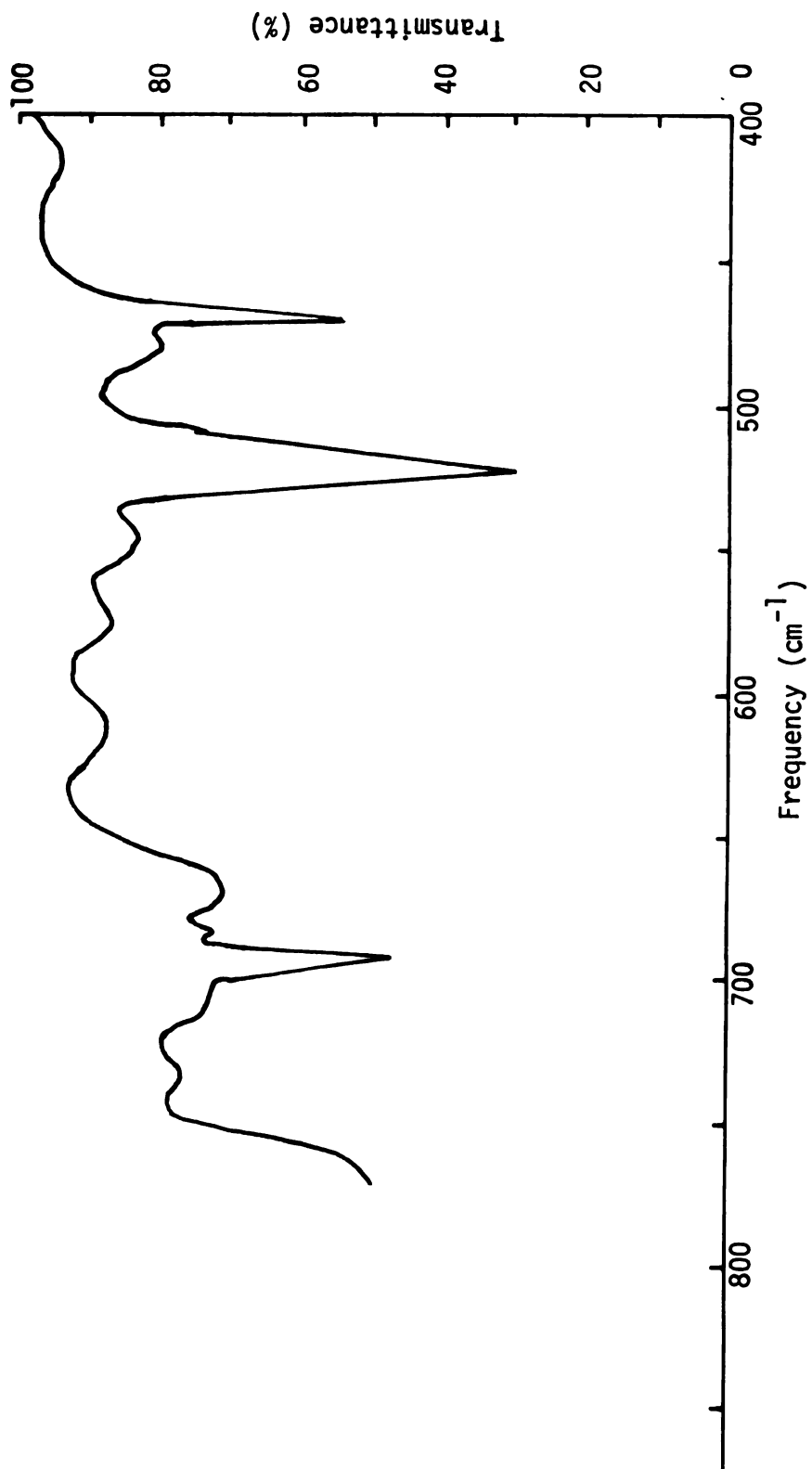
Figure 21.--Infrared Spectrum of Me_2SiCl_2.

significantly less stable than other silandiols. However, the condensation of $Me_2Si(OH)_2$ is base catalyzed to such an extent that the hydroxyl groups in glass cause condensation to occur. To avoid this problem, most researchers recommend the use of quartz materials in the preparation of this compound.

To confirm the assignment of the 510 cm^{-1} to $Me_2Si(OH)_2$, the silandiol was prepared using a technique similar to that of Takiguchi (11). Takiguchi prepared $Me_2Si(OH)_2$ in an ether solution using aniline as a hydrogen chloride acceptor.

To prepare $Me_2Si(OH)_2$, 0.164 moles of Me_2SiCl_2 were slowly added to a cooled 1,2-dimethoxyethane solution (0°C) containing 0.33 moles of aniline and 0.33 moles of water. Infrared spectrum of samples taken while adding Me_2SiCl_2 showed an infrared peak at approximately 510 cm^{-1}. This peak increased in strength as additional Me_2SiCl_2 was added to the solution. However, condensation was a problem and due to heating of the cell, may have occurred while scanning the infrared spectrum.

Figure 22 shows the bands of Me_2SiCl_2, its hydrolysis

and common condensation products, such as
$$\begin{array}{ccc} Me & & Me \\ | & & | \\ HO-Si-O-Si-OH. \\ | & & | \\ Me & & Me \end{array}$$
It is

interesting to note that the spectra of the condensation products do not correspond to any of the spectra obtained during the hydrolysis experiments. This supports the conclusion that little condensation occurs during the hydrolysis experiments.
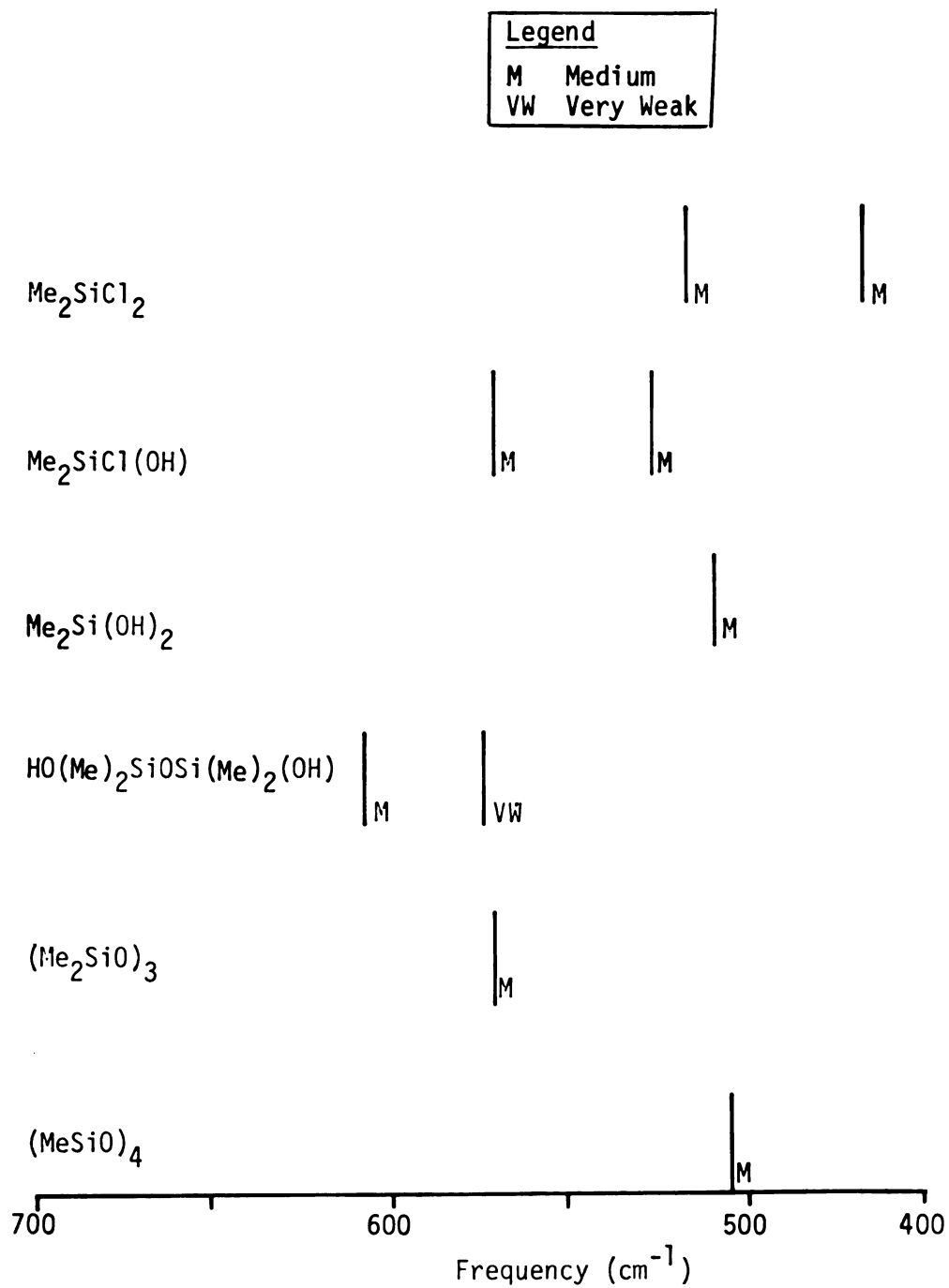
Figure 22.--Infrared Spectrum of Me$_2$SiCl$_2$, Its Hydrolysis and Common Condensation Products.

B. Condensation Reaction

The condensation reaction of $Me_2Si(OH)_2$ has been studied by Chrzczonowicz and Chojnowski (13). The reaction was found to involve S_n2 substitution and to be acid catalyzed. The rate expression used to describe this reaction is:

$$\frac{-d\ [SiOH]}{dt} = K_{III}\ [HCl]\ [SiOH]^2 \tag{4.1}$$

The reaction is first order with respect to hydrogen chloride and second order with respect to the silandiol. At 25°C and using dioxane as a solvent, K_{III} was determined to be 0.33 moles^{-2} liter^2 sec.$^{-1}$. At the concentrations of HCl present during the hydrolysis study, the rate of this condensation reaction at 25°C is 100 times slower than the hydrolysis reaction at 0°C in 1,2-dimethoxyethane. One may expect an increase in the rate of condensation in 1,2-dimethoxyethane. However, Shaffer and Flanigen (6) found mixed results when comparing the combined hydrolysis-condensation reactions of Me_2SiCl_2 and $PhSiCl_3$ in these solvents. The rates of the reactions of Me_2SiCl_2 was three times as fast in dioxane as in 1,2-dimethoxyethane. However, the rates of the reactions of $PhSiCl_3$ were slower in 1,2-dimethoxyethane than in dioxane. Yet, even an increase of three times in the condensation reaction would have little effect on this comparison of the hydrolysis and condensation reactions of Me_2SiCl_2. Therefore, one can conclude that the condensation reaction of $Me_2Si(OH)_2$ does not occur to any significant extent under the conditions present during the hydrolysis reactions experiments.

Several authors state that in comparing the hydrolysis and condensation reactions of halosilanes, hydrolysis occurs first, leading to silanols, -diols, or -triols. These then undergo condensation with loss of water. Various examples are given here as further evidence that condensation does not occur during the time of the hydrolysis reactions studied in this work.

Noll (2: p. 109) gives a general mechanism for the hydrolysis-condensation reactions of halosilanes. Here, complete hydrolysis occurs followed by condensation. Petrov et al (19: p. 1) give the following scheme for the hydrolysis of Me_2SiCl_2.

$$Me_2SiCl_2 \xrightarrow[-2\ HCl]{2\ H_2O} Me_2Si(OH)_2 \longrightarrow (Me_2Si\text{-}O\text{-})_n$$
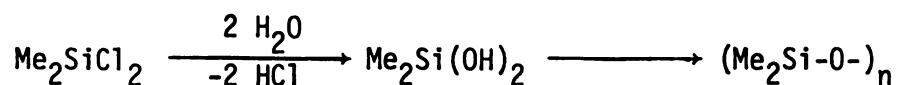
Roberts and Caserio (20: p. 1193) state that the hydrolysis of $MeSiCl_3$ gives $MeSi(OH)_3$ which is unstable and rapidly undergoes condensation with the loss of water.

Condensation can also occur between organohalosilanes and organosilanols as shown below:

$$Si\text{-}X + HO\text{-}Si \longrightarrow Si\text{-}O\text{-}Si + HX$$

Noll (2: p. 204) states that this reaction occurs on heating organohalosilanes and organosilanols. Also, these reactions may also occur during the hydrolysis if the hydrolysis reaction is slow. The fast rate of the hydrolysis reactions of Me_2SiCl_2 makes this type of reaction extremely unlikely.

68

C. Calculation of Concentration

Since Beer's law held for $PhSiCl_3$, it was assumed to hold for Me_2SiCl_2 and its hydrolysis products. The concentrations of Me_2SiCl_2, $Me_2SiCl(OH)$, and $Me_2Si(OH)_2$ were determined from the 532 cm^{-1}, 572 cm^{-1} and 510 cm^{-1}, respectively. The absorption for the various peaks was determined using the base-line technique.

A material balance for the total silane present during several runs was used to determine the extinction coefficients. Using a least square fit, the following extinction coefficients were obtained:

TABLE 8.--Extinction Coefficients for Me_2SiCl_2 and Its Hydrolysis Products.

Extinction Coefficient	Linear Estimate of Standard Deviation
$\varepsilon_{532} = 122.3\ (Mxcm)^{-1}$	4.9
$\varepsilon_{572} = 119.8\ (Mxcm)^{-1}$	7.2
$\varepsilon_{510} = 102.2\ (Mxcm)^{-1}$	15.0

D. Conditions for the Hydrolysis Reactions of Me_2SiCl_2

The reagents were prepared for the hydrolysis experiments using the methods described in Chapter II. They were drawn into the tanks and an initial spectrum of the silane obtained. The initial concentrations of the various silanes were determined from this reference spectrum. These concentrations were corrected for

dilution due to the addition of the water-solvent mixture. The initial conditions for the experiments used to describe the hydrolysis reactions of Me_2SiCl_2 are given in Table A-5 in Appendix A.

Complete hydrolysis of Me_2SiCl_2 was observed in the experiments. However, $Me_2SiCl(OH)$ and $Me_2Si(OH)_2$ followed by the 542 cm^{-1} and 510 cm^{-1} peaks, respectively, reached an equilibrium state. A higher concentration of water shifted the equilibrium toward $Me_2Si(OH)_2$.

Spectra obtained during run 44 are shown in Figure 23. At the end of the run, the peaks at 542 cm^{-1} and 510 cm^{-1} are still present.

E. HCl Effect

To determine the effect of HCl on the reaction, several runs were made with an initial concentration of HCl. The initial HCl concentration of approximately 0.5 moles/liter is considerably stronger than the approximately 0.2 moles/liter of HCl formed during the runs. The data obtained during runs 37 and 38 are given in Table A-6 in Appendix A.

No difference between the rate of reactions was observed for runs with an initial HCl concentration and those with no HCl initially present. Therefore, the reactions with HCl initially present can be described by the same model as those with no HCl initially present.
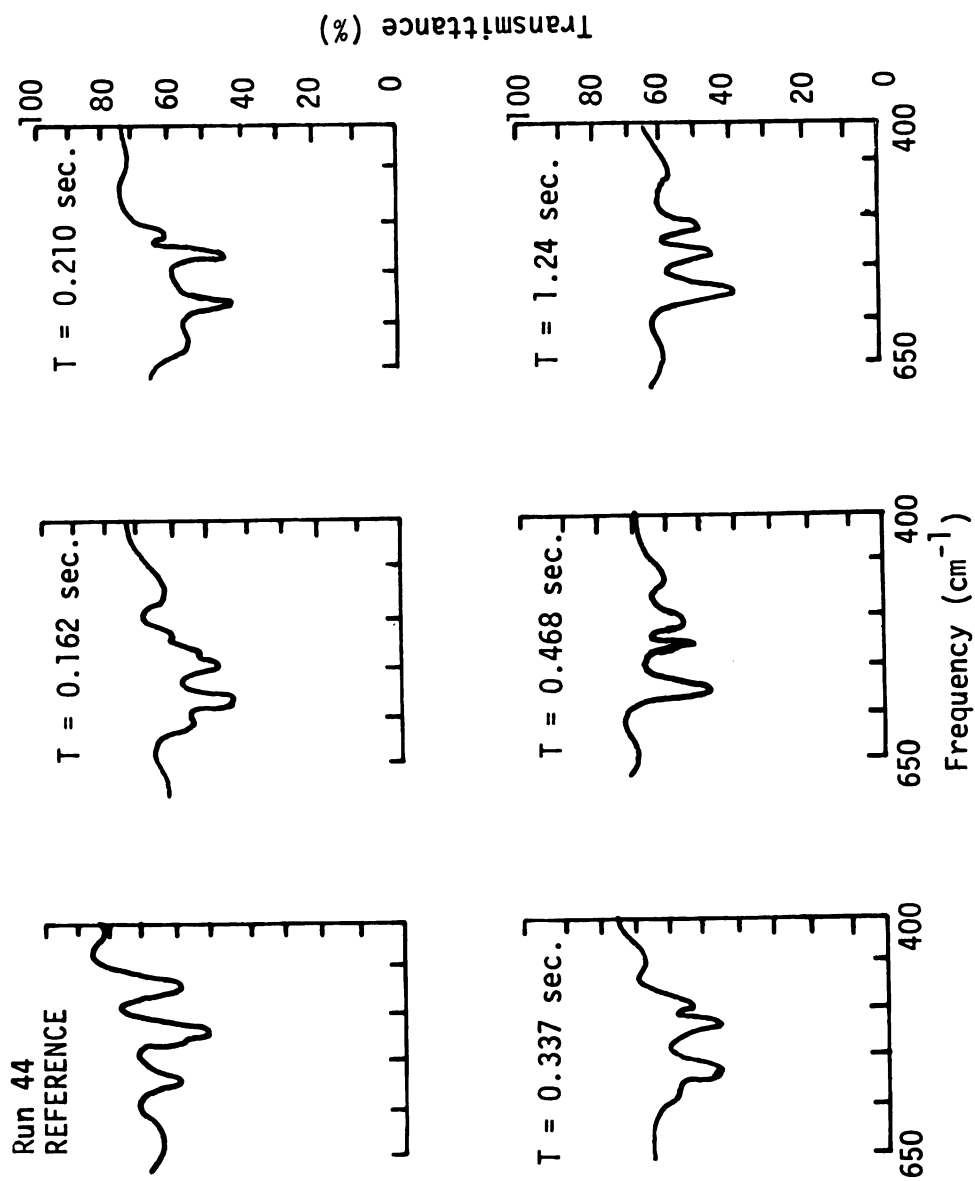
Figure 23.--Spectra Obtained During Run 44.

F. Results and Discussion

The following reaction steps were used to model the hydrolysis reactions of Me_2SiCl_2.

(1) $Me_2SiCl_2 + H_2O \xrightarrow{K_1} Me_2SiCl(OH) + HCl$

(2) $Me_2SiCl(OH) + H_2O \xrightarrow{K_2} Me_2Si(OH)_2 + HCl$

(3) $Me_2Si(OH)_2 + HCl \xrightarrow{K_2'} Me_2SiCl(OH) + H_2O$
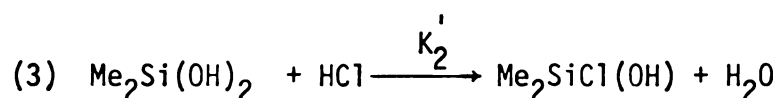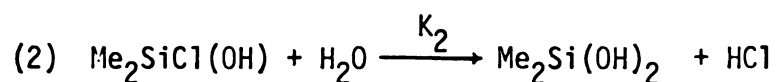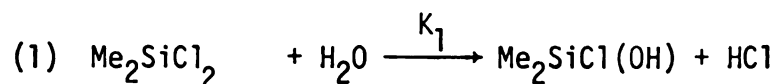
At the concentrations used in this study, HCl had little effect on the reaction rates. The reactions were assumed to be first order with respect to the water and silane and second order overall. The rate expressions used to describe the hydrolysis reactions of Me_2SiCl_2 are:

$$\frac{d[Me_2SiCl_2]}{dt} = -K_1 [MeSiCl_2] [H_2O] \tag{4.2}$$

$$\frac{d[Me_2SiCl(OH)]}{dt} = K_1 [Me_2SiCl_2] [H_2O] - K_2 [Me_2SiCl(OH)] [H_2O]$$

$$+ K_2' [Me_2Si(OH)_2] [HCl] \tag{4.3}$$

$$\frac{d[Me_2Si(OH)_2]}{dt} = K_2 [Me_2SiCl(OH)] [H_2O]$$

$$- K_2' [Me_2Si(OH)_2] [HCl] \tag{4.4}$$

$$[H_2O] = [H_2O]_0 - [Me_2SiCl(OH)] - 2[Me_2Si(OH)_2] \qquad (4.5)$$

$$[HCl] = [HCl]_0 + [Me_2SiCl(OH)] + 2[Me_2Si(OH)_2] \qquad (4.6)$$

Here, $[H_2O]_0$ and $[HCl]_0$ are the initial concentrations of H_2O and HCl, respectively.

Using the data obtained during runs 44, 45, and 46, the constants listed in Table 9 were determined with the aid of a least squares type curve fitting program (15). The data points were weighted based on estimates of their variances.

Figures 24, 25 and 26 are plots of the data points and model (solid lines) versus residence time for runs 44, 45, and 46, respectively. Figures 27 and 28 are plots of the data points and model versus residence time for runs 37 and 38 and illustrate the effect of HCl on the reactions.

The kinetic parameters were determined assuming that the system was isothermal and that plug flow existed. The effect of these assumptions is discussed in Chapter V and results in

TABLE 9.--Parameters Used to Model the Hydrolysis Reactions of Me_2SiCl_2.

Parameter	Linear Estimate of Standard Deviation
K_1 = 38.3 liters/mole-sec.	4.81
K_2 = 11.1 liters/mole-sec.	1.94
K_3' = 20.2 liters/mole-sec.	4.77
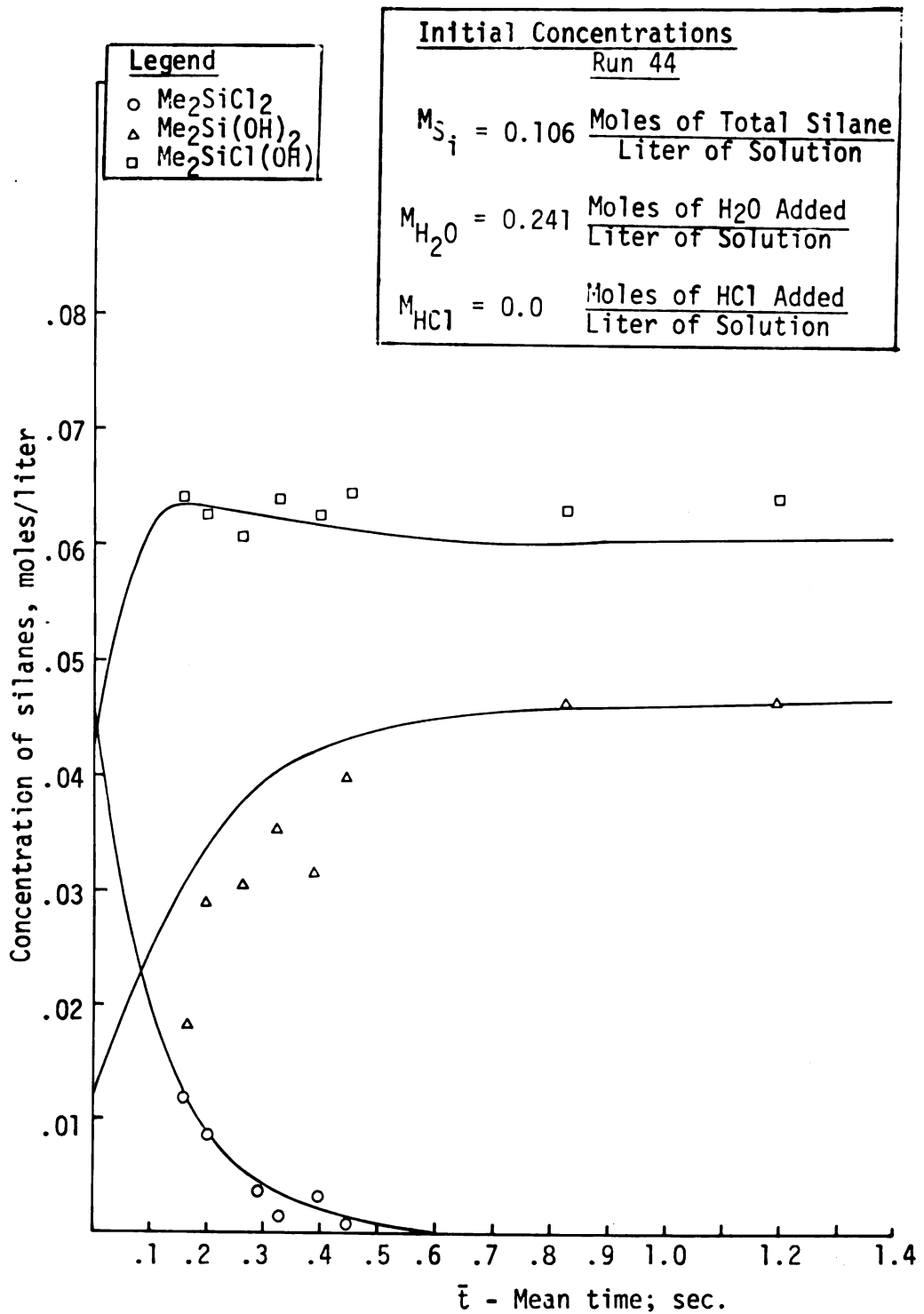
Figure 24.--Concentration of Silanes Versus Mean Reaction
Time for the Hydrolysis of Me_2SiCl_2, Run 44.
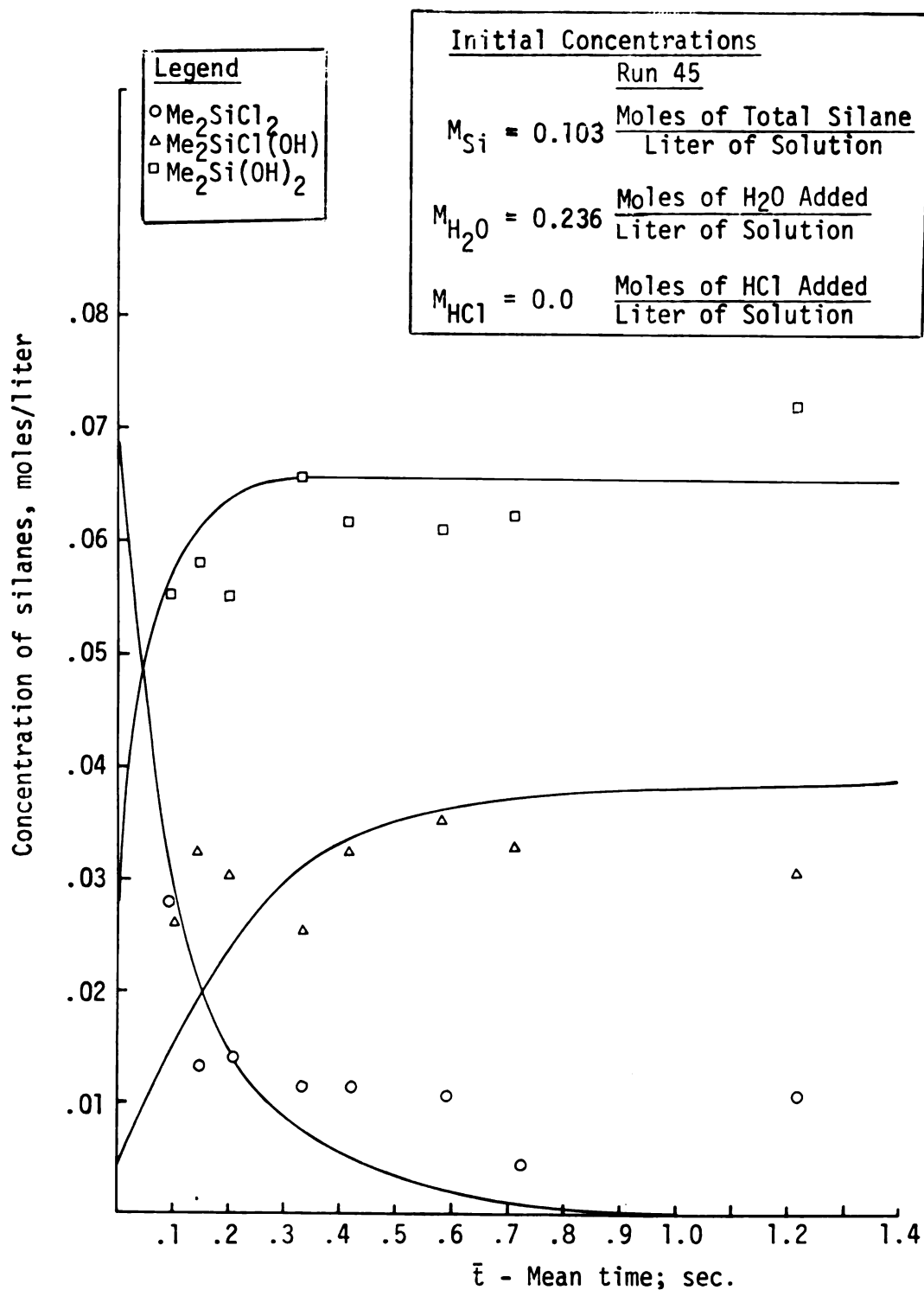
Figure 25.--Concentration of Silanes Versus Mean Reaction
Time for the Hydrolysis of Me_2SiCl_2, Run 45.
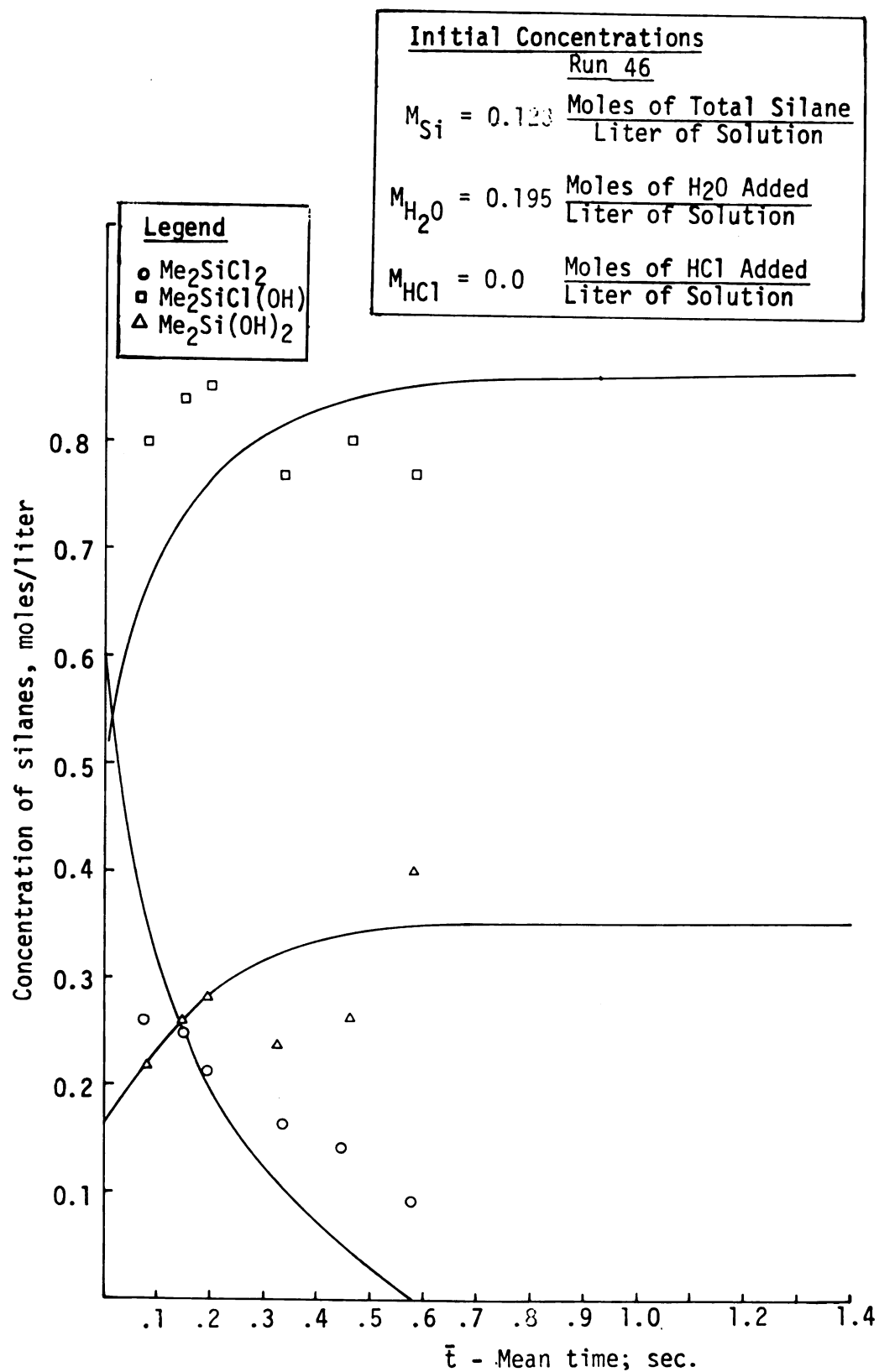
Figure 26.--Concentration of Silanes Versus Mean Reaction Time for the Hydrolysis of Me_2SiCl_2, Run 46.

Initial Concentrations
Run 37

M_{Si} = 0.1283 $\dfrac{\text{Moles of Total Silane}}{\text{Liter of Solution}}$

M_{H_2O} = 0.286 $\dfrac{\text{Moles of } H_2O \text{ Added}}{\text{Liter of Solution}}$

M_{HCl} = 0.569 $\dfrac{\text{Moles of HCl Added}}{\text{Liter of Solution}}$

Legend
o Me_2SiCl_2
△ $Me_2SiCl(OH)$
□ $Me_2Si(OH)_2$
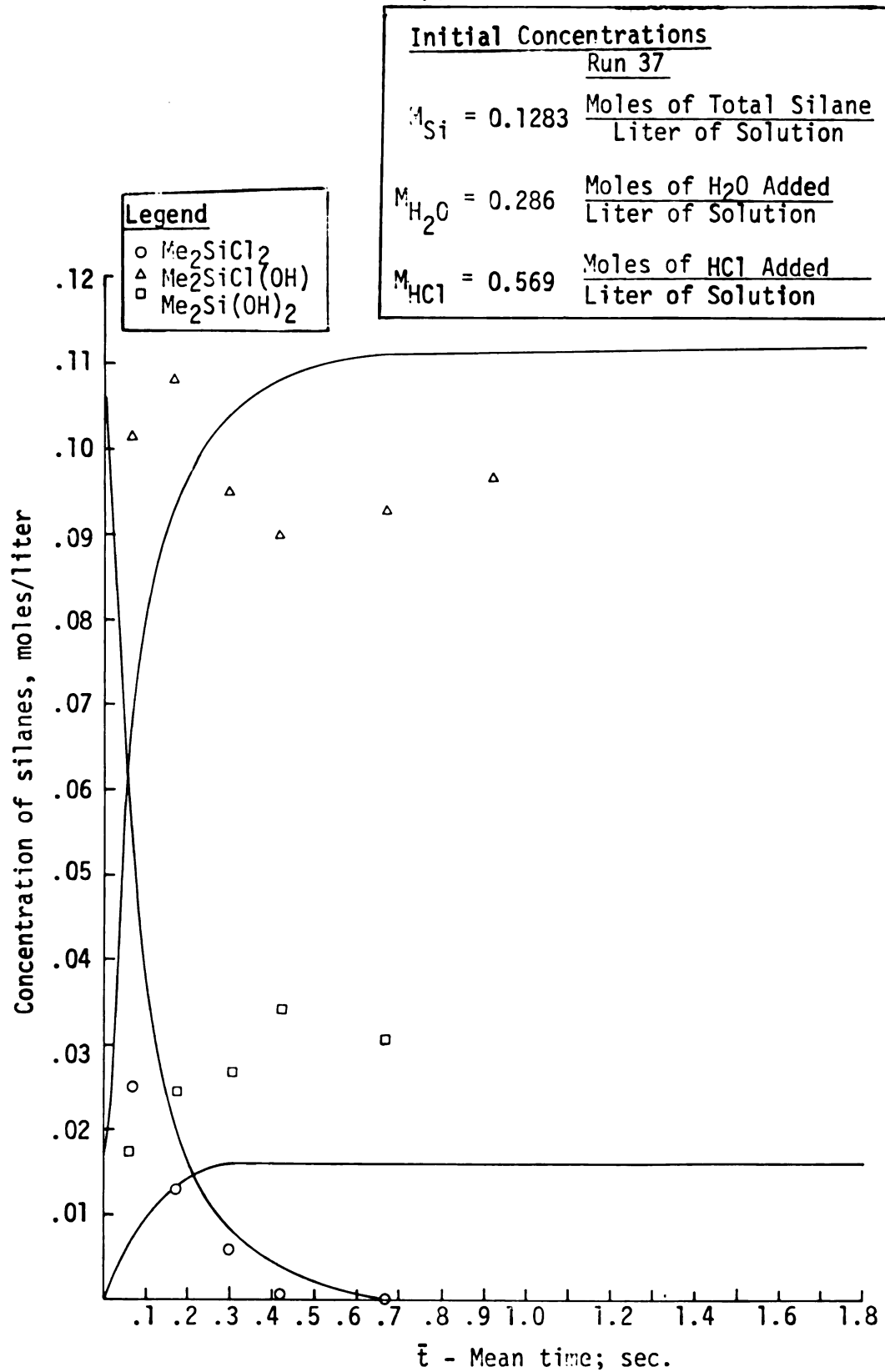
Figure 27.--Concentration of Silanes Versus Mean Reaction Time for the Hydrolysis of Me_2SiCl_2, Run 37.
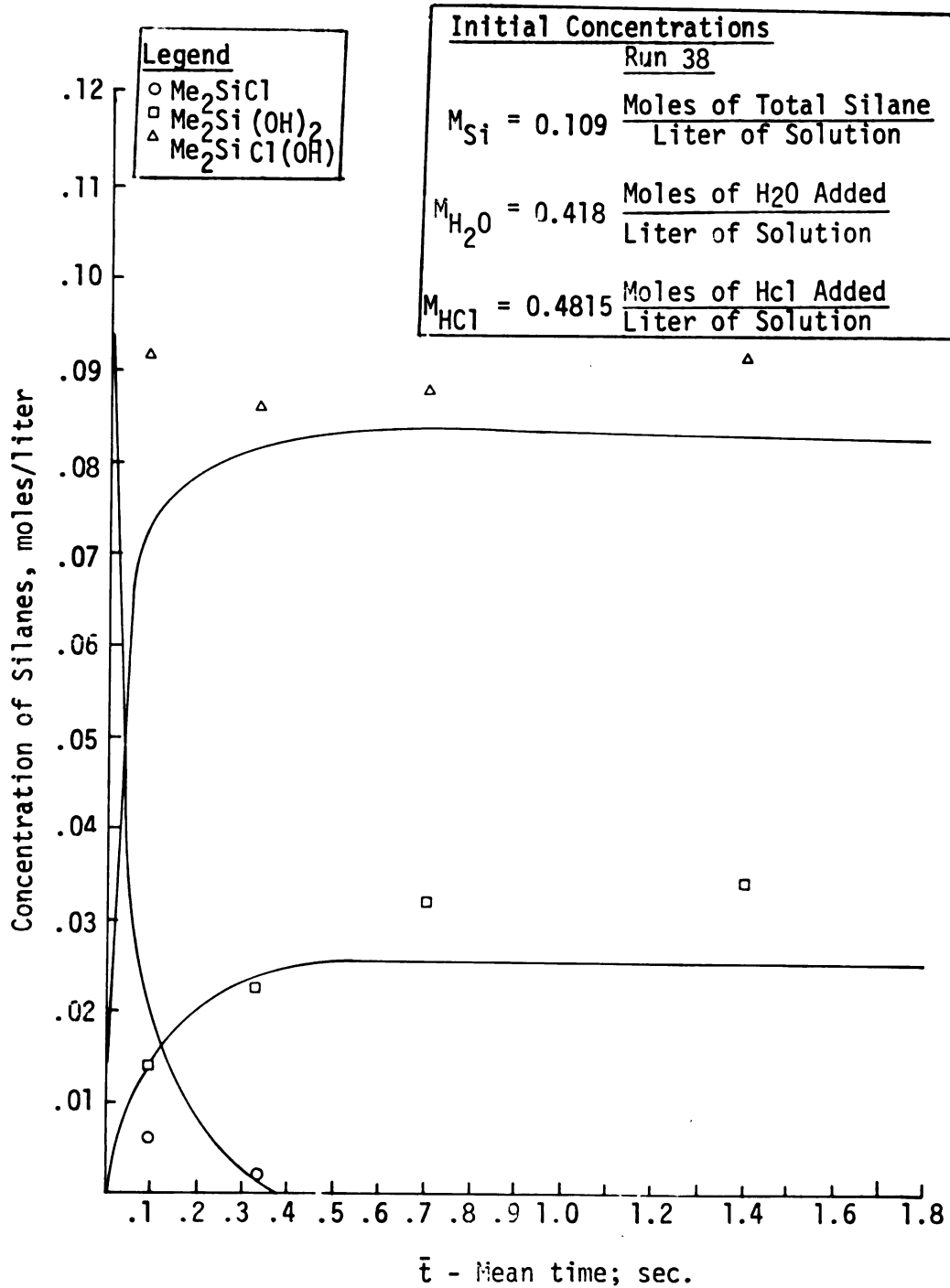
Figure 28.--Concentration of Silanes Versus Mean Reaction
Time for the Hydrolysis of Me_2SiCl_2, Run 38.

approximately a 10 percent bound between the parameters determined assuming isothermal plug flow and those determined assuming laminar flow with heat transfer.

G. Temperature Effect

Only limited information is available on the temperature effect on the hydrolysis reactions of chlorosilanes. Generally, these reactions are highly exothermic due in a large part to the heat of dissolving hydrogen chloride in the water solvent mixture. However, in a sturated solution of hydrogen chloride, there may be an actual cooling effect of the reaction due to the vaporization of the hydrogen chloride.

The only apparent study to calculate the activation energy of the hydrolysis reaction of chlorosilanes was conducted by Shaffer and Flanigen (6). Their technique was described earlier and measures only the rate limiting step in the combined hydrolysis and condensation reactions of chlorosilanes in a sturated solution of hydrogen chloride. For the hydrolysis of Me_2SiCl_2, Shaffer and Flanigen determined that their indicated hydrolysis end product was a chlorine end blocked linear polysiloxane. The rate of reaction was measured at 0°C and 25.7°C. Using the rates calculated at these temperatures, the activation energy was determined to be approximately 25 kcal/mole for the combined hydrolysis condensation reactions.

One objective of this research was to determine the activation energies for the individual hydrolysis reactions of

Me_2SiCl_2. To accomplish this, the hydrolysis reactions of Me_2SiCl_2 were studied at temperatures ranging from 16°C to -21°C. The higher temperature (16°C) was maintained through a combination of an on-off heater, a water circulating pump, and a cooling coil circulating water at 15°C. To obtain temperatures below 0°C, a methanol water solution was used. Here methanol was added to reduce the freezing point of the solution to the desired temperature. A liquid-solid equilibrium was obtained by adding dry ice to the solution. Through the use of these techniques, the temperature was maintained to within 0.5°C of the desired temperature.

The solution in the constant temperature bath was circulated through the heat exchanger surrounding the reactor. At 252°K, a sludge formed in the constant temperature bath, which caused some problems in circulating the solution through the heat exchanger.

A marked difference in the intensities of the absorptions of the infrared bands occurred with the changes in temperature. As the temperature was increased a decrease in band intensity was noted and a similar increase in intensity occurred as the temperature was decreased. This observation has been made by other investigators in the infrared region and has been attributed to one of two effects. Slowinski (21) observed this decrease in intensity of absorption with an increase in temperature. It was observed that a band at 100°C was in some cases only 70 percent as intense as the same band at 25°C. This effect was attributed to the presence of rotational isomers. Brown (22) attributed this effect to collisions of the solute molecules with the walls of the solvent cage.

To correct for this effect, the extinction coefficients obtained at 0°C were multiplied by an appropriate constant based on a material balance on the system. This approximation is based on the fact that the extinction coefficients are all of similar magnitude and are due to similar vibrations. Therefore, one would expect the rate of change of the extinction coefficients with respect to temperature to be similar. It was necessary to use this method of determining the extinction coefficients at different temperatures since not enough data was available for an independent evaluation of the extinction coefficients at each temperature.

At 16°C, the rate of reaction was extremely fast. This plus the loss of accuracy in determination of the concentrations caused by the decrease band intensities made the calculation to the hydrolysis rate at 16°C impossible with the desired degree of accuracy. Therefore, only temperatures at or below 0°C were used to determine the activation energy.

The hydrolysis of Me_2SiCl_2 is described by one irreversible and one reversible reaction. The activation energies were determined by measuring the reaction rates at 0, -5.5 and -21°C. The rates obtained for these reactions at the three temperatures are shown in Table 10. Figures 29 and 30 (on pages 82 and 83) are plots of concentrations versus residence time for the hydrolysis reactions at 267.5 and 252.0°K, respectively.

Due to the slower rates of reaction at 252.0°K, the rate constants were determined with more accuracy at this temperature. This resulted in a smaller linear estimate of standard deviation

TABLE 10.--Rate Constants for the Hydrolysis Reaction of Me_2SiCl_2 at Different Temperatures.

Temperature (°K)	Rate Constant (liter/mole-sec.)	Linear Estimate of Standard Deviation
	K_1	
273.0	38.3	4.81
267.5	34.0	9.91
252.0	23.7	5.71
	K_2	
273.0	11.1	1.94
267.5	7.37	3.94
252.0	3.58	1.3
	K_2'	
273.0	20.2	4.77
267.5	19.2	15.4
252.0	14.6	6.47

for these rate constants compared to those determined at 267.5°K. Considerably more data was available at 273.0°K, which accounts for the smaller standard deviations in the rate constants at this temperature. The standard deviations for the parameters at 267.5°K are high since only one data set was used to determine these parameters. In determining the activation energies for these reactions, the rate constants at the various temperatures were
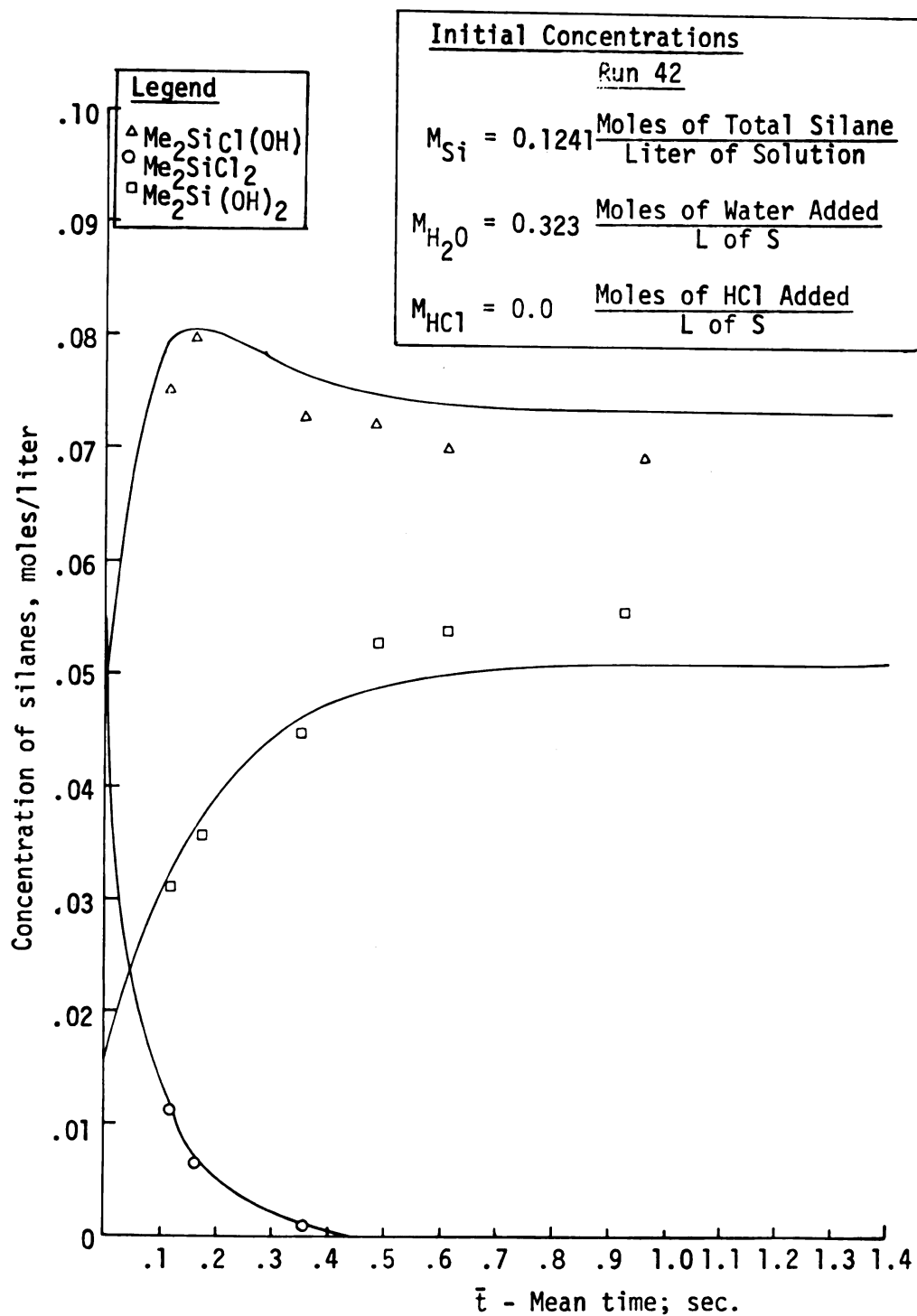
Figure 29.--Concentration of Silanes Versus Mean Reaction Time for the Hydrolysis of Me_2SiCl_2, Run 42.

$T = 267.5°K$
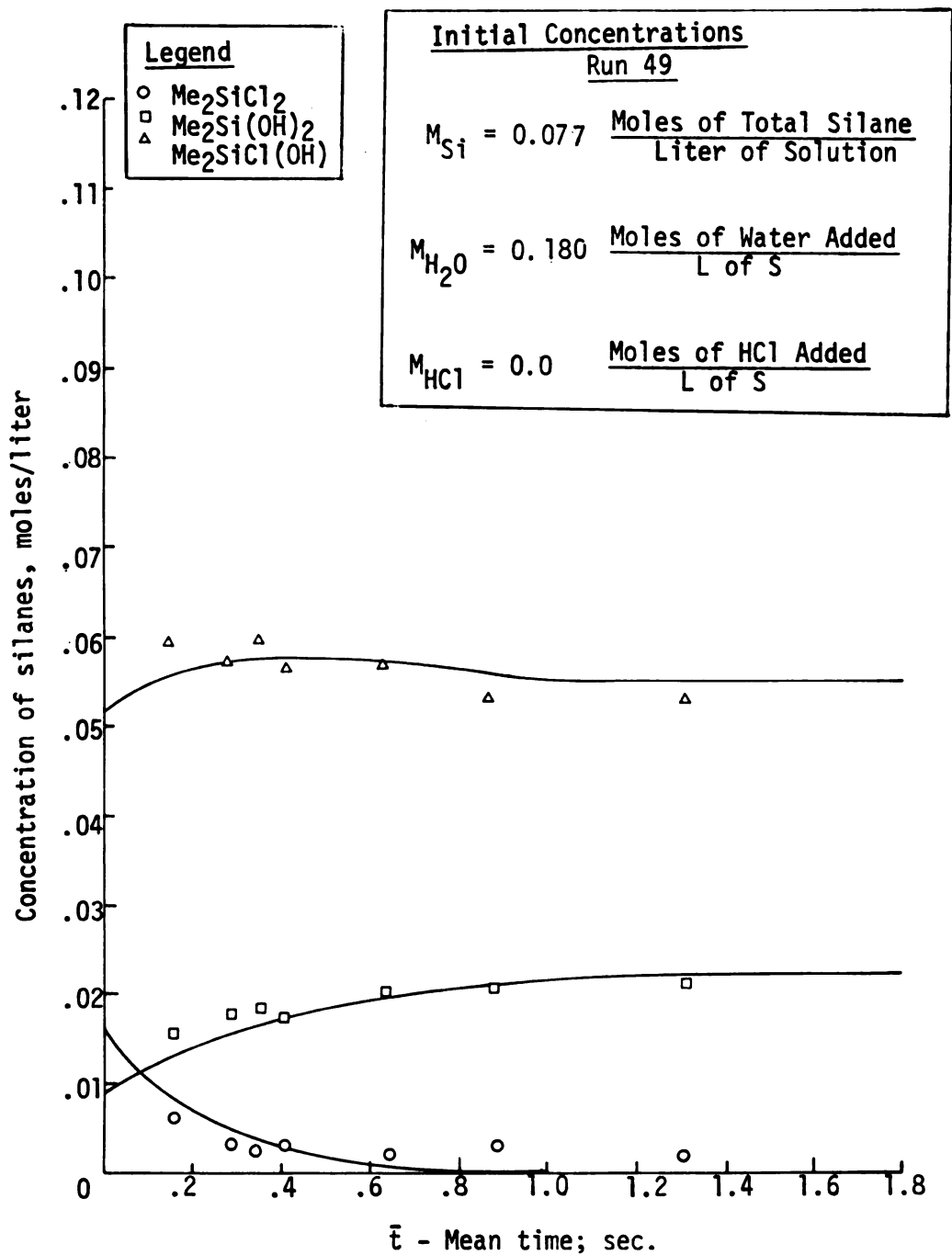
Figure 30.--Concentration of Silanes Versus Mean Reaction Time
for the Hydrolysis of Me_2SiCl_2, Run 49.

$T = 252°K$

given the appropriate weights based on their linear estimate of standard deviation.

The activation energies and frequency factors were calculated for the two forward reactions using the reaction rate constants determined at the different temperatures. The rate constants K_2' were not known accurately enough to allow determination of the activation energy of the reverse reaction. To determine the activation energy of the reverse reaction, the equilibrium constant K_2/K_2' was measured at 273.0, 262.0, 267.5 and 252.0°K. Using these equilibrium constants, the difference between the activation energies of the forward and reverse reactions was calculated using the derivation shown here:

$$K_2 = K_{20} \, e^{-\Delta E_2/RT} \tag{4.7}$$

$$K_2' = K_{20}' \, e^{-\Delta E_2'/RT} \tag{4.8}$$

$$K_2/K_2' = K_{20}/K_{20}' \, e^{(-\Delta E_2 + \Delta E_2')/RT} \tag{4.9}$$

The activation energies and frequency factors for the two forward reactions and for the reverse reaction are given in Table 11.

Figure 31 (on page 86) is a plot of 1/temperature versus $\log_e$ (rate constant) for reactions 1 and 2. This illustrates a graphical technique which may be used to calculate the activation energies. The solid lines are drawn using the values of the activation energies and frequency factors given in Table 11.

TABLE 11.--Activation Energies for the Hydrolysis Reactions of Me_2SiCl_2.

Reaction	Linear Estimate of Standard Deviation
Forward Reaction 1	
Activation energy = 3.6×10^3 cal/mole	5.70×10^1
Frequency factor = 3.05×10^4 liter/mole-sec.	3.34×10^3
Forward Reaction 2	
Activation energy = 1.05×10^4 cal/mole	6.4×10^1
Frequency factor = 3.02×10^9 liter/mole-sec.	3.4×10^8
Reverse Reaction 2	
$\Delta E_2' - \Delta E_2$ = 4.37×10^3 cal/mole	1.2×10^3
Activation energy = 1.4×10^4 cal/mole	

H. Conclusions on the Hydrolysis of Me_2SiCl_2

This study demonstrated that the hydrolysis reactions of Me_2SiCl_2 can be described by rate equations that are first order with respect to water and silane and second order overall. Such expressions are consistent with the S_n2-Si mechanism which is believed to describe the hydrolysis reactions of halosilanes.

The hydrolysis of the first chlorine atom in Me_2SiCl_2 is faster than that of the second. This is similar to the observations made in the case of the hydrolysis reactions of $PhSiCl_3$ and is consistent with the observation of Shaffer and Flanigen (6). Both the first and second hydrolysis reactions of Me_2SiCl_2 appear
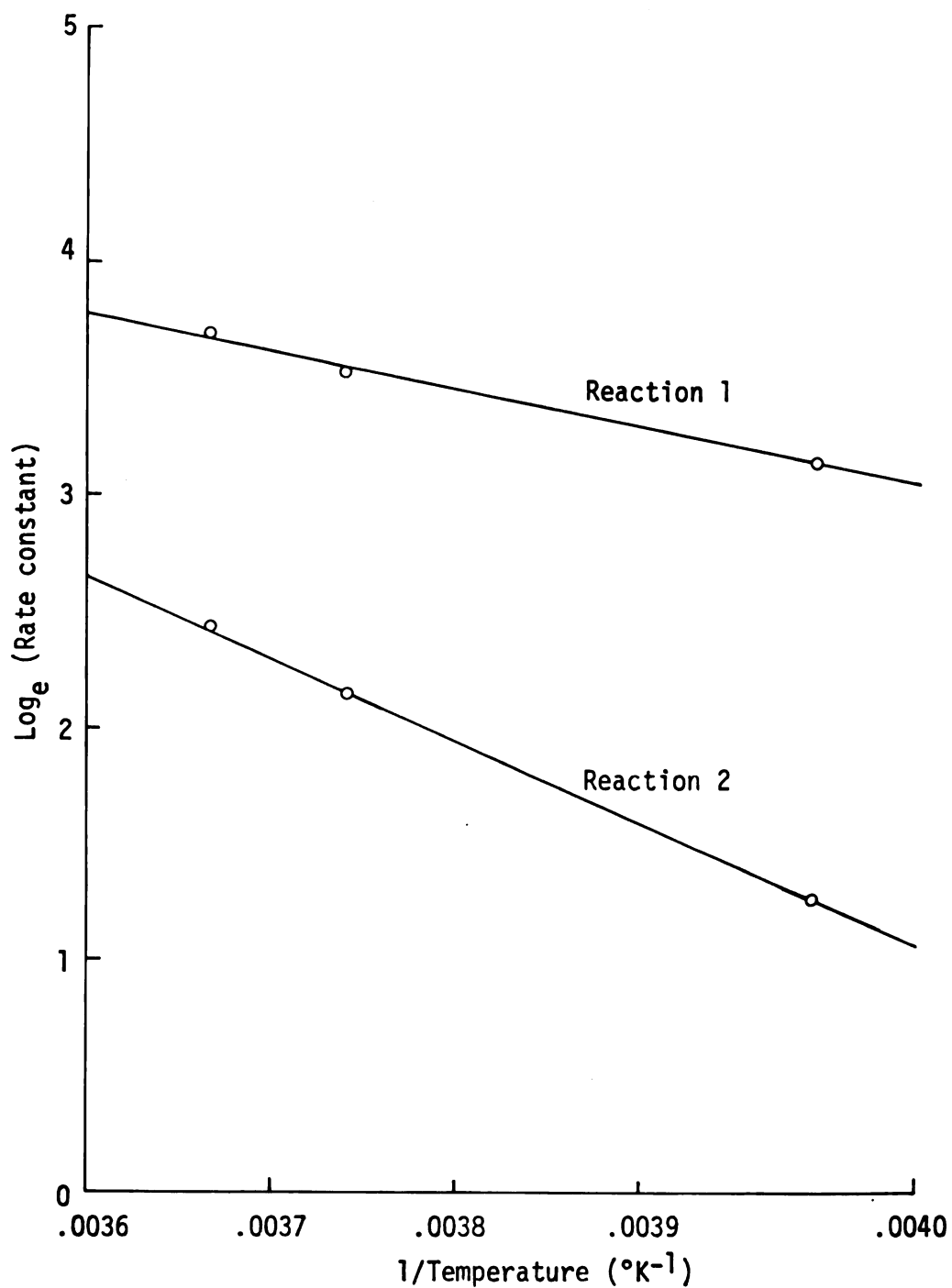
Figure 31.--1/Temperature Versus Log$_e$ (Rate Constant) for the Hydrolysis Reactions of Me$_2$SiCl$_2$.

to be reversible. However, under the conditions of this study, the equilibrium of the first reaction is shifted to the right to such a degree that it can be described as an irreversible reaction.

The presence of HCl had little effect on the rate of reaction. This indicates that the hydronium ion H_3O^+ is more reactive in the hydrolysis of Me_2SiCl_2 than in the hydrolysis of $PhSiCl_3$. Since the condensation reaction is catalyzed by HCl, the presence of HCl still plays an important part in determining the final products of the combined hydrolysis-condensation reactions.

CHAPTER V

ANALYSIS OF A LAMINAR FLOW REACTOR

The analysis of the rate data collected during these studies assumed that the reactor system was isothermal and that plug flow existed. These assumptions are commonly made in studying reactions in flow systems. In this chapter, the significance of these assumptions is investigated.

A. Scope of Past Work

Several authors have studied these assumptions independently by either studying the plug flow assumption in an isothermal reactor or the isothermal assumption in a plug flow reactor. The assumption of plug flow in an isothermal system has been investigated by Kleinhenz and Hawley (7) and by Johnson (23). Johnson calculated the fraction of reagent reacted for both plug and laminar flow for first and second order reactions. From the comparison of the fraction reacted, one can determine the significance of the plug flow assumption in an isothermal reaction system. Kleinhenz and Hawley (7) plotted the ratio of conversion of laminar to plug flow for reaction orders from 0 to 3. They extended this analysis by calculating the reaction rate constants needed to achieve a certain conversion for plus or laminar flow. From the ratios of such rate constants, one can determine the significance of the

plug flow assumption on the determination of the reaction rate
constants. Kleinhenz and Hawley concluded that the reaction rate
constants determined assuming plug flow are a reasonably good
estimate of the actual rate constants.

Huang and Barduhn (24) have analyzed the isothermal
assumption in a plug flow reactor. Considering an exothermic reac-
tion, temperature profiles occur along the length of the reactor,
since the heat generated by the reaction exceeds the heat trans-
ferred through the reactor walls to the surrounding medium. At a
certain length in the reactor, the temperature reaches a maximum
and a hot spot occurs. If the reactor is long enough the tempera-
ture in the reactor eventually reaches that of the surrounding
medium. A factor, which may be used to correct the rate constants
obtained assuming an isothermal reaction, is presented in the
article.

Merrill and Hamrin (25) investigated the laminar flow
assumption with radial molecular diffusion for a three-halves order
reaction. They studied the diffusion effect for an isothermal
reactor, a reactor with heat transfer through the walls of the
reactor, and for an adiabatic reactor. From this study, they con-
cluded that radial diffusion affected the concentration profiles
near the wall but had little effect on the overall conversion.

B. Scope of This Study

The analysis presented here investigates the combined
temperature and laminar flow effects on the concentrations and

temperatures in a flow reactor. Differential equations are developed which describe the laminar flow system with radial heat conduction. These equations are then written in dimensionless form with the appropriate dimensionless constants. Using numerical integration techniques and values for the dimensionless constants from the study of the hydrolysis reactions of Me_2SiCl_2, the equations are integrated to obtain concentration and temperature profiles in the reactor. From these profiles, the extent of reaction for laminar flow is obtained. The extent of reaction for plug flow versus that of laminar flow is plotted for zero, first, and second, order reactions. From such plots, the combined effects of the isothermal and plug flow assumptions can be determined. This data can then be used to determine the effect of these assumptions on the determination of the rate constants.

C. Development of the Laminar Flow Model

The model developed here is based on laminar flow in a circular tube. The aim of this model is to determine the concentrations and temperature profiles in a laminar flow reactor.

Bird, Steward and Lightfoot (26: p. 46) have expressed the change of axial velocity with respect to radial direction for laminar flow in circular tubes as:

$$\frac{dV_z}{dr} = \frac{\Delta P}{2\mu} \frac{r}{L} \qquad (5.1)$$

Here, ΔP is the pressure drop along the length of the tube, r is any radius in the tube, μ is the viscosity of the fluid and L is the length of the tube.

Integrating and applying the boundary conditions that V_z is zero at $r = R$, we have:

$$V_z = \frac{\Delta P\ R^2}{4\mu\ L}\left[1 - (\tfrac{r}{R})^2\right] \tag{5.2}$$

Since at $r = 0$, the maximum velocity is obtained, equation (5.2) may be written as:

$$V_z = V_{max}\left[1 - (\tfrac{r}{R})^2\right] \tag{5.3}$$

where

$$V_{max} = \frac{\Delta P\ R^2}{4\mu\ L} \tag{5.4}$$

The average velocity $<V_z>$ in the tube may be calculated by integrating V_z over the area of the tube and dividing by the area.

$$<V_z> = \frac{\iint \pi\ r^2\ V_z\ dr\ d\theta}{\iint \pi\ r^2\ dr\ d\theta} = \frac{\Delta P\ R^2}{8\mu\ L} \tag{5.5}$$

Hence, the average velocity in the tube is equal to one-half the maximum velocity.

$$<V_z> = \frac{1}{2}<V_{max}> \tag{5.6}$$

Figure 32 illustrates a cylindrical element in reactor with laminar flow.

An energy balance over the cylindrical element gives the following terms:

Energy in by conduction at r	$q_r\|_r \cdot 2\pi \; r \; \Delta z$
Energy out by conduction at r + Δr	$q_r\|_{r+\Delta r} \cdot 2\pi \; (r + \Delta r) \; \Delta z$
Energy in by conduction at z	$q_z\|_z \cdot 2\pi \; r \; \Delta r$
Energy out by conduction at z + Δz	$q_z\|_{z+\Delta r} \cdot 2\pi \; r \; \Delta r$
Energy in with flowing fluid at z	$\rho \; \hat{C}_p \; V(T - T_0)\|_z \cdot 2\pi \; r \; \Delta r$
Energy out with flowing fluid at z + Δz	$\rho \; C_p \; V(T - T_0)\|_{z+\Delta z} \cdot 2\pi \; r \; \Delta r$
Energy produced in ring-shaped element	$2\pi \; r \; \Delta z \; \Delta r \; (-r_e) \; (-\Delta H)$

For an nth order reaction, we have:

$$r_e = \frac{dC_A}{dt} = -K_0 \; e^{-\Delta E/RT} \; C_0^N (1 - X)^N \tag{5.7}$$

Equating the energy outputs to the energy inputs plus the energy produced in the element and dividing by $2\pi \; \Delta r \; \Delta z$ gives:

$$\frac{(rq_r)\|_{r+\Delta r} - (rq_r)\|_r}{\Delta r} + r \; \frac{q_z\|_{z+\Delta z} - q_z\|_z}{\Delta z}$$

$$+ r \; \rho \; \hat{C}_p \; V_z \; \frac{T\|_{z+\Delta z} - T\|_z}{\Delta z} + r \; r_e \; (-\Delta H) = 0 \tag{5.8}$$
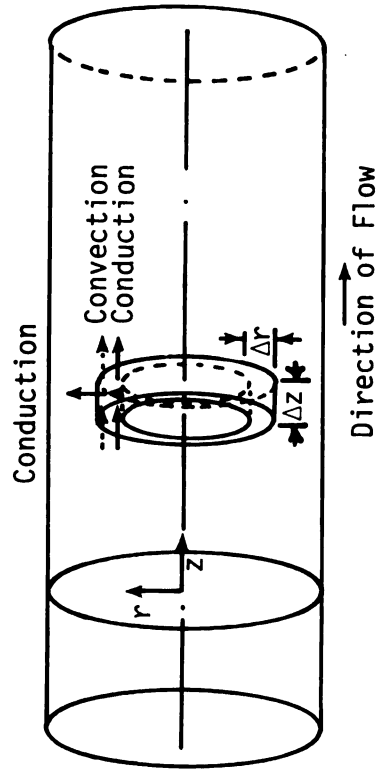
Figure 32.--A Cylindrical Element in a Laminar Flow Reactor.

Taking the limit as Δz, $\Delta r \rightarrow 0$:

$$\rho \, \hat{C}_p \, V_z \, \frac{\partial T}{\partial z} = - \frac{1}{r} \frac{\partial}{\partial r} (r q_r) - \frac{\partial q_z}{\partial z} + (-\Delta H) r_e \qquad (5.9)$$

Introducing the velocity distribution for laminar flow and Fourier's law for heat conduction:

$$q_r = -K \frac{\partial T}{\partial r} \; ; \qquad q_z = -K \frac{\partial T}{\partial z} \qquad (5.10)$$

We now have the partial differential equation:

$$\rho \, \hat{C}_p \, V_M \left[1 - (\frac{r}{R})^2 \right] \frac{\partial T}{\partial z} = K \left[\frac{1}{r} \frac{\partial}{\partial r} \left(r \frac{\partial T}{\partial r} \right) - \left(\frac{\partial^2 T}{\partial z^2} \right) \right]$$

$$- (-\Delta H) r_e \qquad (5.11)$$

The heat conduction in the z direction is normally small in comparison with the heat convection term. Therefore, the heat conduction term $(\partial^2 T / \partial z^2)$ may be dropped from equation (5.11) and we obtain the following equation:

$$\rho \, \hat{C}_p \, V_M \left[1 - (\frac{r}{R})^2 \right] \frac{\partial T}{\partial z} = \frac{K}{r} \frac{\partial}{\partial r} \left(r \frac{\partial T}{\partial r} \right)$$

$$- \Delta H K_o e^{-\Delta E / RT} \, c_o^N (1 - X)^N \qquad (5.12)$$

This is a partial differential equation describing the temperature distribution in a laminar flow reactor.

The following boundary conditions may be applied to equation (5.12).

B.C. 1: at $r = 0$, $\frac{\partial T}{\partial r} = 0$

B.C. 2: at $r = R$, $T = T_{wall}$

B.C. 3: at $z = 0$, $T = T_0$ (for all r)

In this analysis, we will consider only reactors where the initial temperature, T_0, is equal to the temperature at the wall, T_{wall}.

To simplify the manipulations involved, equation (5.12) is written in dimensionless form through the introduction of the following dimensionless variables.

$$\theta = \frac{\rho \hat{C}_p T}{(-\Delta H)C_0} \qquad \text{(Dimensionless temperature)}$$

$$\eta = z/R \qquad \text{(Dimensionless length)}$$

$$\xi = r/R \qquad \text{(Dimensionless radius)}$$

Equation (5.12) is now written as:

$$\rho \hat{C}_p V_M (1 - \xi^2)\frac{(-\Delta H)C_0}{\rho C_p R}\frac{d\theta}{d\eta} = \frac{K}{rR}\left[\frac{\partial}{\partial \xi}\left[\frac{r(-\Delta H)C_0}{R \rho C_p}\right]\frac{\partial \theta}{\mu \xi}\right]$$

$$- \Delta H K_0 e^{-\Delta E/RT}C_0^N(1-X)^N \qquad (5.13)$$

Through the use of the following dimensionless constants, equation (5.13) is:

$$(1 - \xi^2) \frac{d\theta}{d\eta} = \frac{\alpha}{\xi} \left[\frac{\partial\theta}{\partial\xi} + \xi\frac{\partial^2\theta}{\partial\xi^2} \right] + \beta e^{-\gamma/\theta}(1 - X)^N \qquad (5.14)$$

$$\gamma = \frac{\Delta E \, \rho \, \hat{C}_p}{R_c(-\Delta H)C_o}$$

$$\alpha = \frac{K}{\rho \, \hat{C}_p \, V_M \, R}$$

$$\beta = \frac{R \, K_o \, C_o^{N-1}}{V_M}$$

Equation (5.14) represents the final form of the partial differential equation describing the temperature distribution in a laminar flow reactor. This equation is a function of the extent of reaction, X. Therefore, the extent of reaction must be determined for the laminar flow system.

Merrill and Hamrin (25) have shown that the radial diffusion has a small effect on the overall conversion in a laminar flow system. Therefore, the radial diffusion term can be neglected in considering the conversion in laminar flow. Since the flow in the tube is quite high, we can also neglect the axial diffusion in the reactor. Writing a material balance on the ring-shaped element in Figure 31, we have:

Material in at z with flowing fluid	$V_z \, 2\pi \, r \, \Delta r \, C$
Material out at z + Δz with flowing fluid	$V_z \, 2\pi \, r \, \Delta r \, C$
Material reacted in ring-shaped element	$2\pi \, r \, \Delta r \, \Delta z \, (-r_e)$

Equating the inputs and outputs for this system, we have:

$$V_z \ 2\pi \ r \ \Delta r \ C|_z - V_z \ 2\pi \ r \ \Delta r \ C|_{z+\Delta z} - 2\pi \ r \ \Delta r \ \Delta z \ (-r_e) = 0 \qquad (5.15)$$

Dividing by Δz and taking the limit as Δz goes to zero:

$$V_z \ \frac{\partial C}{\partial z} = r_e \qquad (5.16)$$

When substituting the laminar velocity profiles for V_z, the reaction equation for r_e and the extent of reaction for concentration, equation (5.16) becomes:

$$V_M \left(1 - (r/R)^2\right) \frac{dX}{dz} = K_o e^{-\Delta E/R_c T} (1 - X)^N C_o^{N-1} \qquad (5.17)$$

Equation (5.17) written in dimensionless form along with equation (5.14) describe the temperature and concentration profiles in the laminar flow reactor.

$$\frac{dx}{d\eta} = \frac{\beta}{(1 - \xi^2)} e^{-\gamma/\theta} (1 - X)^N \qquad (5.18)$$

$$(1 - \xi^2) \frac{\partial \theta}{\partial \eta} - \beta(1 - X)^N e^{-\gamma/\theta} = \frac{\alpha}{\xi} \left[\frac{\partial \theta}{\partial \xi} + \xi \frac{\partial^2 \theta}{\partial \xi^2}\right] \qquad (5.19)$$

B.C. 1 for equation (5.18) at $\eta = 0$, $X = 0$ for all ξ ⟵ *H x V* *10/14/96*

B.C. 1 for equation (5.19) at $\eta = 0$, $\theta = \dfrac{\rho \ C_p \ T_w}{(-\Delta H) C_o}$ for all ξ

B.C. 2 for equation (5.19) at $\xi = 1$, $\theta = \dfrac{\rho \ C_p \ T_w}{(-\Delta H) C_o}$ for all η

B.C. 3 for equation (5.19) at $\xi = 0$, $\frac{\partial \theta}{\partial \xi} = 0$ for all η

The integration of equations (5.18) and (5.19) gives the radial temperature and concentration profiles along the length of the reactor. Equations (5.20) and (5.21) are used to find the average concentration and mixing cup temperature in the reactor. This is the concentration and temperature that would be measured if at one point along the length of the reactor, the reaction was stopped and the solution allowed to flow into a cup. The temperature in this cup is the mixing cup temperature and the concentration is the average concentration.

$$X_{ave} = \frac{2\pi \int_0^R x(\xi,\eta,\theta)V(\xi)}{\pi V_{ave} R^2} \qquad (5.20)$$

$$T_{mixing\ cup} = \frac{2\pi \int_0^R \theta(\xi,\eta,\theta)V(\xi)}{\pi V_{ave} R^2} \qquad (5.21)$$

In equations (5.20) and (5.21), the radial concentration and temperature profiles are multiplied by the velocity at their radial position and integrated over the area of the reactor. These are then divided by the average velocity multiplied by the area of the reactor.

The numerical integration technique, numerical values for the constants used in the integration, and a computer listing of the program are given in Appendix B.

D. Conclusions

This analysis of the isothermal and plug flow assumptions in a laminar flow reactor enables the significance of these assumptions to be studied. In the case of the hydrolysis reactions of Me_2SiCl_2, this analysis shows that the isothermal and plug flow assumptions have little effect on the extent of reaction. This is seen in Figure 33, where the extent of reaction for laminar flow with heat transfer follows quite closely the extent of reaction for isothermal plug flow, especially for a second order reaction. Since the laminar flow assumption results in the measurement of a lower rate constant, the slight increase in temperature actually reduces the difference between laminar and plug flow. The temperature rise is not great enough to significantly affect the concentrations in the reactor. The extent of reaction predicted considering laminar flow, heat of reaction, and radial heat transfer are still below those of an isothermal plug flow reactor.

This analysis demonstrates that it is possible to study reactions in laminar flow and predict the temperature and laminar flow effects. Kleinhenz and Hawley (7) demonstrated the magnitude of the laminar flow assumption on the rate constants. The maximum error introduced by this assumption is approximately 16 percent. When the temperature effect is introduced, the maximum error is reduced to approximately 10 percent. Due to the mixing in the reactor, this error will be further reduced. Therefore the values of the rate constants determined in this study are well within this 10 percent bound.
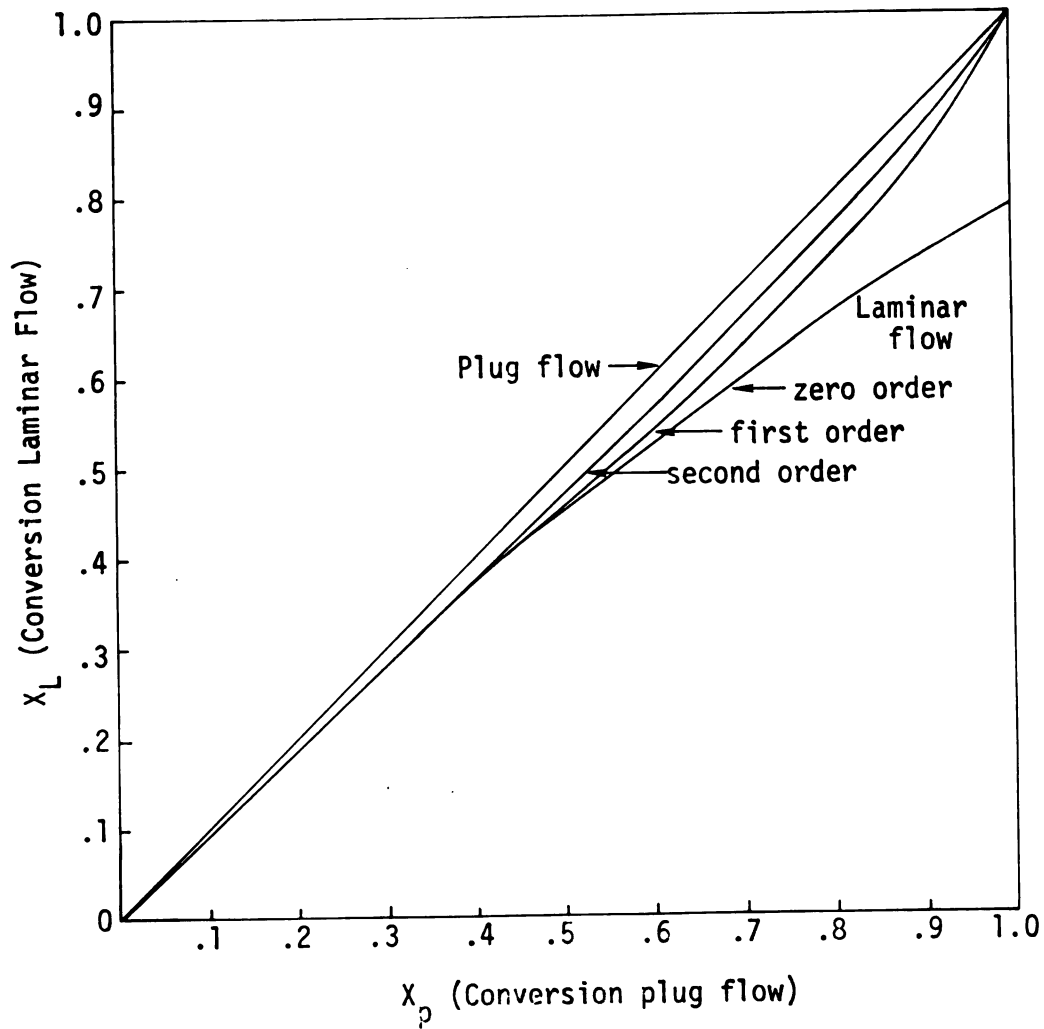
Figure 33.--Extent of Reaction for Laminar Flow With Heat
Transfer Versus Extent of Reaction for Isothermal
Plug.

Using rate and thermodynamic constants similar to those found in the hydrolysis reactions of Me_2SiCl_2 with an initial temperature of 0°C, the extent of reaction for laminar flow with heat transfer to the wall was obtained. Figure 34 illustrates the extent of reaction for an isothermal plug flow reactor versus that for the laminar flow reactor with zero, first, and second order reactions with heat transfer. To indicate the effect of laminar flow with heat transfer to the wall of the reactor on the rate constants, the ratio of the rate constants for an isothermal plug flow versus those for laminar flow with heat transfer are plotted in Figure 35.

The temperature effect for a second order reaction with constants similar to those for Me_2SiCl_2 hydrolysis reactions is shown in Figure 34. In the adiabatic case the temperature reaches a maximum of 2.6°C above the initial temperature at the completion of the reaction. With heat transfer to the sides of the reactor, the temperature rise follows that of the adiabatic reactor until the extent of reaction reaches 0.1; from here the temperature falls below that for the adiabatic case. At an extent of reaction of 0.9, the temperature for the laminar flow reactor is approximately 1.2°C below that of the adiabatic reactor. As the reaction reaches completion, the rate of reaction falls and heat transfer is more significant. If the reactor is long enough, the temperature in the reactor will eventually reach that of the surrounding medium in the heat exchanger. As Huang and Barduhn (24) have shown in their analysis, the temperature in a plug flow reactor
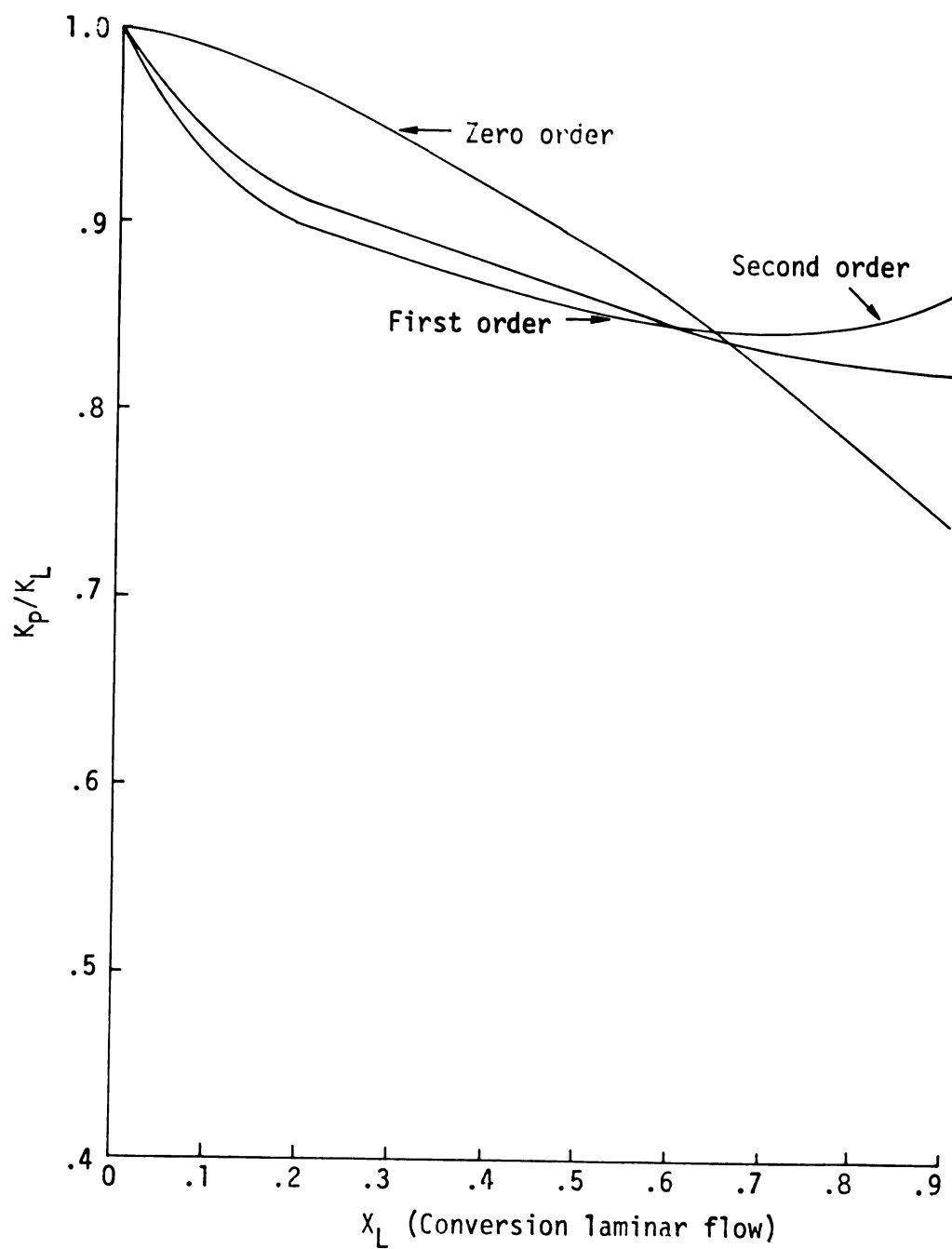
Figure 34.--Ratio of Rate Constants Versus Extent of Reaction
for Zero, First, and Second Order Reactions.

Adiabatic Rise

Temperature Rise °C

X_L (Extent of Reaction)
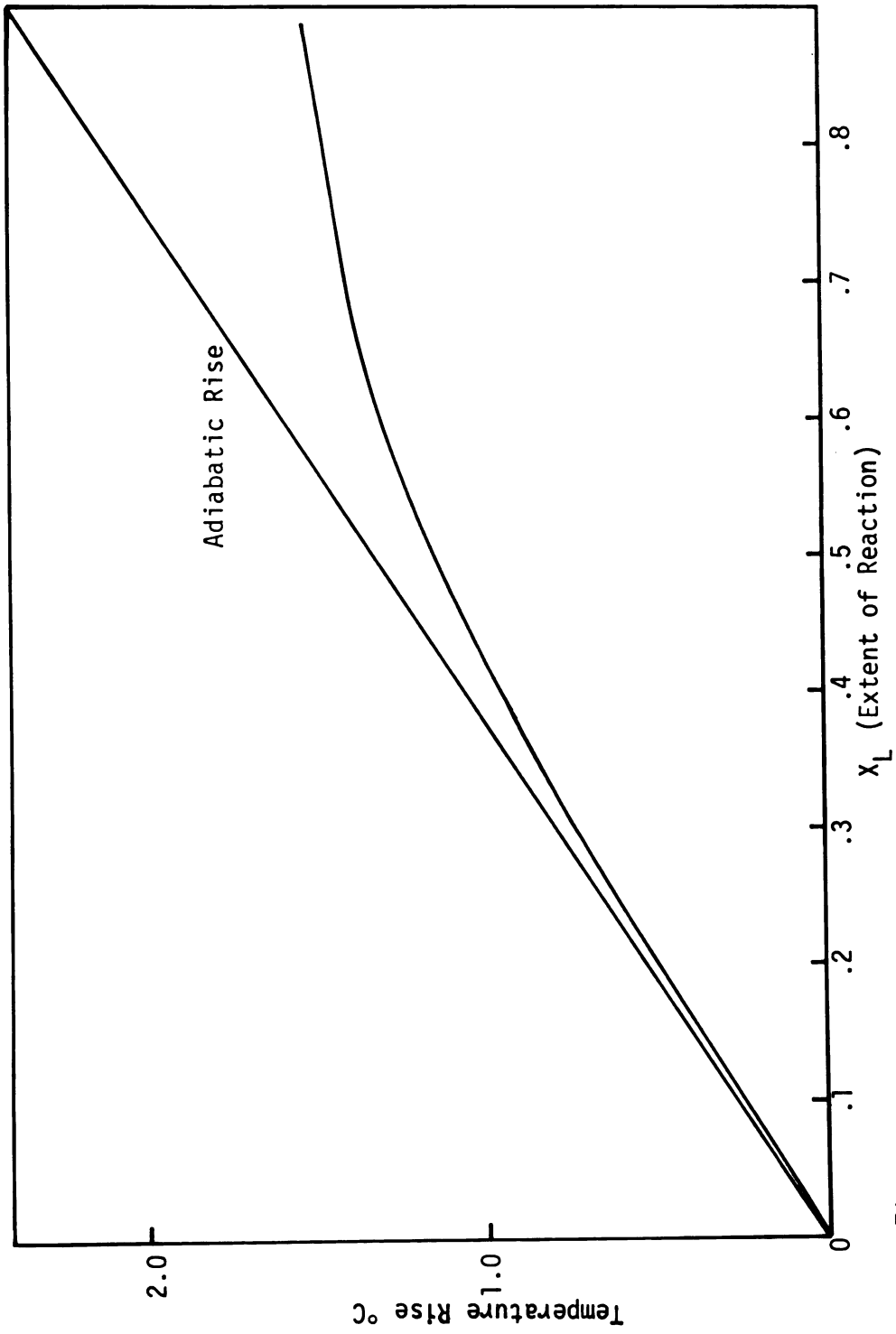
Figure 35.--Temperature Rise in a Laminar Flow Reactor With Heat Transfer to the Wall.

also reaches a maximum. However, since heat transfer in the plug flow reactor is grăter than the heat transfer in the laminar flow reactor, the maximum temperature will be lower in the plug flow reactor.

This analysis can be applied to flow reactors to determine the accuracy of the values of the rate constants determined from data on such reactors. It would be possible to predict at what initial concentrations a large error is introduced into the values of the rate constants by the laminar flow and isothermal assumptions. This should aid investigators collecting data on existing processes containing flow reactors.

CHAPTER VI

CONCLUSIONS

This study demonstrates the use of a laminar flow reactor to investigate fast reactions. The unique design of the flow system enables the residence time of the reactants to be varied without changing flow rates or location of the detector. Chapter V of this study shows the effect of the plug flow and isothermal assumptions on the rate constants determined using these assumptions.

In both the hydrolysis reactions of $PhSiCl_3$ and Me_2SiCl_2, the chlorines were replaced by hydroyl groups in series. In these studies, the hydrolysis of the first chlorine atom was considerably faster than that of the remaining chlorines. This is similar to the observation of Shaffer and Flanigen (6) in their study of various hydrolysis reactions of chlorosilanes.

It is proposed that the hydrolysis reactions of chlorosilanes proceed through the following mechanism:

$$(1) \quad H_2O \quad + \; \underset{}{>}Si\text{-}Cl \; \rightleftharpoons \; M \cdots {}^+H_2O\text{-}\overset{\diagup}{\underset{|}{Si}}\text{-}Cl^- \cdots M$$

$$(2) \; M \cdots {}^+H_2O\text{-}\overset{\diagup}{\underset{|}{Si}}\text{-}Cl^- \cdots M \longrightarrow HO\text{-}Si\overset{\diagup}{\diagdown} + \quad HCl$$
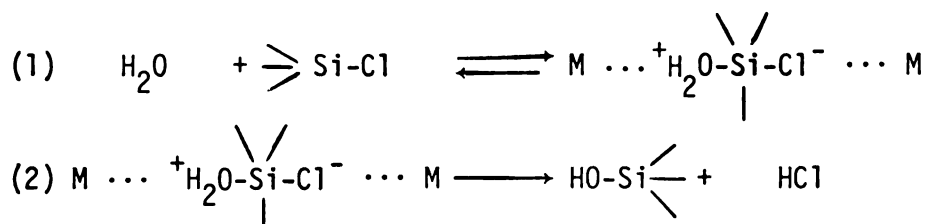
Reaction (1) represents the fast formation of the transition state intermediate and is followed by the slower breakdown

105

of the transition intermediate, reaction (2). M represents stabilization of the intermediate by the medium.

In both the hydrolysis reactions of $PhSiCl_3$ and Me_2SiCl_2, rate expressions first order with respect to water were used to describe the reaction. These rate equations were developed to model the reactions in a polar solvent. In a nonpolar solvent, the order of reaction with respect to water should be greater than one due to changes in the medium. Water has the ability to stabilize the transition state intermediate in the hydrolysis reactions. Hence, the addition of water to a nonpolar medium would noticeably increase the ability of the medium to stabilize the intermediate and thus increase the rate of reaction.

One of the principal aims of this study was to investigate the effects of HCl on the hydrolysis reactions of the chlorosilanes. The addition of HCl to the initial reagents markedly suppressed the rate of the hydrolysis reaction of $PhSiCl_3$. This effect can be explained by the reaction of the ion H^+ with with water to form the hydronium ion H_3O^+. Due to its positive charge, the hydronium ion is considerably less reactive toward the silane than the water molecule.

No effect on the rate of the hydrolysis reactions of Me_2SiCl_2 was observed with changes in the initial HCl concentration. This difference in the effect of HCl compared to its effect on $PhSiCl_3$ can be explained by the nature of the substitutent groups attached to the silicone. In the case of $PhSiCl_3$, the phenyl group is electron withdrawing which decreases the electron

density on the silicon. In Me_2SiCl_2, the methyl groups do not exhibit this electron withdrawing effect. Therefore, the hydronium ion is more reactive toward the silicon in Me_2SiCl_2. These different polar effects demonstrate the importance of the polar nature of the substituents on the rate of reaction.

A similar effect of the substituents has been observed in the case of base or acid catalyzed condensation reactions of silandiols (2: p. 213). In acid catalyzed condensation, electron negative groups decrease the electron density of the oxygen on the silanol, thus making attack by H^+ more difficult. In the case of base catalyzed condensation, the electron withdrawing groups have the opposite effect and facilitate the nucleophilic attack of OH^- on the silicon.

Under certain conditions, it may be reasonable to expect that HCl may actually catalyze the hydrolysis reaction of organo-chlorosilanes. One example of this may be a pseudo-first order reaction where H_2O is present in excess. Here, the amount of water in the hydronium form would not be sufficient and the increase in HCl would increase the polarity of the medium. Thus, an actual increase in the rate of reaction would result.

The significant aspects of this study are the demonstration of the laminar flow technique to study fast reactions, the description of the reaction models and mechanism, the effect of HCl on the systems, and the investigation of the plug flow and isothermal assumptions.

The reactions studied were modeled assuming that plug flow existed and that the system was isothermal. A principal aspect of this study was to determine the magnitude of the error introduced by these assumptions. The study of these assumptions begins with a concentration-temperature model of a laminar flow tubular reactor with heat transfer to the wall of the reactor. The model is based on a ring-shaped element in the reactor with conduction and convection of energy in the axial direction and with conduction in the radial direction.

Plots of concentration for a laminar flow reactor with heat transfer versus an isothermal plug flow reactor are presented. From this analysis, the effect of these assumptions on the rate constants is determined.

BIBLIOGRAPHY

BIBLIOGRAPHY

1. Sommer, L. H., Stereochemistry, Mechanism, and Silicon, McGraw Hill, New York (1965).

2. Noll, W., Chemistry and Technology of Silicones, Academic Press, New York (1968).

3. Mileshkevick, V. P.; Nikolaev, G. A.; Evdokimov, V.F.; and Karlin, A.V., Zh. Ohsch. Klim., 41 (3), 643 (1971).

4. Allen, A. D., and Modena, G., J. Chem. Soc., 3567 (1963).

5. Chipperfield, J. R., and Prince, R. H., J. Chem. Soc., 3657 (1963).

6. Shaffer, L. H., and Flanigen, E. M., Phys. Chem., 61, 1591 (1957).

7. Kleinhenz, T. A., and Hawley, M. C., M.S. Thesis, Mich. State Univ. (1970).

8. Kriengsmann, H., and Schowtka, K. H., Z. Physik. Che., 209, 261 (1958).

9. Smith, A. L., Spectrochim. Acta., 23A, 1075 (1967).

10. Sadtle Standard Spectra, Sadtler Research Laboratories, Philadelphia, Penn. 12137 (1972).

11. Takiguchi, T., J. Am. Chem. Soc., 2359 (1959).

12. Tyler, L. J., J. Amer. Chem. Soc., 77, 770 (1955).

13. Chrzczonowicz, S., and Chojnowski, J., Rochzinki Chemii. Ann. Soc. Chim. Polororum, 36, 1293 (1962).

14. Smith, D. C., and Miller, E. C., J. Opt. Soc. Am., 34: 130 (1944).

15. Dye, J. L., and Nicely, V. A., J. Chem. Ed. 48: 443 (1971).

16. Brown, T. L., J. Chem. Phys., 24, 1281 (1956).

17. Smith, A. L., J. Chem. Phys., 21, 1997 (1953).

18. Kendall, D. N., Applied Infrared Spectroscopy, Reinhold Publishing Corp., New York (1966).

19. Petrov, A. D.; Mironov, B. F.; Ponomarenko, V.A.; and Cherngshev, E. A., Synthesis of Organisolicon Monomers, New York, Consultants Bureau (1964).

20. Roberts, J. D., and Caserio, M. C. Modern Organic Chemistry, W. A. Benjamin, New York (1967).

21. Slowinski, E. J., and Claver, G. C., J. Opt. Soc. Am., 45, 1281 (1956).

22. Brown, T. L., J. Chem. Phys., 24, 1281 (1956).

23. Johnson, M. M., Ind. Eng. Chem. Fundam., 9, 681 (1970).

24. Huang, J. S., and Barduhn, A. J., A. I. Ch. E. J., 20,6,1228

25. Merrill, L. W., and Hamrin, C. E., A. I. Ch. E. J., 16, 194 (1970).

26. Bird, R. B.; Stewart, W. E.; and Lightfoot, E. N., Transport Phenomena, John Wiley & Sons, Inc., New York (1960).

A	Absorption
A_o	Base line absorption
C	Constant in equation (3.15)
C	Concentration (moles/liter)
C_b	Average concentration in reactor (moles/liter)
C_o	Initial concentration (moles/liter)
C_p	Heat capacity (cal/g-°C)
d	Infrared cell diameter (cm)
ΔE	Activation energy (cal/mole)
ΔH	Heat of reaction (cal/mole)
K	Thermal conductivity (cal/sec-cm-°C)
K_L	Rate Constant for laminar Flow
K_P	Rate constant for plug flow
K_o	Frequency factor
K_1, K_2, K_3	Rate constants defined by equations (3.3)-(3.6) $(liters/mole)^{1+n}/sec$
K_1, K_2, K_2'	Rate constants defined by equations (4.2)-(4.6) (liters/mole-sec)
K_1, K_2	Rate constants defined by equations (3.9)-(3.14) (liters/mole-sec)
L	Length of reactor (cm)
M	Moles/liter
n	Power to which concentrations are raised
n	Number of maximum equation (3.2)

n_1, n_2	Refractive index of solvent
P	Pressure drop in reactor (dyne/cm^2)
q_r	Heat flux (cal/cm^2-sec)
q_z	Heat flux (cal/cm^2-sec)
R	Reactor radius (cm)
R_c	Gas constant
r	Reactor radius (cm)
r_e	Rate of reaction
T	Temperature (°C)
T_0	Reference temperature (°C)
T_w	Temperature at wall of reactor (°C)
V_z	Velocity in reactor (cm/sec)
V_M	Maximum velocity in reactor (cm/sec)
X	Extent of reaction
z	Axial direction in reactor
ε	Extinction coefficient (liters/cm-mole)
η	Dimensionless length
θ	Dimensionless temperature
μ	Viscosity (poise)
μ_1, μ_2	Wave numbers (cm^{-1})
ξ	Dimensionless radius
ρ	Density (g.cm^3)

APPENDICES

APPENDIX A

DATA USED TO MODEL THE HYDROLYSIS

REACTIONS OF PhSiCl$_3$

AND Me$_2$SiCl$_2$

APPENDIX A

DATA USED TO MODEL THE HYDROLYSIS REACTIONS

OF $PhSiCl_3$ AND Me_2SiCl_2

TABLE A-1.--Summary of Initial Run Conditions for the Hydrolysis Reactions of $PhSiCl_3$.

Concentration* (Moles/Liter)	Run				
	20	21	22	24	26
$PhSiCl_3$	0.0379	0.0672	0.0849	0.0329	0.061
$PhSiCl(OH)_2$	0.0351	0.0278	0.00712	0.0447	0.0242
Total Silane	0.073	0.095	0.0918	0.0776	0.0852
Water	0.215	0.291	0.242	0.259	0.0807
HCl	1.21	1.463	0.338	0.0	0.0
Temperature	273.0°K	273.0°K	273.0°K	273.0°K	273.0°K

*Concentrations are based on mixed reactants.

TABLE A-2.--Absorption and Concentration Values at Various Residence Times for the Hydrolysis Experiments of $PhSiCl_3$.

$\bar{t}$ (Sec.)	Absorption			Concentration (Moles/Liter)		
	$518\ cm^{-1}$	$527\ cm^{-1}$	$465\ cm^{-1}$	$PhSiCl_3$	$PhSiCl_2(OH)$	$PhSi(OH)_3$

Run 20 initial concentrations (moles/liter): $M_{H_2O} = 0.215$, $M_{HCl} = 1.21$ Cell spacing = 0.116 cm.

$\bar{t}$ (Sec.)	$518\ cm^{-1}$	$527\ cm^{-1}$	$465\ cm^{-1}$	$PhSiCl_3$	$PhSiCl_2(OH)$	$PhSi(OH)_3$
0.066	trace	0.272	0.024	trace	0.05997	0.008693
0.165	0.0	0.223	0.028	0.0	0.0492	0.01014
0.231	0.0	0.199	0.035	0.0	0.0439	0.0127
0.297	0.0	0.191	0.045	0.0	0.0421	0.0163
0.429	0.0	0.142	0.090	0.0	0.0313	0.326
0.561	0.0	0.118	0.095	0.0	0.0260	0.0344
0.752	0.0	0.084	0.095	0.0	0.0186	0.0344

Run 21 initial concentrations (moles/liter): $M_{H_2O} = 0.291$, $M_{HCl} = 1.463$ Cell spacing = 0.0113 cm.

$\bar{t}$ (Sec.)	$518\ cm^{-1}$	$527\ cm^{-1}$	$465\ cm^{-1}$	$PhSiCl_3$	$PhSiCl_2(OH)$	$PhSi(OH)_3$
0.066	trace	0.322	0.013	trace	0.07275	0.004825
0.159	0.0	0.276	0.046	0.0	0.0624	0.0171
0.224	0.0	0.273	0.049	0.0	0.0617	0.0182
0.291	0.0	0.225	0.053	0.0	0.0508	0.0197
0.357	0.0	0.226	0.075	0.0	0.0511	0.02784
0.423	0.0	0.174	0.085	0.0	0.0393	0.03155
0.489	0.0	0.155	0.090	0.0	0.0350	0.0334
0.753	0.0	0.105	0.122	0.0	0.0237	0.0453

TABLE A-2.--Continued.

$\bar{t}$ (Sec.)	Absorption			Concentration (Moles/Liter)		
	518 cm^{-1}	527 cm^{-1}	465 cm^{-1}	PhSiCl$_3$	PhSiCl$_2$(OH)	PhSi(OH)$_3$

Run 22 initial concentrations (moles/liter): $M_{H_2O} = 0.242$, $M_{HCl} = 0.338$
Cell spacing = 0.0154 cm.

0.066	0.0	0.456	0.033	0.0	0.0757	0.009
0.159	0.0	0.351	0.082	0.0	0.0583	0.02237
0.198	0.0	0.286	0.096	0.0	0.0465	0.0262
0.291	0.0	0.192	0.135	0.0	0.0319	0.0368
0.423	0.0	0.222	0.161	0.0	0.03687	0.0439
0.489	0.0	0.207	0.184	0.0	0.0344	0.0502
0.621	0.0	0.144	0.210	0.0	0.0239	0.0573
0.753	0.0	0.119	0.211	0.0	0.01976	0.0576
0.951	0.0	0.126	0.220	0.0	0.0209	0.0600
1.083	0.0	0.054	0.218	0.0	0.00897	0.0595

Run 24 initial concentrations (moles/liter): $M_{H_2O} = 0.259$, $M_{HCl} = 0.0$
Cell spacing = 0.0119 cm.

0.066	0.0	0.189	0.076	0.0	0.0406	0.0268
0.1387	0.0	0.129	0.135	0.0	0.0277	0.0477
0.217	0.0	0.056	0.156	0.0	0.0120	0.0551
0.299	0.0	0.036	0.176	0.0	0.0077	0.0621
0.386	0.0	0.020	0.183	0.0	0.00429	0.0646
0.482	0.0	0.015	0.206	0.0	0.00322	0.0727
0.614	0.0	0.014	0.209	0.0	0.0301	0.0737
1.926	0.0	0.010	0.218	0.0	0.00215	0.077

TABLE A-2.--Continued.

t (Sec.)	Absorption			Concentration (Moles/Liter)		
	$518\ cm^{-1}$	$527\ cm^{-1}$	$465\ cm^{-1}$	$PhSiCl_3$	$PhSiCl_2(OH)$	$PhSi(OH)_3$
Run 26 initial concentrations (moles/liter): $M_{H_2O} = 0.0807$, $M_{HCl} = 0.0$ Cell spacing = .0121 cm						
0.066	0.0	0.383	0.0010	0.0	0.0812	0.000349
0.1023	0.0	0.373	0.0028	0.0	0.079	0.000573
0.168	0.0	0.36	0.00563	0.0	0.0763	0.00196
0.234	0.0	0.3096	0.0105	0.0	0.0656	0.00366
0.300	0.0	0.322	0.0164	0.0	0.0682	0.00572
0.366	0.0	0.336	0.0136	0.0	0.0712	0.00474
0.433	0.0	0.342	0.0206	0.0	0.0725	0.00718

TABLE A-3.--Summary of Initial Run Conditions for the Hydrolysis Reactions of $PhSiCl_3$ in Acetonitrile.

Concentration* (Moles/Liter)	Run	
	16	17
$PhSiCl_3$	0.0669	0.064
$PhSiCl_2(OH)$	0.0032	0.0046
Total Silane	0.0701	0.069
H_2O	0.218	0.22
Temperature	273.0°K	273.0°K

*Concentrations are based on mixed reactants.

TABLE A-4.--Absorption and Concentration Values at Various Residence Times for the Hydrolysis Reactions of $PhSiCl_3$ in Acetonitrile.

$\bar{t}$ (Sec.)	Absorption			Concentration (Moles/Liter)		
	$518\ cm^{-1}$	$527\ cm^{-1}$	$465\ cm^{-1}$	$PhSiCl_3$	$PhSiCl_2(OH)$	$PhSi(OH)_3$
Run 16 initial concentrations (moles/liter): $M_{H_2O} = 218$, $M_{HCl} = 0.0$ Cell spacing = 0.0121 cm.						
0.0735	0.076	0.049	0.136	0.141	0.0103	0.0474
0.0735	0.088	0.068	0.133	0.163	0.0144	0.0464
0.147	0.028	0.073	0.146	0.005	0.0154	0.0509
0.220	0.026	0.051	0.171	0.005	0.0110	0.0596
0.294	0.014	0.055	0.158	0.002	0.0116	0.0551
0.441	0.001	0.033	0.181	trace	0.0070	0.0631
0.6613	0.0	0.01	0.195	0.0	0.0021	0.0680
1.0286	0.0	0.0	0.207	0.0	0.0	0.0722
2.79	0.0	0.0	0.216	0.0	0.0	0.0753
Run 17 initial concentrations (moles/liter): $M_{H_2O} = 0.22$, $M_{HCl} = 0.0$ Cell spacing = 0.0123 cm.						
0.095	0.059	0.112	0.144	0.0107	0.023	0.0494
0.142	0.022	0.085	0.223	0.0040	0.0176	0.0765
0.190	0.038	0.097	0.210	0.0069	0.0201	0.0720
0.237	0.055	0.098	0.188	0.0100	0.0202	0.0645
0.248	0.055	0.104	0.190	0.0100	0.0216	0.0650
0.379	0.035	0.057	0.214	0.0064	0.0118	0.0734
0.474	0.030	0.065	0.220	0.0055	0.0135	0.0755
0.569	0.024	0.043	0.232	0.0044	0.0089	0.0796
0.663	0.030	0.037	0.227	0.0055	0.0114	0.0779
0.853	0.001	0.001	0.237	trace	trace	0.0813
1.396	0.0	0.0	0.242	0.0	0.0	0.0831

122

TABLE A-5.--Summary of Initial Run Conditions for the Hydrolysis
Reactions of Me_2SiCl_2.

Concentration* (Moles/Liter)	Run						
	37	38	42	44	45	46	49
Me_2SiCl_2	0.1108	0.0937	0.0575	0.0546	0.07	0.0595	0.017
$Me_2SiCl(OH)$	0.0175	0.0148	0.0503	0.0394	0.0279	0.048	0.05125
$Me_2Si(OH)_2$	0.0	0.0	0.0163	0.011	0.0051	0.0155	0.00884
Total Silane	0.1283	0.109	0.1241	0.106	0.103	0.123	0.077
HCl	0.569	0.4815	0.0	0.0	0.0	0.0	0.0
H_2O	0.286	0.418	0.323	0.241	0.236	0.195	0.180
Temperature (°K)	273.0	273.0	267.5	273.0	273.0	273.0	252.0

*Concentrations are based on mixed reactants.

TABLE A-6.--Absorption and Concentration Values at Various Residence
Times for the Hydrolysis Experiments of Me_2SiCl_2.

$\bar{t}$ Sec.)	Absorption			Concentration (Moles/Liter)		
	532 cm^{-1}	572 cm^{-1}	510 cm^{-1}	Me_2SiCl_2	$Me_2SiCl(OH)$	$Me_2Si(OH)_2$

Run 37 initial concentrations: $M_{H_2O} = 0.320$, $M_{HCl} = 0.569$; temperature = 273.0°K; cell spacing = 0.0115 cm.

0.0637	0.038	0.141	0.021	0.026	0.102	0.0179
0.1687	0.018	0.149	0.029	0.0123	0.108	0.0247
0.2961	0.0085	0.130	0.325	0.0058	0.094	0.0277
0.4234	0.001	0.123	0.040	0.0007	0.089	0.0341
0.6781	0.0	0.128	0.036	0.0	0.0926	0.03069
1.187	0.0	0.125	0.038	0.0	0.0904	0.0324
1.569	0.0	0.131	0.039	0.0	0.0947	0.0333
1.888	0.0	0.130	0.040	0.0	0.0940	0.0341
2.524	0.0	0.129	0.039	0.0	0.0933	0.0333

Run 38 initial concentrations: $M_{H_2O} = 0.459$, $M_{HCl} = 0.4815$; temperature = 273.0°K; cell spacing = 0.0115 cm.

0.0913	0.01	0.127	0.017	0.0068	0.0922	0.0145
0.333	0.003	0.121	0.026	0.0020	0.0878	0.0222
0.6985	0.001	0.121	0.039	0.0007	0.0878	0.0333
1.410	0.0	0.128	0.040	0.0	0.0929	0.0342
1.794	0.0	0.128	0.039	0.0	0.0929	0.0333
2.251	0.0	0.127	0.041	0.0	0.0922	0.0350
2.707	0.0	0.132	0.035	0.0	0.0958	0.0299
3.62	0.0	0.131	0.037	0.0	0.0951	0.0316

TABLE A-6.--Continued.

t (Sec.)	Absorption			Concentration (Moles/Liter)		
	532 cm^{-1}	572 cm^{-1}	510 cm^{-1}	Me_2SiCl_2	$Me_2SiCl(OH)$	$Me_2Si(OH)_2$

Run 42 initial concentrations: $M_{H_2O} = 0.180$, $M_{HCl} = 0.0$; temperature = 267.5°K; cell spacing = 0.010 cm.

0.121	0.01127	0.0918	0.032	0.00606	0.0744	0.0304
0.121	0.01127	0.0918	0.0322	0.00529	0.0744	0.0306
0.161	0.0081	0.0931	0.0300	0.00388	0.0754	0.0285
0.3565	0.009	0.0988	0.0472	0.00274	0.0801	0.0450
0.484	0.0	0.09503	0.0565	0.00139	0.0771	0.0538
0.611	0.0	0.0962	0.057	0.00689	0.0781	0.0543
0.930	0.0	0.0956	0.0583	0.00767	0.0776	0.0555
2.39	0.0	0.0954	0.0589	0.0	0.0774	0.0561
2.62	0.0	0.0954	0.0585	0.0	0.0774	0.0553

Run 44 initial concentrations: $M_{H_2O} = .241$, $M_{HCl} = 0.0$; temperature = 273.0°K; cell spacing = 0.00961 cm.

0.0156	0.0137	0.0746	0.0172	0.0112	0.0648	0.0175
0.202	0.00888	0.0729	0.0282	0.0073	0.0633	0.0287
0.265	0.00478	0.0709	0.0287	0.0039	0.0616	0.0292
0.327	0.001	0.0747	0.0344	0.0008	0.0649	0.0350
0.389	0.0032	0.0726	0.0308	0.0026	0.063	0.0313
0.452	0.0	0.0749	0.0386	0.0	0.065	0.0392
0.826	0.0	0.0726	0.0450	0.0	0.063	0.0457
1.20	0.0	0.0742	0.0455	0.0	0.0644	0.0462
1.823	0.0	0.0746	0.0450	0.0	0.0647	0.0457
2.1342	0.0	0.0765	0.0448	0.0	0.0663	0.0455

TABLE A-6.--Continued.

$\bar{t}$ (Sec.)	Absorption			Concentration (Moles/Liter)		
	532 cm^{-1}	572 cm^{-1}	510 cm^{-1}	Me_2SiCl_2	$Me_2SiCl(OH)$	$Me_2Si(OH)_2$

Run 45 initial concentrations: M_{H_2O} = .236 M, M_{HCl} = 0.0; temperature = 273.0°K; cell spacing = 0.0098 cm.

0.0921	0.0348	0.065	0.025	0.0279	0.0554	0.0250
0.0921	0.0274	0.066	0.028	0.0220	0.0562	0.0280
0.143	0.0162	0.0687	0.0315	0.0130	0.0585	0.0315
0.207	0.0172	0.065	0.0303	0.0138	0.0554	0.0303
0.334	0.0140	0.070	0.0313	0.0112	0.0597	0.0313
0.416	0.0155	0.075	0.0300	0.0124	0.0640	0.0300
0.588	0.013	0.074	0.0318	0.0104	0.0631	0.0318
0.715	0.0052	0.0701	0.034	0.0042	0.0598	0.0340
1.224	0.013	0.0672	0.046	0.0104	0.0573	0.0460
1.86	0.006	0.0669	0.0517	0.0048	0.0570	0.0517

Run 46 initial concentrations: M_{H_2O} = 0.195 M, M_{HCl} = 0.0; temperature = 273.0°K; cell spacing = 0.0105 cm.

0.0792	0.0337	0.105	0.02365	0.0252	0.0835	0.0220
0.0792	0.0356	0.0993	0.0241	0.0266	0.0790	0.0224
0.142	0.03128	0.1063	0.02859	0.0234	0.0846	0.0266
0.206	0.2592	0.1091	0.03192	0.0194	0.0868	0.0297
0.3328	0.02141	0.0975	0.02556	0.0160	0.0776	0.0238
0.4596	0.02158	0.09832	0.0275	0.0161	0.0783	0.0232
0.5864	0.0158	0.0967	0.0430	0.0122	0.0770	0.0363

TABLE A-6.--Continued.

$\bar{t}$ (Sec.)	Absorption			Concentration (Moles/Liter)		
	$532\ cm^{-1}$	$572\ cm^{-1}$	$510\ cm^{-1}$	Me_2SiCl_2	$Me_2SiCl(OH)$	$Me_2Si(OH)_2$

Run 49 initial concentrations: $M_{H2O} = 0.180$, $M_{HCl} = 0.0$; temperature = 262.0°K; cell spacing = .0104 cm.

$\bar{t}$ (Sec.)	$532\ cm^{-1}$	$572\ cm^{-1}$	$510\ cm^{-1}$	Me_2SiCl_2	$Me_2SiCl(OH)$	$Me_2Si(OH)_2$
0.158	0.0242	0.211	0.0453	0.00643	0.0596	0.015
0.281	0.0124	0.203	0.0515	0.00329	0.0573	0.017
0.3456	0.0112	0.194	0.0548	0.00297	0.0548	0.0160
0.410	0.0127	0.206	0.0527	0.00337	0.0582	0.0154
0.5394	0.0124	0.203	0.0584	0.00329	0.0574	0.0171
0.8721	0.0131	0.207	0.0605	0.00348	0.0585	0.0177
1.315	0.00796	0.202	0.0623	0.00211	0.0571	0.0182
1.638	0.00351	0.203	0.0577	0.00093	0.0574	0.0169
1.961	0.001	0.206	0.07328	0.00026	0.0582	0.0215
2.284	0.001	0.204	0.0707	0.00026	0.0576	0.0207
3.059	0.0	0.205	0.07945	0.0	0.0579	0.0233
4.803	0.0	0.190	0.09938	0.0	0.0549	0.0291

TABLE A-7.--Absorbance Data Obtained During the Condensation Reaction of $PhSi(OH)_3$.

Time (sec.)	0.0	0.195	0.30	0.49	0.625	0.945	1.29
Absorbance of $PhSi(OH)_3$	1.6	1.31	1.12	0.735	1.01	0.64	.608

APPENDIX B

NUMERICAL METHOD AND FORTRAN PROGRAM

USED TO ANALYZE A LAMINAR FLOW

REACTOR WITH HEAT TRANSFER

APPENDIX B

NUMERICAL METHOD AND FORTRAN PROGRAM USED TO ANALYZE

A LAMINAR FLOW REACTOR WITH HEAT TRANSFER

As developed in Chapter V, the differential equations describing the temperature and concentration profiles in laminar flow are:

$$\frac{dX}{d\eta} = \frac{\beta}{(1 - \xi^2)} e^{-\gamma/\theta} (1 - X)^N \qquad (B.1)$$

$$(1 - \xi^2) \frac{\partial\theta}{\partial\eta} - \left[(1 - X)^N e^{-\gamma/\theta}\right] = \frac{\alpha}{\xi} \left[\frac{\partial\theta}{\partial\xi} + \xi \frac{\partial^2\theta}{\partial\xi^2}\right] \qquad (B.2)$$

with the following boundary conditions:

B.C. 1 for equation (B.1) at $\eta = 0$, $X = 0$ for all ξ

B.C. 1 for equation (B.2) at $\eta = 0$, $\theta = \frac{\rho C_p T_w}{(-\Delta H)C_0}$ for all ξ

B.C. 2 for equation (B.2) at $\xi = 1$, $\theta = \frac{\rho C_p T_w}{(-\Delta H)C_0}$ for all η

B.C. 3 for equation (B.2) at $\xi = 0$, $\frac{\partial\theta}{\partial\xi} = 0$ for all η

128

Here, an explicit method is developed to integrate these partial differential equations. The partial derivatives may be approximated by the following finite-difference formulas:

$$\frac{\partial X}{\partial \eta} = \frac{X_{j+1,i} - X_{j,i}}{\Delta \eta} \tag{B.3}$$

$$\frac{\partial \theta}{\partial \eta} = \frac{\theta_{j+1,i} - \theta_{j,i}}{\Delta \eta} \tag{B.4}$$

$$\frac{\partial \theta}{\partial \xi} = \frac{\theta_{j,i+1} - \theta_{j,i}}{\Delta \xi} \tag{B.5}$$

$$\frac{\partial^2 \theta}{\partial \xi^2} = \frac{\theta_{j,i+1} - 2\theta_{j,i} + \theta_{j,i-1}}{\Delta \xi^2} \tag{B.6}$$

Substituting these expressions into equations (B.1) and (B.2), we have:

$$(1 - \xi^2)\left[\frac{\theta_{j+1,i} - \theta_{j,i}}{\Delta \eta}\right] = \beta(1 - X_{j,i}) \; e^{-\gamma/\theta_{j,i}}$$

$$+ \frac{\alpha}{\xi}\left[\left(\frac{\theta_{j,i+1} - \theta_{j,i}}{\Delta \xi}\right)\right.$$

$$\left.+ \xi\left(\frac{\theta_{j,i+1} - 2\theta_{j,i} + \theta_{j,i-1}}{\Delta \xi^2}\right)\right] \tag{B.7}$$

$$\frac{X_{j+1,i} - X_{j,i}}{\Delta \eta} = \frac{\beta}{(1 - \xi^2)} \; e^{-\gamma/\theta_{j,i}} \; (1 - X)^N \tag{B.8}$$

Solving for $\theta_{j+1,i}$ and $X_{j+1,i}$:

$$\theta_{j+1,i} = \left[\Delta\eta/(1 - \xi^2)\right] * \left[\beta * (1 - X_{j,i})^2\right] * e^{-\gamma/\theta_{j,i}}$$

$$+ (\alpha/\xi) * \left[(\theta_{j,i+1} - \theta_{j,i})/\Delta\xi\right] + \alpha * (\theta_{j,i+1} - 2 * \theta_{j,i}$$

$$+ \theta_{j,i-1})/\Delta\xi^2) + \theta_{j,i} \tag{B.9}$$

$$X_{j+1,i} = \left[(\Delta\eta * \beta)/(1 - \xi^2)\right] * e^{-\gamma/\theta_{j,i}} * (1 - X_{j,i})^N$$

$$+ X_{j,i} \tag{B.10}$$

The following constants were used to model the reactions in the laminar flow reactor.

Constant	Symbol	Value	Units	Derivation
Heat capacity	C_p	.438	cal/g.°C	1,2-dimethoxyethane
Density	ρ	.8683	g/ml	1,2-dimethoxyethane
Initial temperature	T_o	273.0	°K	system
Heat of reaction	ΔH	-10000.0	cal/g-mole	bond energy differences = -7000 cal/ gmole for 1 Cl replaced by 1 OH
Initial concentration	C_o	.1	g-mole/liter	system
Thermal conductivity	K	.00033	cal/sec cm^2 °C/cm	ethyl ether
Maximum velocity	V_m	34.	cm/sec	system
Reactor radius	R	.108	cm	system

Constant	Symbol	Value	Units	Derivation
Frequency factor	K_o	1.4×10^8	$mole^{-1}sec^{-1}$	half life of .5 sec. for second order reaction
Activation energy	ΔE	10000.0	cal/g-mole	range of experimental values
Gas constant	R_c	1.987	cal/g-mole/°C	constant

Dimensionless parameters for equations (B.9) and (B.10) used for second order reaction.

Constant	Derivation	Value	Symbol in Program
Initial temperature	$\dfrac{\rho * C_p * T_w}{(-\Delta H) * C_o}$	103.826	Const (1)
Alpha	$\dfrac{K}{\rho * \hat{C}_p * V_m * R}$	2.363×10^{-4}	ALPHA
Beta	$\dfrac{R * K_o}{V_m \, C_o^{n-1}}$	6.44×10^5	BETA
Gamma	$\dfrac{\Delta E * \rho * C_p}{R_c * \Delta H * C_o}$	1.914×10^3	GAMMA
Temperature			THETA (J,I)
Extent of reaction			X (J,I)

Program LAM begins with the input and output of the data necessary for this integration. The sum of the point velocities multiplied by the area is then calculated. This value is used to calculate the mixing cup temperature and the extent of reaction. Next the concentration and temperature profiles are calculated

using equations (5.20) and (5.21). The inner DO loop calculates the temperature and extent of reaction across the radial direction and the outer DO loop advances along the axial direction of the reactor. The mixing cup temperature and extent of reaction are then calculated and printed. These values are compared to the isothermal plug flow reactor and their ratio to that of the isothermal plug flow case printed.

```
      PROGRAM LAM  (INPUT,TAPE60=INPUT,OUTPUT,TAPE61=OUTPUT)
      DIMENSION CONST(5),THETA(21,200),X(21,200),AX(21,21),AVET(21,21)
C
C     THIS PROGRAM COMPUTES THE CONCENTRATION AND TEMPERATURE PROFILES
C     FOR A LAMINAR FLOW REACTOR.  THESE PROFILES ARE THEN USED TO
C     CALCULATE THE AVERAGE EXTENT OF REACTION AND MIXING CUP
C     TEMPERATURE.  THE EXTENT OF REACTION IS THEN COMPARED TO THAT FOR
C     AN ISOTHERMAL PLUG FLOW REACTOR.
C
C     INPUT DATA USED IN THIS CALCULATION
C
      PI=3.1416
      RADIUS = .108
      IB=0
      READ(60,100)(CONST(NI) ,NI=1,4)
  100 FORMAT(4F20.10)
      READ(60,101) N,M
  101 FORMAT(2I5)
      READ (60,102) CO,AK,VB,TW,NUR
  102 FORMAT( 4F10.5,I5)
      DXI=1./N
      DETA=.5
```

134

```
C
C        OUTPUT OF DATA
C
      WRITE(61,214) NOR
      WRITE(61,211) N
211 FORMAT( // * NUMBER OF RADIAL INCREMENTS EQUALS *,I3)
214 FORMAT( // * ORDER OF REACTION IS * ,I3)
      ALPA=CONST(2) $ GAMMA=CONST(4) $ BETA=CONST(3)
      WRITE(61,212) ALPA, GAMMA, BETA
      WRITE(61,213) CONST(1), TW
212 FORMAT( // * ALPHA EQUALS *, F10.5, // * GAMMA EQUALS *, F10.5,
   1 // * BETA EQUALS *F15.5)
213 FORMAT(// * INITIAL DIMENSIONAL TEMPERATURE IS *,F10.5,// * INITIAL
   1 TEMPERATURE IS *,F10.5)
C
C        SET THE INITIAL AND BOUNDARY CONDITIONS
C
      M1=N+2
      M2=N+1
      XI=0.0 $ ETA =0.0
      DO 10 J = 1,M
      DO 10 I = 1,M
      X(J,I) = 0.0
10 THETA(J,I) =0.0
      DO 11 I=1,M1
11 THETA (1,I)=CONST(1)
      DO 12 J=1,M
12 THETA(J,1)=CONST(1)
```

```
C        CALCULATION OF AVERAGE VOLECITY
C
         SVMB=0.0
         VM=34.
         XI=DXI/2.
         DO 20 IA = 1, N
         V = VM * ( 1.-XI**2)
         VMB = V * 2.*PI * XI * DXI
         XI = DXI + XI
   20    SVMB = SVMB + VMB
         VB = SVMB + VMB
         WRITE (61,210) SVMB
  210    FORMAT(//* THE BULK VELOCITY EQUALS *,F10.5)
C
C        CALCULATION OF TEMPERATURE AND CONCENTRATION PROFILES
C
         DO 13 J=1,M
         ETA=ETA+DETA
         TIME=ETA *RADIUS/VB
         WRITE(61,201)ETA,TIME
  201    FORMAT( //* VALUES AT LENGTH ETA = *,F10.5,*   TIME = *,F10.5,*
        1 SEC *)
         THETA(J,M2+1) = THETA(J,M2)
         XI=1.0
         DO 14 I = 2, M2
         XI=XI-DXI
         THETA(J,I+1) =(DETA/(1.-XI**2))*(BETA*((1.-X(J,I))**NOR)*EXP(-GA
        1 MMA/THETA(J,I))+(ALPA/XI)*((THETA(J,I+1)-THETA(J,I))/DXI)
        2+ALPA * (THETA(J,I+1) - 2.*THETA(J,I) + THETA(J,I-1)))/
        3( DXI**2)) + THETA(J,I)
         X(J,I+1)=(DETA*BETA)/(1. -  XI**2) * EXP(-GAMMA/THETA(J,I))
        1*((1.-X(J,I))**NOR)+X(J,I)
         IF(X(J+1,I).GT. 1.0) X(J+1,I)=1.0
```

```
C
C        OUTPUT OF CONCENTRATION PROFILES
         WRITE(61,202) XI,THETA(J+1,I),X(J+1,I)
202 1FORMAT(* RADIUS = *,F10.5,* TEMPERATURE = *,F10.5,* EXTEN
      1T OF REACTION = *,F10.5)
 14 CONTINUE
         IF(IB.GT. 4.) GO TO 30
         IB=IB+1
         GO TO 13
C
C        CALCULATION OF EXTENT OF REACTION AND AVERAGE TEMPERATURE
C
 30 CONTINUE
         STB=0.0
         X2=0.0
         XI=1.0
         XI=DXI/2.0
         XB=0.0
         DA=31  JK=1,N
         AVET(J+1,IA) =(THETA(J+1,IA) + THETA(J+1,IA-1))/2.0
       T = AVET(J+1,IA)*VM*(1.-XI**2)*2. *PI*XI*DXI/SVMB
         STB = STB + T
         AX(J+1,IA) =(X(J+1,IA) + X(J+1,IA-1))/2.0
         X2=AX(J+1,IA)*VM*(1.-XI**2)2.*PI*XI*DXI /SVMB
         XI=XB+DXI
 31 CONTINUE
       TEM =(STB/CONST(1))*TW
```

```
C
C      OUTPUT OF EXTENT OF REACTION AND MIXING CUP TEMPERATURE
C
       WRITE(61,221) TEM
   221 FORMAT(//* THE MIXING CUP TEMPERATURE IS *, F10.5)
       WRITE(61,203) STB,XB
   203 FORMAT(/* THE DIMENSIONLESS TEMPERATURE IS *,F10.5,/* THE EXTENT
      1 OF REACTION IS *,F10.5,/)
C
C      COMPUT EXTENT OF REACTION IN PLUG FLOW
C
       T=ETA*RADIUS/VB
       X1 = (AK*CO*T/(1. + AK*CO*T))
       IF(X1.GT. 1.0) X1 = 1.0
       XR=XB/X1
C
C      OUTPUT OF RATIO OF EXTENT OF REACTION
C
       WRITE(61,220) XR
   220 FORMAT(// * THE RATIO OF CONVERSION IS * F10.5)
       IB=0
    13 CONTINUE
```

138

VALUES AT LENGTH ETA =   24.00000   TIME =   .15247 SEC

RADIUS =   .95000   TEMPERATURE = 103.98667   EXTENT OF REACTION = .61882
RADIUS =   .90000   TEMPERATURE = 104.02806   EXTENT OF REACTION = .45425
RADIUS =   .85000   TEMPERATURE = 104.05783   EXTENT OF REACTION = .36289
RADIUS =   .80000   TEMPERATURE = 104.07180   EXTENT OF REACTION = .30469
RADIUS =   .75000   TEMPERATURE = 104.07063   EXTENT OF REACTION = .26446
RADIUS =   .70000   TEMPERATURE = 104.05926   EXTENT OF REACTION = .23518
RADIUS =   .65000   TEMPERATURE = 104.04328   EXTENT OF REACTION = .21310
RADIUS =   .60000   TEMPERATURE = 104.02688   EXTENT OF REACTION = .19602
RADIUS =   .55000   TEMPERATURE = 104.01234   EXTENT OF REACTION = .18255
RADIUS =   .50000   TEMPERATURE = 104.00034   EXTENT OF REACTION = .17176
RADIUS =   .45000   TEMPERATURE = 103.99073   EXTENT OF REACTION = .16305
RADIUS =   .40000   TEMPERATURE = 103.98306   EXTENT OF REACTION = .15597
RADIUS =   .35000   TEMPERATURE = 103.97694   EXTENT OF REACTION = .15021
RADIUS =   .30000   TEMPERATURE = 103.97205   EXTENT OF REACTION = .14556
RADIUS =   .25000   TEMPERATURE = 103.96819   EXTENT OF REACTION = .14184
RADIUS =   .20000   TEMPERATURE = 103.96521   EXTENT OF REACTION = .13893
RADIUS =   .15000   TEMPERATURE = 103.96301   EXTENT OF REACTION = .13676
RADIUS =   .10000   TEMPERATURE = 103.96152   EXTENT OF REACTION = .13524
RADIUS =   .05000   TEMPERATURE = 103.96068   EXTENT OF REACTION = .13435
RADIUS = -.00000   TEMPERATURE = 103.96040   EXTENT OF REACTION = .13405

THE MIXING CUP TEMPERATURE IS   273.49021

THE DIMENSIONALESS TEMPERATURE IS 104.01243
THE EXTENT OF REACTION IS   .21448

THE RATIO OF CONVERSION IS   .91783

Sample Output